Synthetic Aperture Radar Application for Tropical Peatlands Monitoring Activity in Indonesia

（インドネシアにおける熱帯泥炭地管理のための
合成開口レーダー画像の応用に関する研究）

Dandy Aditya Novresiandi

2018

Synthetic Aperture Radar Application for Tropical Peatlands Monitoring Activity in Indonesia

A dissertation presented to

The United Graduate School of Agricultural Sciences, Tottori University

in partial fulfillment of the requirements for a degree of Doctor of Philosophy

by

Dandy Aditya Novresiandi

Approved by -

Professor Ryota NAGASAWA

Faculty of Agriculture, Tottori University

The United Graduate School of Agricultural Sciences

Tottori University, Japan

March, 2018

Dandy Aditya NOVRESIANDI (2018)

Synthetic Aperture Radar Application for Tropical Peatlands Monitoring Activity in Indonesia
The United Graduate School of Agricultural Sciences, Tottori University, Japan

March 2018

Ph.D Thesis

Declaration

This thesis is submitted for the degree of Doctor of Philosophy at the United Graduate School of Agricultural Sciences, Tottori University. This dissertation is the result of my own work and has not been and is not being, in part or wholly, submitted for another degree, diploma, or similar qualification.

Dandy Aditya Novresiandi

Acknowledgements

First and foremost, praise and thanks is to Allah SWT, the Almighty, the greatest of all, for everything that He has given to me and my family, *Al-hamdu lillahi rabbil 'alamin*. This dissertation could finally be possible by the synergy of significant efforts and utmost contributions which came from many individuals as well as organizations. In the first place, I owe my deepest gratitude to my academic supervisor, Professor Ryota Nagasawa, in providing such useful guidance, understanding, suggestions, and supports during my study in Japan. In addition to being an excellent academic supervisor, he is a man of principles and has immense knowledge and experience of research in general and his subject in particular. I would also like to extend my appreciation for all his contributions of time, encouragement and ideas. I am deeply grateful to my teacher, Professor Ketut Wikantika, for his utmost guidance and motivation, as well as his valuable contribution in introducing me to the world of remote sensing. Furthermore, I would like to show my gratitude to Drs. Wahyunto, M.Sc from the Indonesian Agency for Agricultural Research and Development for his help, supports, and ideas on my study. In addition, I would like to thanks Professor Yoshiyuki Hioki, Associate Professor Takaaki Fujimoto, Associate professor Hirokazu Haga, and Associate Professor Masako Kubo for their fruitful suggestions on my study. My appreciation also extends to my colleagues in Landscape Ecology and GIS Laboratory, Tottori University, including Lissa Fajri Yayusman, Kansuma Burapapol, Prima Rizky Mirelva, Koera Takuya, and Kono Tatsuya for considerable helps, supports, discussions, and enjoyable times during my study in Japan. In addition, I would also thank all Indonesian, Japanese, Thai, and Malaysian friends in Tottori. I owe everything to my lovely Wife, Nuli Rahmasari, my precious Son, Mauyama Erste Maresi, my proud Brother, Daffa Afia Rizfazka, my sincere Father, Sigit Tri Nuswantoro, and my beloved Mother, Retno Sri Sayekti, who always encourage and support me at every stage of my personal and academic life. Thank you for always have a faith in me. I love you all with all my heart. Finally, I would like to acknowledge the financial support of the Ministry of Education, Culture, Sports, Science, and Technology Japan during my study in Japan. I am really grateful for the valuable opportunity that has been given to me to pursue my study in Tottori University, Japan.

Table of contents

List of Figures

List of Tables

List of Abbreviation

ALOS : Advanced Land Observing Satellite
ASAR : Advanced Synthetic Aperture Radar
ASTER : Advanced Spaceborne Thermal Emission and Reflection Radiometer
AVNIR-2 : Advanced Visible and Near Infrared Radiometer type 2
AWP : Annual Work Plans
BRG : *Badan Restorasi Gambut* (in Indonesian) or Peat Restoration Agency
DEM : Digital Elevation Model
DF : Distance Factor
DT : Decision Tree
ENSO : El Niño Southern Oscillation
ENVISAT : Environmental Satellite
ERS : European Remote Sensing
ESA : European Space Agency
FBD : Fine Beam Dual Polarization
GDEM : Global Digital Elevation Model
GIS : Geographic Information System
GRD : Ground Range Detected
HH : Horizontal transmit - Horizontal receive polarization
HV : Horizontal transmit - Vertical receive polarization
IAARD : Indonesian Agency for Agricultural Research and Development
ISODATA : Iterative Self-Organizing Data Analysis Technique
ISPO : Indonesian Sustainable Palm Oil
IW : Interferometric Wide
JAXA : Japanese Aerospace Exploration Agency
JERS : Japanese Earth Resources Satellite
K : Kappa coefficient
MRP : Mega Rice Project
OA : Overall Accuracy
P4S : *Proyek Pembukaan Persawahan Pasang Surut* (in Indonesian) or Project for Tidal Swamp Reclamation
PA : Producer's Accuracy
PALSAR : Phased Array L-band Synthetic Aperture Radar
PD : Polarimetric Decomposition
PLR : Fully Polarimetric
PolSARpro : Polarimetric SAR Data Processing and Educational Tool

RS	**:** Remote Sensing
RVI	: Radar Vegetation Index
SAR	: Synthetic Aperture Radar
SNAP	: Sentinel Application Platform
SRTM	: Shuttle Radar Topography Mission
TRMM	: Tropical Rainfall Measuring Mission
UA	: User's Accuracy
UTM	: Universal Transverse Mercator
VH	: Vertical transmit - Horizontal receive polarization
VV	: Vertical transmit - Vertical receive polarization
WGS84	: World Geodetic System 84

Chapter 1

Introduction

1.1 Research Background

The tropical peatlands are characterized by areas in between the Tropics of Cancer and Capricorn (23.5^{o}N and 23.5^{o}S, respectively) which contains peat soil. Peat is a type of soil where the remains of organic matter accumulating under more or less water-saturated condition due to incomplete decomposition and anaerobic environment for a long period (Rydin and Jeglum 2006; Page et al. 2011; Rudiyanto et al. 2016). Tropical peatlands are mostly situated at low altitudes where the peat swamp forest is found above a thick mass of organic matter that has been contributed over thousands of years, forming accumulated deposits up to 20 m of peat depth (Anderson 1983).

The largest deposit of tropical peatlands are found in Southeast Asia, followed by South America, Africa, the Caribbean and Central America, mainland Asia and the Pacific region, where favorable regional environmental and topographic circumstances have allowed peat to form under high precipitation-high temperature conditions (Andriesse 1988; Page et al. 2011). In Southeast Asia, Indonesia has obviously the largest portion of the tropical peatlands area and tropical peat carbon store, followed by Malaysia, with Brunei, Myanmar, Papua New Guinea, the Philippines, Thailand and Vietnam, collectively, having much smaller measures of the total estimation of both tropical peatlands area and tropical peat carbon store.

Tropical peatlands acknowledged as one of key ecosystems among the high-carbon reservoir ecosystems due to their huge carbon and water storage, their effect on coastal ecosystems, and their role in preserving bio-resources and biodiversity (Osaki and Tsuji 2016; Osaki et al. 2016b). Thus, the amount of carbon stored in tropical peatlands is recognized as one of the largest terrestrial carbon storage (Jauhiainen et al. 2005). In addition, tropical peatlands have a great contribution to the global carbon cycle, which is associated with the fluxes of two significant greenhouse gases (i.e., carbon dioxide (CO_2) and methane (CH_4)), and thus have a direct relationship with global climate change processes (Jaenicke et al. 2008, Shimada et al. 2016a). In their natural state, tropical peatlands are vast carbon sink and store but once the carbon input is

discontinued by land clearance activities (e.g., deforestation) and the peat is drained, the exposed air oxidizes the peat, so that the stored carbon release rapidly to the atmosphere, which result in continuous subsidence of the peat surface and thus contribute to climate change processes (Agus et al. 2011; Osaki and Tsuji 2016; Osaki et al. 2016a).

Unfortunately, tropical peatlands are now being subjected to a rapid economic development without full consideration to the sustainable management principles and practices of tropical peatlands, which has led to large increases in carbon emission (Rieley et al. 2008). Tropical peatlands are mostly located at low altitudes in coastal and sub-coastal areas, so they tend to have a higher rate of development when compared to the other types of peatlands (Rieley 2007; Rieley et al. 2008). This is well advanced in Southeast Asia, especially in Indonesia and Malaysia archipelago, where a certain amount of tropical peatlands area has already been deforested, drained and converted to commercial plantations (often using fire, as the cheapest way of land clearance tool by some irresponsible groups of people). Consequently, in addition to biodiversity losses, there have been significant greenhouse gases emissions and large losses of carbon from the peat store, further contributing to climate change processes (Rieley and Page 2016).

In Indonesia, tropical peatlands are distributed along the low altitudes in the coastal and sub-coastal areas of Sumatra Island, Kalimantan (Indonesian territory of Borneo Island) and Papua (Indonesian territory of the western part of the island of New Guinea) (Ritung et al. 2012). In former times, tropical peatlands were considered as a wasteland due to their infertility. However, along with the increasing needs as a consequence of the growing human population, tropical peatlands are more extensively being developed for various economic purposes such as for agriculture and settlement (Agus et al. 2011). The history of the development of tropical peatlands for various economic purposes (e.g., agriculture, plantation and exploitation practices for commercial logging) in Indonesia has been started since the pre-colonialism era, and is still continuing up until now (Noor 2012). The background of the development of tropical peatlands for various economic purposes is initially comes from the successful attempts of indigenous people who utilized tropical peatlands as traditional land resources for producing food crops, fruits, and spices to support their daily life, so that inspired the government, policy makers and stakeholders to open tropical peatlands extensively as an effort for expanding the area of agriculture and for supporting the food security program since the 1970s (Notohadiprawiro 1998; Osaki et al. 2016a).

However, due to the lack of understanding of the complexities (i.e., the particular biological, chemical and physical attributes) of this sensitive ecosystem and the lack of consideration to the sustainable management principles and practices of tropical peatlands, not all location that were opened resulting a success, even leaving very serious damages to tropical peatlands ecosystem as a consequence of land degradations and fires (Rieley et al. 2008). Moreover, in the past two decades, the development of tropical peatlands utilization in Indonesia for various economic purposes have become greater due to the excessive land use/cover conversion to commercial plantations (i.e., oil palm and timber plantations), which approximately 2.0–2.5 million ha of tropical peatlands in Indonesia were converted for the development of oil palm plantations (Rieley and Page 2005; Osaki et al. 2016a).

Concurrently, the importance of tropical peatlands as a long-term carbon sinks and stores, their tendency to become a short-term source of carbon emission, and their significant role in climate change processes, have been receiving tremendous interest during the past two decades (Miettinen et al. 2017). Moreover, there are considerable debates in the matter of whether or not tropical peatlands are globally net absorbers or emitters of carbon, as well as under what circumstances they may sequester or release carbon (Rieley et al. 2008). Consequently, these concerns should be initially responded to via an accurate inventory of tropical peatlands to obtain a better understanding of tropical peatlands management, as well as to improve the foundation of knowledge in tropical peatlands monitoring activity (Osaki et al. 2016a). The accurate inventory of tropical peatlands, i.e., developing methodologies for tropical peatlands monitoring activity, is very important for accurately calculating their spatial distributions, for correctly quantifying their carbon storage, for properly estimating the magnitude of their carbon emissions, for appropriately evaluating the effect of land use/cover changes on tropical peatlands due to the rapid economic development, and for providing information that aids in the sustainable management principles and practices of tropical peatlands, particularly in Indonesia where the largest portion of the tropical peatlands is located (Hirano et al. 2016; Miettinen et al. 2017). Hence, tropical peatlands monitoring activity has become vitally important towards the sustainable management of tropical peatlands (Page et al. 2002; Jaenicke et al. 2008; Wahyunto and Agus 2012). Nevertheless, tropical peatlands cover relatively large areas and are primarily located in remote areas that are difficult to access. Thus, it is obviously challenging to develop

methodologies for monitoring tropical peatlands, especially in Indonesia.

Remote sensing (RS) applications can serve as an advantageous tool for monitoring the vast areas of tropical peatlands, as the traditional ground surveys are generally time-consuming, labor-intensive, and limited by accessibility. The RS applications serve as an advantageous tool owing to the periodic monitoring systems at wide-scale synoptic view, especially in remote sites (Lu 2006). Hence, RS is the most effective tool for tropical peatlands monitoring activity at various spatial and temporal scales, particularly when combined with field measurement data (Shimada et al. 2016a). Furthermore, the recent development of synthetic aperture radar (SAR)-based RS satellites has introduced an advanced prospect that enables continuous monitoring and cloud-free observation in humid tropical regions, particularly for tropical peatlands monitoring activity in Indonesia (Kuntz 2010).

To date, the use of SAR-based RS applications for tropical peatlands monitoring activity has increasing expeditiously, along with the growing availability of SAR data sets. Several studies have investigated the potential of SAR data for tropical peatlands monitoring activity, e.g., Romshoo et al. (2002) applied the combination of L-band Japanese Earth Resources Satellite (JERS-1) SAR time-series data and optical data to recognize land use/cover changes on tropical peatlands in Kalimantan, Indonesia, by observing the backscatter coefficients in distinct land use/cover types. Page et al. (2002) examined the combination of C-band European Remote Sensing (ERS) SAR and Landsat data for estimating the total amount of carbon that had been emitted by tropical peatlands in Central Kalimantan, Indonesia, in the event of the 1997 El Niño Southern Oscillation (ENSO). Wijaya et al. (2010) evaluated the potential of X-band TerraSAR-X dual-polarization data and fusion images with optical data to characterize different peat depth categories in Central Kalimantan, Indonesia. Another report demonstrated the use of L-band Advanced Land Observing Satellite (ALOS) Phased Array type L-band SAR (PALSAR) for wide-area mapping of tropical forest and land cover, including several categories for tropical peatlands on Borneo Island (Hoekman and Vissers 2010). Jaenicke et al. (2010) applied the combination of C-band Environmental Satellite (ENVISAT) Advanced Synthetic Aperture Radar (ASAR) dual-polarization and L-band ALOS PALSAR single- and dual-polarization data for monitoring the hydrological effects of tropical peatlands restoration by canal blocking in the ex-Mega Rice Project (MRP) area, Central Kalimantan, Indonesia. Watanabe et al. (2011) used the L-band

ALOS PALSAR fully polarimetric data for evaluating the radar scattering mechanism on tropical peatlands in Central Kalimantan, Indonesia. Englhart et al. (2016) examined C-band Sentinel-1 dual-polarization data for producing burned area maps, including those in tropical peatlands areas in Central Kalimantan, Indonesia. Another study applied the integration of L-band ALOS PALSAR dual-polarization data, optical data, and digital elevation model (DEM)-derived data for tropical peatlands mapping in the Cuvette Centrale, Congo Basin (Dargie et al., 2017). Despite all the previous research, detailed information is lacking on the performances of SAR data to identify and classify the spatial distributions of tropical peatlands, as well as to classify their peat depth categories, in response to the emerging SAR-based RS applications for tropical peatlands monitoring activity.

In fact, the L-band ALOS PALSAR data that operated in 1.27 GHz offer the cloud penetration ability and reported to be capable of passing through a certain level of vegetation cover to verify the underlying soil characteristics (Takada et al. 2009; Antropov et al. 2011). These data are provided by the Japan Aerospace Exploration Agency (JAXA). The L-band ALOS PALSAR dual-polarization data comprise two channels — horizontal transmit–horizontal receive (HH) and horizontal transmit–vertical receive (HV) — of polarization, whereas the fully polarimetric data include four channels — HH, HV, vertical transmit-horizontal receive (VH) and vertical transmit-vertical receive (VV) — of polarization. These potentials make the L-band ALOS PALSAR dual-polarization and fully polarimetric data, as well as their data combinations, particularly promising for use in tropical peatlands identification and classification.

In addition, the C-band Sentinel-1 data, which provided by the European Space Agency (ESA), are of interest owing to the fact that they are available at no cost and have global coverage. The Sentinel-1 mission encompasses a constellation of two polar-orbiting satellites (Sentinel-1A and Sentinel-1B). This data collection method operates at a center frequency of 5.405 GHz and includes two polarization channels — VH and VV — with a very short repeat cycle (12 days with one satellite and 6 days with two) and rapid product delivery. These characteristics make C-band Sentinel-1 data particularly promising for use in tropical peatlands monitoring activity, specifically for classifying peat depth distributions. Hence, further studies are absolutely necessary involving the use of these potential SAR data (i.e., L-band ALOS PALSAR and C-band

Sentinel-1 data) to improve the foundation of knowledge regarding tropical peatlands monitoring activity in Indonesia, especially for use in tropical peatlands identification and classification, as well as in peat depth classification.

1.2 Research Objectives

The primary objectives of this study are to explore the ability of L-band ALOS PALSAR fully polarimetric data for tropical peatlands identification, to evaluate the performance of L-band ALOS PALSAR dual-polarization and fully polarimetric data for tropical peatlands classification, as well as to investigate the potential of C-band Sentinel-1 for peat depth classification, in response to the emerging SAR-based RS applications for tropical peatlands monitoring activity. Therefore, to obtain those primary objectives, the present study concentrated on the following specific objectives:

(1) to explore the characteristic of tropical peatlands from the viewpoint of L-band ALOS PALSAR fully polarimetric data,

(2) to develop methodology for tropical peatlands identification using L-band ALOS PALSAR fully polarimetric data,

(3) to develop methodology for tropical peatlands classification by means of four combinations of L-band ALOS PALSAR data: (i) the combination of two scenes of dual-polarization data, (ii) the single scene of fully polarimetric data, (iii) the combination of two scenes of dual-polarization data and the single scene of the fully polarimetric data, and (iv) the combination of two scenes of dual-polarization data, the single scene of the fully polarimetric data, and the additional topographic-derived feature "distance to river,"

(4) to compare and investigate the performance of L-band ALOS PALSAR data for tropical peatlands classification when utilized as single usage (i.e., only dual-polarization data or only fully polarimetric data), combined (i.e., the combination of dual-polarization and fully polarimetric data), and integrated with topographic-derived feature (i.e., added the feature "distance to river" to the combination of dual-polarization and fully polarimetric data),

(5) to compare and evaluate the performance of features derived after the ground-range radar cross section (sigma naught or σ^0) and slant-range perpendicular radar cross section (gamma naught or γ^0) of C-band Sentinel-1 data for discriminating peat depth classes, and

(6) to develop methodology for peat depth classification on oil palm plantations using C-band Sentinel-1 data.

1.3 Outline of Dissertation

This dissertation is organized into six chapters. The focus of this chapter (Chapter 1) is to describe the general background of the study, purposes and motivations that significantly encourage for performing this study, as well as several goals to be obtained by conducting the present study.

Chapter 2 provides succinct information regarding the distribution of tropical peatlands of the world and in Indonesia, the development of tropical peatlands utilization in Indonesia, the issues of tropical peatlands utilization in Indonesia, as well as their current status towards the sustainable management of tropical peatlands in Indonesia. In additional, a brief description on the subject of the basic theory of SAR, an introduction to SAR system, the characteristics of SAR, SAR measures and features that used in the present study are explained.

Chapter 3 principally discusses about the methodology development to identify tropical peatlands using L-band ALOS PALSAR fully polarimetric data. This chapter demonstrates the contribution of polarimetric decomposition (PD) theorems and the radar vegetation index (RVI) for characterizing tropical peatlands from the viewpoint of L-band SAR fully polarimetric data.

Chapter 4 particularly reports the performance of L-band ALOS PALSAR dual-polarization data, fully polarimetric data, and their data combinations for classifying tropical peatlands, as well as describes the methodology development to classify tropical peatlands using L-band ALOS PALSAR dual-polarization and fully polarimetric data. Moreover, the details regarding the seasonal variation of tropical peatlands from the viewpoint of L-band SAR dual-polarization data is given in this chapter.

Chapter 5 specifically describes about the methodology development for peat depth classification on oil palm plantations using C-band Sentinel-1 data. This chapter gives details of the evaluation of features derived after the ground-range radar cross section (sigma naught or σ^0) and slant-range perpendicular radar cross section (gamma naught or γ^0) of C-band Sentinel-1 data for discriminating peat depth classes. Additionally, the

analysis of the seasonal variation of peat depth classes from the viewpoint of C-band SAR dual-polarization data is explained in this chapter.

Finally, in the Chapter 6, the general discussion, conclusion and recommendation are given.

Chapter 2

Theoretical Framework

2.1 The Tropical Peatlands

Tropical peatlands are considered to be important due to their functions, products and values, both for the people and for the environment. The functions (i.e., direct and indirect functions), products and values of tropical peatlands are listed as follows (Maltby 1997):

a. The direct functions of tropical peatlands

   Direct functions of tropical peatlands encompass water flow regulation (i.e., water storage, filtration and supply), environmental protection against natural hazards (e.g., erosion prevention and flood mitigation), macro-climate stabilization, recreational and educational facilitation, as well as other resources for supporting local communities (i.e., land resource for food production).

b. The indirect functions of tropical peatlands

   Indirect functions of tropical peatlands are associated with the ecological functions, such as sediment retention, nutrient detention, carbon balance and storage, and micro-climate stabilization.

c. The products of tropical peatlands

   Tropical peatlands products are connected to their role in water provision to other ecosystems and human communities, forest resources (i.e., fuel wood, timber and bark), resins and medicines supplies, wildlife resources, agricultural and horticultural resources, as well as energy resources (Page and Rieley 1998).

d. The values of tropical peatlands

   Values of tropical peatlands are closely related to the maintenance of environmental quality, which are genetic reservoirs for various endemic animals and plants (Joosten and Clarke 2002).

In addition to their functions, products and values, tropical peatlands have become a long-term provider of goods and services that supporting lives for local communities (e.g., provide hunting grounds and fishing areas, construction materials, food and medicines, as well as traditional land resource for agriculture practices) (Riley et al. 2008).

2.1.1 The tropical peatlands of the world

The total area and total carbon store of tropical peatlands worldwide are estimated at 441,025 km^2 (nearly 11% of global peatlands area) and at 88.6 Gt (Gigatonnes) (nearly 19% of the global peat carbon store), for the total area and total carbon store, respectively (Page et al. 2011). **Table 2.1** shows the estimation of tropical peatlands area in distinct regions of the world, which describes that the Southeast Asia region contains the largest area of tropical peatlands (56% of total tropical peatlands area), followed by South America (24%), Africa (13%), the Caribbean and Central America (5%), other Asia (1%) and the Australia and Pacific Island (less than 1%). In addition to those estimates, as well as presented in **Table 2.1**, the largest carbon store of tropical peatlands is also calculated in Southeast Asia (77% of total tropical peat carbon store), followed by South America (11%), Africa (8%), the Caribbean and Central America (3%) and other Asia combined with the Australia and Pacific Island (less than 1%).

Table 2.1 Best estimate area and carbon store of tropical peatlands in distinct regions of the world (Based on Page et al. 2011).

Region	Best Estimate Area (km^2) (%)	Best Estimate Carbon Store (Gt) (%)
Asia (Southeast)	247,778 (56%)	68.5 (77%)
South America	107,486 (24%)	9.7 (11%)
Africa	55,860 (13%)	6.9 (8%)
Central America and Caribbean	23,374 (5%)	3.0 (3%)
Asia (Other)	6,337 (1%)	0.4 (0%)
Australia and Pasific Island	190 (0%)	0.0 (0%)
Total	**441,025 (100%)**	**88.6 (100%)**

Therefore, the largest area of tropical peatlands and tropical peat carbon store are estimated in Southeast Asia with 56% of the total tropical peatlands area and 77% of the total estimation of tropical peat carbon store, owing to the large extent of tropical peatlands and the considerable depth of peat deposit (regularly exceeding 10 m) in this region (Rieley and Page 2016). Within the Southeast Asia region, Indonesia is estimated to contain the largest tropical peatlands area (47% of total tropical peatlands area) as well as the biggest tropical peat carbon store (65% of total tropical peat carbon store), followed by Malaysia (6% of total tropical peatlands area; 10% of total tropical peat

carbon store) with Brunei, Myanmar, Papua New Guinea, the Philippines, Thailand and Vietnam, collectively, having much smaller measures of both estimates (around 3% of total tropical peatlands area; around 2% of total tropical peat carbon store) (**Table 2.2**).

Table 2.2 Best estimate area and carbon store of tropical peatlands in different countries wihin Southeast Asia region (Based on Page et al. 2011).

Country	Best Estimate Area (km^2) (% Global)	Best Estimate Carbon Store (Gt) (% Global)
Brunei	909 (0%)	0.3 (0%)
Indonesia	206,950 (47%)	57.4 (65%)
Malaysia	25,889 (6%)	9.1 (10%)
Myanmar	1,228 (0%)	0.1 (0%)
Papua New Guinea	10,986 (3%)	1.4 (2%)
Philippines	645 (0%)	0.2 (0%)
Thailand	638 (0%)	0.0 (0%)
Vietnam	533 (0%)	0.0 (0%)
Total	**247,778 (56%)**	**68.5 (77%)**

2.1.2 The tropical peatlands in Indonesia

Current inventories of tropical peatlands area, peat depth and their carbon stores are contaminated by uncertainties and knowledge gaps so that their accuracies are vary not only from region to region but also country to country (Page et al. 2007; Rieley and Page 2016). These issues also affecting the development of tropical peatlands inventory activities in Indonesia. Since the 1970s, there are several attempts made by researchers and organization worldwide to calculate the total area of tropical peatlands in Indonesia. As shown in **Table 2.3**, there is a wide variation (ranging from 13.5 to 26.5 million ha) between the estimated amounts of the total area of tropical peatlands in Indonesia.

Ritung et al. (2012) estimated that in Indonesia there are 14.91 million ha of tropical peatlands that distributed widely along the low altitudes in the coastal and sub-coastal areas of Sumatra Island (6.44 million ha, 43% of the total tropical peatlands area in Indonesia), Kalimantan (4.78 million ha, 32%) and Papua (3.69 million ha, 25%). Moreover, the influence of tides of rivers that flowing through the tropical peatlands in Indonesia could significantly reaches the distance inland (Osaki et al. 2016a). Tropical peatlands in Indonesia are generally categorized in to four types of peat depth classes, i.e., shallow-peat class (0.5 to 1 m of peat depth), medium-peat class (1 to 2 m of peat

depth), deep-peat class (2 to 4 m of peat depth), and very deep-peat class (more than 4 m of peat depth). Thus, based on the peat depth, about 5.24 million ha (35%) of tropical peatlands in Indonesia are situated in the shallow-peat class, 3.91 million ha (26%) in the medium-peat class, 2.76 million ha (19%) in the deep-peat class, and 2.98 million ha (20%) in the very deep-peat class (Ritung et al. 2012).

Table 2.3 Total area of tropical peatlands in Indonesia estimated by various authors or sources (Modified from Najiyati et al. 2005).

Authors or Sources (Publication Year)	Total Area of Tropical Peatlands in Indonesia (million ha)
Driessen (1978)	16.10
Puslittanah (1981)	26.50
Euroconsult (1984)	17.20
Soekardi and Hidayat (1988)	18.40
Deptrans (1988)	20.10
Subagyo et al. (1990)	14.90
Deptrans (1990)	17.80
Nugroho et al. (1992)	13.50*
Radjagukguk (1993)	20.10
Dwiyono and Rachman (1996)	20.00
Wetlands International (2002-2006)	21.00
Page et al. (2011)	20.69
Ritung et al. (2012)	14.91

*exclude tropical peatlands associated with saline land and floodplain (2.46 million ha)

In Sumatra Island, the Riau Province dominates the provincial level of tropical peatlands distribution, which consisting of around 3.86 million ha (60% of the total tropical peatlands area in Sumatra). In this province, tropical peatlands are mainly situated in the very deep-peat class (42% of the total tropical peatlands area in Riau Province), followed by the medium-peat class (23% of the total tropical peatlands area in Riau Province), the deep-peat class (22% of the total tropical peatlands area in Riau Province), and the shallow-peat class (13% of the total tropical peatlands area in Riau Province). Meanwhile, in Kalimantan, the Central Kalimantan Province dominates the provincial level of tropical peatlands distribution, which consisting of around 2.66 million ha (56% of the total tropical peatlands area in Kalimantan). In this province, tropical peatlands are mostly situated in the very deep-peat class (36% of the total tropical peatlands area in Central Kalimantan Province), followed by the deep-peat class

(24% of the total tropical peatlands area in Central Kalimantan Province), the shallow-peat class (21% of the total tropical peatlands area in Central Kalimantan Province), and the medium-peat class (19% of the total tropical peatlands area in Central Kalimantan Province). In Papua, the Papua Province dominates the provincial level of tropical peatlands distribution, which consisting of around 2.64 million ha (72% of the total tropical peatlands area in Papua). In this province, tropical peatlands are largely situated in the shallow-peat class (57% of the total tropical peatlands area in Papua Province), followed by the medium-peat class (31% of the total tropical peatlands area in Papua Province), the deep-peat class (12% of the total tropical peatlands area in Papua Province), and no tropical peatlands are situated in the very deep-peat class.

2.1.3 The development of tropical peatlands utilization in Indonesia

Tropical peatlands in Indonesia were once considered as marginal agricultural lands, however, they are gradually utilized for the development of various economic purposes (e.g., agriculture, settlement, plantation and exploitation practices for commercial logging). The development of the utilization of tropical peatlands for various economic purposes in Indonesia could be divided into several periods. The periods of tropical peatlands utilization in Indonesia are briefly described as follows (Nugroho 2012; Noor 2012):

a. The period of pre-colonialism era to colonialism era

   The first ever recorded attempt of land clearance activity in tropical peatlands areas for various economic purposes in Indonesia was conducted by the Majapahit Empire in the 13th century. In this period, tropical peatlands areas situated in West Kalimantan Province, Kalimantan, were utilized for agriculture and settlement purposes. Furthermore, during the colonialism era, the Dutch East India Company was recorded in the attempt of land clearance activity in tropical peatlands areas for developing settlement and plantation areas in Sumatra (Lampung Province), Kalimantan (South Kalimantan Province), and Papua (Merauke Regency, Papua Province) around 1920s.

b. The period of late 1940s to 1960s

   The first effort of land clearance activity in tropical peatlands area after the independence of Indonesia was recorded in 1950s. During this period, the government was initiated the Dredge, Drain, and Reclamation Project to build

canals in tropical peatlands area for developing extensive agriculture areas in South Kalimantan and Central Kalimantan Province, Kalimantan. Simultaneously, several polders were constructed in several tropical peatlands areas in Sumatra Island for supporting the agriculture program initiated by the government.

c. The period of 1970s to early 1990s

On this period, the severe condition of food security in Indonesia has motivated the government to establish another substantial agricultural project for increasing national food supplies, so that alleviating the food security problem. The Project for Tidal Swamp Reclamation (*Proyek Pembukaan Persawahan Pasang Surut* or P4S in Indonesian), initiated in Kalimantan (West Kalimantan, South Kalimantan and Central Kalimantan Province) and Sumatra (Lampung, South Sumatra, Riau, and Jambi Province), has converted 1.24 million ha of tropical peatlands into agriculture areas.

d. The period of mid 1990s to 2000s

The issue on food security has one more time becomes the major background to set up another large-scale agricultural project in Indonesia. On this period, the Mega Rice Project (MRP) was established with the objective to develop one million ha of paddy field in tropical peatlands areas in Central Kalimantan Province, Kalimantan. Additionally, during this period, there was an increasing trend in the development of oil palm plantations in tropical peatlands areas. In Sumatra, the total area of oil palm plantations situated in tropical peatlands areas has increased nearly four times (from 0.26 to 1.01 million ha) between 1990 to 2005 (Sabiham and Kartawisastra 2012).

e. The period of late 2000s to 2010s

On this period, the development of oil palm plantations in tropical peatlands areas has continue to increase along with the increasing global demand for palm oil, particularly in Sumatra, Kalimantan, and Papua. The total area of oil palm plantations situated in tropical peatlands areas in Sumatra has increased more than six times (from 0.26 to 1.39 million ha) between 1990 to 2010. Meanwhile, in Kalimantan, the total area of oil palm plantations situated in tropical peatlands areas has increased tremendously to nearly sixteen times (from 0.02 to 0.31 million ha) between 2000 to 2010. Thus, by 2010, there were nearly 1.7 million ha of tropical peatlands have been exploited for the development of oil palm plantations in

Indonesia (Sabiham and Kartawisastra 2012).

To conclude, the development of tropical peatlands utilization for various economic purposes (e.g., agriculture, settlement, plantation and exploitation practices for commercial logging) has been carried out in Indonesia, which providing employment, local income, new industries and business opportunities, as well as contributing to the national income, but at the expense of the ecosystem and the environment.

2.1.4 The issues of tropical peatlands utilization in Indonesia

Tropical peatlands are recognized as one of key ecosystems among the high-carbon reservoir ecosystems due to their huge carbon and water storage, their effect on coastal ecosystems, and their role in preserving bio-resources and biodiversity (Osaki and Tsuji 2016; Osaki et al. 2016). Therefore, under their natural state, fire occurrence in tropical peatlands areas is extremely rare. However, tropical peatlands become highly susceptible to fire when damaged by land clearance activities, such as logging, drainage, and conversion to plantations (Jaenicke et al. 2008). Since the late 1990s, reoccurring large-scale fire events have significantly affected tropical peatlands in Indonesia, especially in Sumatra, Kalimantan, and Papua (Miettinen et al. 2016).

In 1997, a severe drought that was directly related to the event of El Niño Southern Oscillation (ENSO) attacked Southeast Asia and triggered an enormous forest fire in Central Kalimantan Province, Kalimantan, specifically in the area of the Mega Rice Project (MRP) that was initiated by the Indonesian government from 1995 to 1999. Page et al. (2002) estimated that about 0.73 million ha of tropical peatlands were burnt, and around 0.19 to 0.23 Gt of carbon released to the atmosphere through peat combustion, induced by the 1997 ENSO event in this area. Moreover, in 2002 and 2006, fire reoccurred not only in Kalimantan but also in Sumatra and burnt tropical peatlands areas and the overlying vegetation (Jaenicke et al. 2008).

Recently, in 2015, Indonesia experienced a very strong ENSO, leading to rainfall anomalies and a more severe dry season, as well as resulting in elevated fire occurrence equivalent with the previous catastrophic fire event in 1997 (Englhart et al. 2016). This phenomenon generated a state of emergency due to poisonous smoke and the transboundary haze pollution across Southeast Asia, as well as suffering great financial costs to the government (Lohberger et al. 2017). The transboundary haze pollution threatened several countries in Southeast Asia, including Brunei, Indonesia (particularly

in Sumatra and Kalimantan), Malaysia, Singapore, southern Thailand, Vietnam, Cambodia and the Philippines. The daily emission from this event was extremely large, and estimated in surpassing the average daily emissions from the entire USA (Van Der Werf 2015; Huijnen et al., 2016). Thus, interactions between land clearance activities, which involve drainage of the surface peat, and severe drought events have caused massive uncontrolled and repeated fire events in tropical peatlands areas, particularly in Indonesia (Siegert et al. 2004).

2.1.5 Towards the sustainable management of tropical peatlands in Indonesia

The considerable significance of tropical peatlands as a long-term carbon sinks and stores, their susceptibility to become a short-term source of carbon emission, and their notable role in climate change processes, have been receiving tremendous interest during the past two decades (Miettinen et al. 2017). Thus, in order to increase regulations regarding the worldwide-criticized tropical peatlands utilization in Indonesia, the Indonesian government announced a series of regulations towards the sustainable management of tropical peatlands in Indonesia. These regulations are listed as follows (Carmenta et al. 2017):

a. In 2011, Indonesia government announced a moratorium on granting new licenses of concession in both primary forests and tropical peatlands areas for two years. In that period of time, the government were working on a land use planning reforms that would help Indonesia successfully reaches their greenhouse gas reduction targets (Austin et al. 2012).
b. In 2014, the Government Regulation 71/2014 on protection and management of tropical peatlands (PP71), Article 23 Clause 3(a) was announced, which describes an order to maintain water table depth of 40 cm within tropical peatlands areas.
c. In 2015, the Ministry of Environment Circular Letter no.S.494/MENLHK-PHPL/2015 on the prohibition to open tropical peatlands was announced, which forbidding new permits on tropical peatlands, assisting to operationalize the tropical peatlands moratorium, clarifying land use plans, demanding companies to review their Annual Work Plans (AWP) to ensure these are in alignment with latest regulations, and forcing companies to guarantee future plans reduce impacts on forests and fires on tropical peatlands.
d. In 2015, the Ministry of Agriculture Regulation no. 11/Permentan/OT.140/3/2015

on Indonesian Sustainable Palm Oil (ISPO) Certification System was also announced, which demanding companies to comply with zero burning, through mandatory ISPO certification.

e. In 2015, Presidential Decree 8/2015 on moratorium on new grants on tropical peatlands and primary forests was announced. This regulation instructed the Ministry of Environment and Forests should extend the moratorium, which was first started in 2011, on issuance of concession permits on tropical peatlands and forests, as well as removing exemptions allowed under previous versions of the moratorium.
f. In 2016, Indonesia government announced a new moratorium on expansion of oil palm plantations and mining operations that forbids further expansion on tropical peatlands associated with oil palm cultivation and mining activities.
g. In 2016, Presidential Decree 1/2016 on peat restoration agency *(Badan Restorasi Gambut* or BRG in Indonesian) was announced, which initiated the establishment of a new peat restoration agency mandated to rewet 2 million ha of drained tropical peatlands within 5 years (by 2020).

Concurrently, along with the immense global attentions in alleviating the issues on tropical peatlands utilization in Indonesia, the implementation of sustainable management principles and practices is absolutely necessary. Thus, as one of the initial steps for actualizing the sustainable management of tropical peatlands, the accurate inventory of tropical peatlands, i.e., developing reliable methodologies for tropical peatlands monitoring activity, is vitally important for enhancing the foundation of knowledge of tropical peatlands monitoring activity, particularly in Indonesia where the largest portion of the tropical peatlands is located (Page et al. 2011; Shimada et al. 2016b).

2.2 Basic Theory of Synthetic Aperture Radar (SAR)

Remote sensing (RS) is defined as science and art of obtaining information about an object, area, or phenomenon through the analysis of data acquired by a device that is not in contact with the object, area, or phenomenon under investigation (Lillesand et al. 2008). RS applications have already been proven as an effective alternative tool for monitoring various land use/cover over large areas due to its periodic monitoring system at a wide-scale synoptic view, and has been widely used to support worldwide

environmental and agricultural monitoring activities, as well as for tropical peatlands monitoring activity (Lu 2006; Shimada et al. 2016b). The significance development of RS satellites that based on synthetic aperture radar (SAR), one of the active RS sensor systems, has introduced an advanced prospect that enables continuous monitoring and cloud-free observation in humid tropical regions (Kuntz 2010). These advantages make SAR-based RS applications is significantly superior for tropical peatlands monitoring activity in humid tropical regions, such as in Indonesia, compared to those using the passive sensor-based RS applications.

2.2.1 Introduction to SAR system

Lee and Pottier (2009) describe that the imaging synthetic aperture radar (SAR) system is an active radar system operating in the microwave region of the electromagnetic spectrum (typically between P-band and Ka-band, as showed in **Figure 2.1**), which generally mounted on a moving platform (e.g., airplane, UAV, space-shuttle, or satellite) and operates in a side-looking geometry with an illumination perpendicular to the flight line direction (as illustrated in **Figure 2.2**). This system illuminates objects in the earth's surface with microwave pulses and receives the electromagnetic signal backscattered from the illuminated terrain.

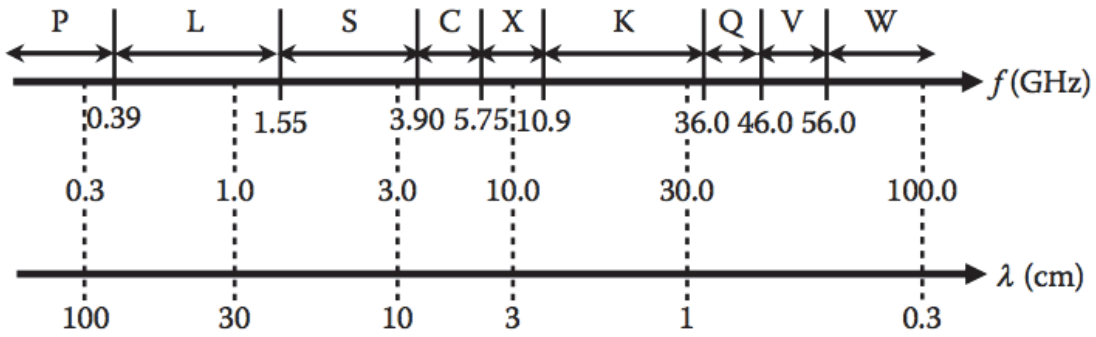

Figure 2.1 The pertinent microwave region of the electromagnetic spectrum (Taken from Lee and Pottier 2009).

Furthermore, SAR system applies signal processing to synthesize a two-dimensional (2-D) high spatial resolution image of the earth's surface reflectivity from all the received signals. Owing to its active RS sensor system, SAR is independent of solar illumination, so that allows day and night operation. Additionally, SAR system allows

an almost all-weather and continuous global-scale earth monitoring due to the utilization of the microwave spectral region on its operation. To date, SAR is a coherent and state-of-the-art microwave RS technique for providing large-scaled 2-D high spatial resolution images of the earth's surface reflectivity.

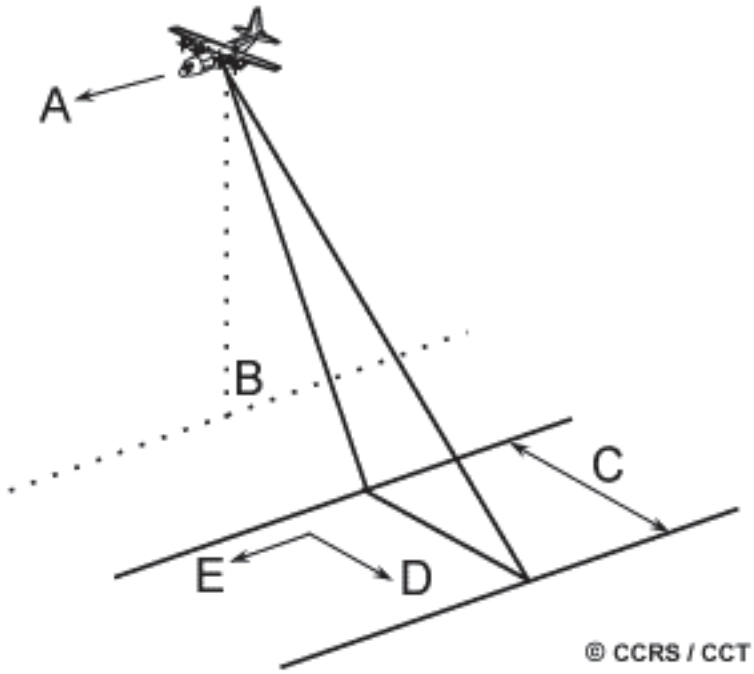

Figure 2.2 The imaging geometry of a radar system: (A) Flight direction; (B) Nadir; (C) Swath; (D) Range; and (E) Azimuth (Taken from CCRS 2014).

2.2.2 Characteristics of SAR

The characteristics of SAR system are often distinguished by wavelength and frequency. The common wavelength ranges (or bands) and their frequency used in SAR-based RS applications are X-band (2.4-3.75 cm of wavelength; 8-12.5 GHz of frequency), C-band (3.75-7.5 cm of wavelength; 4-8 GHz of frequency) and L-band (15-30 cm of wavelength; 1-2 GHz of frequency). Furthermore, the polarization of the microwave radiation is also important for characterizing SAR, and is connected with the orientation of the electric field. Polarization is specifically defined as the attitude of the electric field vector in the electromagnetic wave perpendicular to the direction of propagation. SAR is designed to transmit microwave radiation either horizontally or vertically polarized. In parallel, SAR antennas receive either the horizontally or vertically polarized backscattered energy, and some of them are able to receive both.

Thus, the combinations of SAR ability to transmit and receive microwaves are horizontal transmit–horizontal receive (HH), horizontal transmit–vertical receive (HV), vertical transmit-horizontal receive (VH) and vertical transmit-vertical receive (VV) polarization channels. Consequently, the wavelength and polarization are both influence the way in which SAR senses the object on the earth's surface. Hence, SAR image collected using different polarization and wavelength combinations may yield different and complementary information regarding the object on the earth's surface (CCRS 2014).

2.3 Backscatter coefficients

The information about the object on the earth's surface observed by SAR is often represented by the backscatter coefficients. This measure describes as normalized measure of the radar return from a distributed target. There are several measures utilized to express radar backscatter coefficients, i.e., the slant-range radar cross section (beta-naught or β^0), the ground-range radar cross section (sigma-naught or σ^0) and slant-range perpendicular radar cross section (gamma-naught or γ^0).

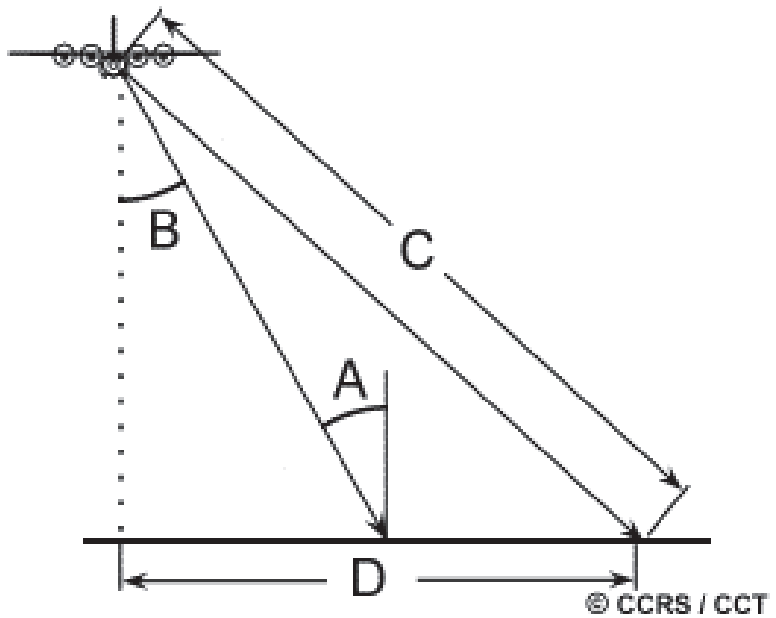

Figure 2.3 The viewing geometry of a radar system: (A) Incidence angle; (B) Look angle; (C) Slant-range distance; and (D) Ground-range distance (Taken from CCRS 2014).

Beta-naught (β^0) or the radar brightness coefficient, is a dimensionless measure, and

is defined as the radar cross section per unit area in the radar's line-of-sight (i.e., slant range). Afterwards, sigma-naught (σ^0) or the scattering coefficient, is the conventional measure of the strength of radar signals reflected by a distributed scatterer (usually expressed in decibel unit or dB), and is defined as the radar cross section per unit area in the ground-range. Subsequently, gamma-naught (γ^0) is defined as the radar cross section per unit area of the incident wavefront (i.e., perpendicular to the slant-range), and generally also expressed in dB. Furthermore, the γ^0 is commonly used to minimize the incidence angle dependency of the radar backscatter for a distributed target (Shimada 2010; El-Darymli et al. 2014). The geometry of slant-range and ground-range distance of a radar system is illustrated in **Figure 2.3**.

2.4 Polarimetric Decomposition (PD)

The main objective of polarimetric decomposition (PD) theorems is to provide interpretation for obtaining earth's surface characteristics from polarimetric SAR data. Specifically, Cloude and Pottier (1996) state that many targets of interest in radar RS demand a multivariate statistical description owing to the combination of coherent speckle noise and random vector scattering effects from surface and volume. Hence, for those targets, it is important to generate the concept of an average or dominant scattering mechanism for the purposes of classification or inversion of scattering data. PD theorems are developed for providing such an interpretation based on sensible physical constraints such as the average target being invariant to changes in wave polarization basis. To date, there are several PD theorems for extracting information from polarimetric SAR data. This study is concentrated in three commonly used PD theorems for SAR-based RS applications, which are listed as follows:

a. The Cloude-Pottier decomposition

   Cloude and Pottier (1997) suggest the Cloude-Pottier decomposition (or H/A/α decomposition) theorem, which based on the types of scattering process (eigenvectors) or their relative magnitudes (eigenvalues) analysis of the covariance matrix (C) or coherency matrix (T). This PD theorem produces three polarimetric features, namely, entropy (H), anisotropy (A) and the alpha angle (α). Entropy (H) indicates the degree of randomness of the scattering that ranges from $0 \leq H \leq 1$, values of H equal to 0 indicates a deterministic scattering process, whereas those equal to 1 showed a degenerate eigenvalues spectrum with high random scattering.

Anisotropy (A) describes the scattering component, and considers as identification properties for the secondary scattering mechanism. The alpha angle (α) shows characteristic of the dominant scattering mechanism.

b. The Freeman-Durden decomposition

Freeman and Durden (1998) define the Freeman-Durden three-component decomposition theorem as a physical scattering model-based decomposition, and model the 3 x 3 covariance matrix (C3) as the contribution of three component scattering mechanisms, i.e., surface, double-bounce, and volume scattering mechanisms. Principally, surface scattering describes the scattering information from moderately rough surface, whereas the double-bounce scattering represents the reflection from tree trunk and ground. Furthermore, the volume scattering characterizes the random distribution of very thin, cylinder-like scatterers associate with the branch of canopy cover.

c. The Yamaguchi decomposition

Yamaguchi et al. (2005) proposes the Yamaguchi four-component decomposition theorem that incorporates the non-reflecting symmetry condition of co-polarization (combinations of polarization where the transmit and receive polarizations are the same) and cross-polarization (combinations of polarization where the transmit and receive polarizations are differ) radar channels. Thus, this PD theorem modeled the 3 x 3 covariance matrix (C3) as the contribution of four-component scattering mechanisms, i.e., surface, double-bounce, volume and helix scattering mechanisms. The additional helix scattering is advantageous for explaining the correlation of both co-polarization and cross-polarization that often occurs in the scattering process of complex urban area but vanishes in scattering process of natural target.

2.5 Radar Vegetation Index (RVI)

Kim and Van Zyl (2004) introduce a feature for quantifying the amount of biomass presented in each pixel of polarimetric SAR data. This feature is specified as the radar vegetation index (RVI), and expressed as follows:

$$\mathrm{RVI} = \frac{8\sigma^0{}_{HV}}{\sigma^0{}_{HH}+\sigma^0{}_{VV}+2\sigma^0{}_{HV}}, \qquad \text{(Eq. 2.1)}$$

where σ^0_{ij} is the backscatter coefficient in linear units, transmitted in the *i* polarization plane, and received in the *j* polarization plane. This feature generally ranges between 0 and 1 and increases with the vegetation cover. Thus, the RVI defines the vegetation behavior in scattering mechanisms, and is useful to examine the complexity of scattering mechanisms in the bare surface due to the presence of vegetation layer (McColl et al. 2014).

Chapter 3

Tropical Peatlands Identification using ALOS PALSAR Imageries: A Case Study in Kahayan River Catchment Area, Central Kalimantan, Indonesia

3.1 Introduction

Tropical peatlands are acknowledged as one of the largest terrestrial carbon stores (Jauhiainen et al. 2005). The total area of tropical peatlands is estimated at only 11% of the global peatland area, but these peatlands store nearly 19% of the global peat carbon pool (Page et al. 2011). Therefore, tropical peatlands play an important role in the global carbon balance, and thus have a direct relationship with global climate change processes (Jaenicke et al. 2008). Unfortunately, tropical peatlands are now being subjected to a rapid economic development that harms this type of ecosystem, and alters their function from carbon storage to carbon emission (Rieley et al. 2008). These peatlands are mostly located at low altitudes in coastal and sub-coastal areas, so tropical peatlands tend to have a higher rate of development when compared with other types of peatlands (Rieley 2007).

The tropical peatlands situated in Central Kalimantan Province, Indonesia, is a particular concern, as they have been damaged by intensive logging, drainage, and conversion to plantations. They are also threatened by several issues, including the Mega Rice Project from 1995 to 1999 and an enormous forest fire during the abnormally long dry season (El Niño Southern Oscillation or ENSO) from 1997 to 1998. These issues have generated significant disturbances to the environment of this tropical peatlands ecosystem and have led to increased carbon emissions (Page et al. 2002; Hoekman and Vissers 2007).

Sustainable management of tropical peatlands is necessary for the control of carbon emissions. One initial step for actualizing the sustainable management principles and practices of tropical peatlands is the establishment of a reliable monitoring technique. Given the vast areas of tropical peatlands, Remote Sensing (RS) can be considered as suitable for use, as traditional ground surveys are generally time-consuming, labor-intensive and limited by accessibility. Therefore, one of the most advantageous RS

tools, Synthetic Aperture Radar (SAR), could be applied in tropical peatlands monitoring activity by an RS application.

The use of SAR data in tropical peatlands monitoring activity has been expanding rapidly and attracting much interest. Several studies have applied SAR-based RS applications for tropical peatlands monitoring activity (Romshoo et al. 2002; Page et al. 2002; Hoekman and Vissers 2007; Wijaya et al. 2010; Watanabe et al. 2011). However, few of these studies have attempted to identify tropical peatlands using L-band SAR fully polarimetric data. These SAR data are operated in L-band (1.27 GHz) and equipped with four channels of polarization. Their advantage of cloud penetration makes L-band SAR fully polarimetric data very suitable for monitoring tropical environments. Moreover, a previous study has reported that L-band SAR fully polarimetric data are permitted to pass through a certain level of vegetation cover (Takada et al. 2009). These advantages make L-band SAR fully polarimetric data particularly promising for use in tropical peatlands monitoring activity.

The present study was carried out to identify tropical peatlands using L-band ALOS PALSAR fully polarimetric data. Three polarimetric decomposition (PD) theorems and a radar vegetation index (RVI) were evaluated to examine the characteristics of tropical peatlands from the viewpoint of L-band SAR fully polarimetric data. Three PD theorems were used to examine the scattering mechanisms of tropical peatlands, while the RVI was used to measure the amount of vegetation cover in the scattering mechanisms. The integration of these two methods was applied to identify tropical peatlands. Furthermore, tropical peatlands identification maps were also established to support tropical peatlands monitoring activity, especially when using L-band SAR fully polarimetric data.

3.2 Materials and Methods

3.2.1 Study Area

Two study areas, 5 x 5 km in size, were chosen in the Kahayan River catchment area, Central Kalimantan, Indonesia (**Figure 3.1**). Basically, these areas are characterized by flat topography with surface elevation ranging up to 55 m above sea level. The average temperature and humidity of these areas are 26.9^{o}C and 83.1%, respectively, which represent the typical hot and humid condition of areas near the equatorial line. The

amounts of precipitation on these areas are ranging from 1,840 to 3,117 mm per year on average, with a typical tropical periodically concentrated rain. The first study area is located in the Pulang Pisau District, and the second study area is located in Palangka Raya City. The tropical peatlands in Central Kalimantan overall is mostly in a severely degraded condition (Jaenicke 2010), and is covered by sparse to medium vegetation in the form of shrubs. These two study areas were selected to represent the condition of tropical peatlands in Central Kalimantan. The common tropical peatlands condition in both study areas are provided in **Appendix 1** and **Appendix 2**.

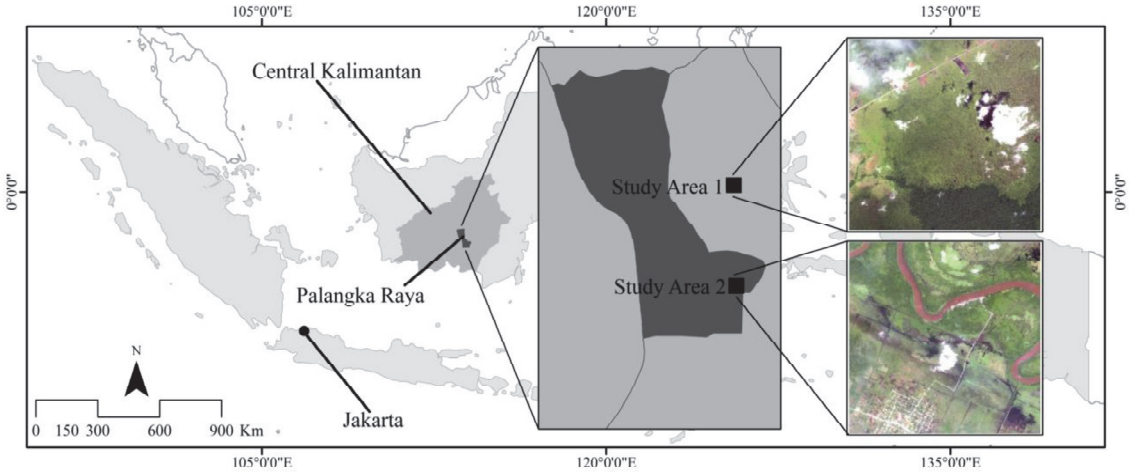

Figure 3.1 Map of Indonesia showing the location of the study areas in the Kahayan River catchment area, Central Kalimantan Province, Indonesia.

3.2.2 Data

A set of L-band ALOS PALSAR fully polarimetric data acquired on May 24, 2009 in the ascending orbit was used as the primary data. The off-nadir angle of these data was 23.1°. The fully polarimetric mode includes four channels of polarization, i.e. horizontal transmit–horizontal receive (HH) and horizontal transmit–vertical receive (HV), vertical transmit-horizontal receive (VH) and vertical transmit-vertical receive (VV). For accuracy assessment procedures, an existing land use/cover map (**Figure 3.2**) and an existing tropical peatlands identification map of the study areas (**Figure 3.3**), derived from ALOS Advanced Visible and Near Infrared Radiometer type 2 (AVNIR-2) data acquired on January 11, 2009, were used as reference maps. In addition, data collected from a ground truth survey conducted on August 23-28, 2013 were used to provide basic information about the study areas (**Appendix 3**).

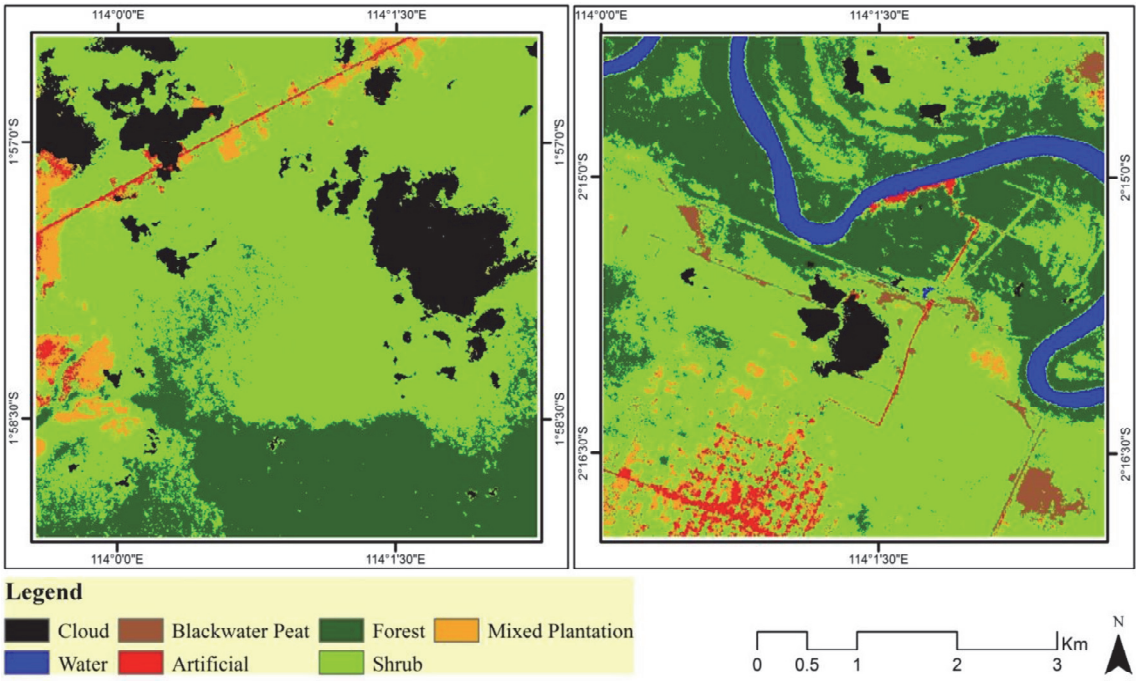

Figure 3.2 The existing land use/land cover maps of the study area 1 (left) and study area 2 (right) derived from ALOS AVNIR-2 data.

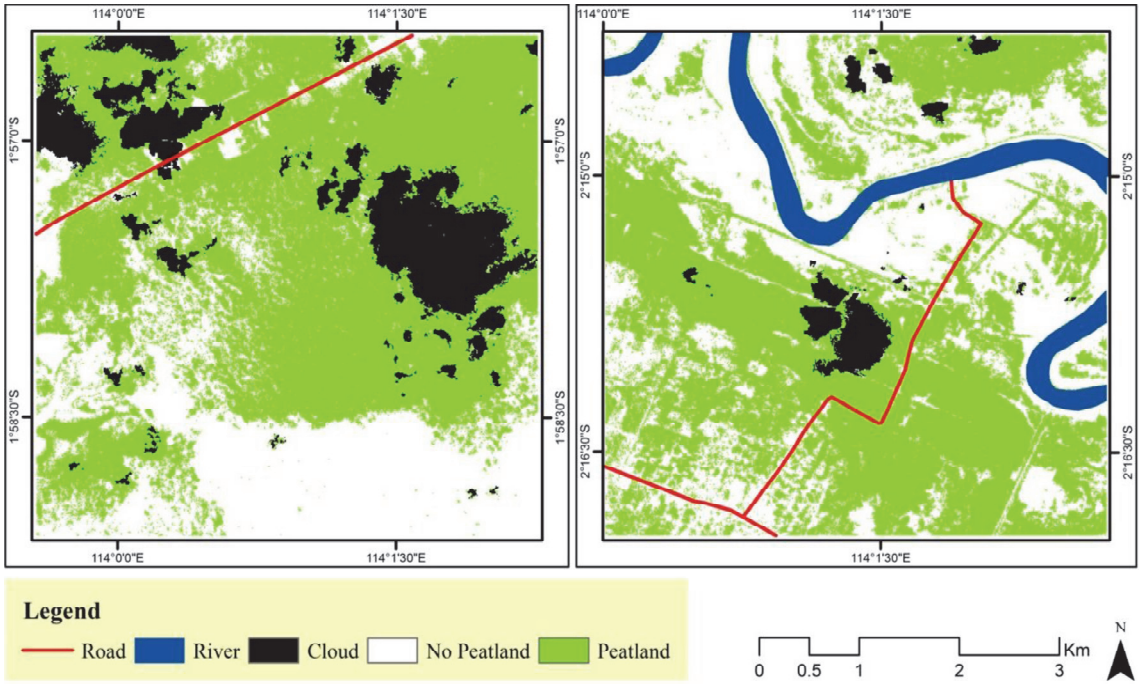

Figure 3.3 The existing tropical peatlands identification maps of the study area 1 (left) and study area 2 (right) derived from ALOS AVNIR-2 data.

3.2.3 Tropical peatlands identification method

A previous study has reported that tropical peatlands, from the viewpoint of L-band SAR fully polarimetric data, generate surface scattering or weak backscattering, but the presence of sparse vegetation cover must also be considered (Watanabe et al. 2011). The tropical peatlands in Central Kalimantan is mostly covered by shrubs. These features were used as an initial approach to identify tropical peatlands by analyzing the scattering mechanisms and vegetation cover of the tropical peatlands using PD theorems integrated with RVI. The aim of PD theorems were to extract characteristics from polarimetric data sets (Lee and Pottier 2009), while RVI was used to generate a value that would represents the amount of vegetation cover in the scattering mechanisms (McColl et al. 2014).

Data were analyzed using the Polarimetric SAR Data Processing and Educational Tool (PolSARpro), a SAR data processing and educational computer software program developed by the European Space Agency (ESA). Speckle noise was reduced by applying a Lee-refined filter with a window size of 5 x 5 pixels, followed by conversion to the coherency matrix (T) and covariance matrix (C) as inputs for PD theorems. Three well-known PD theorems — the Cloude-Pottier decomposition (Cloude and Pottier 1996), the Freeman-Durden three-component decomposition (Freeman and Durden 1998), and the Yamaguchi four-component decomposition (Yamaguchi et al. 2005) — were applied to generate polarimetric features. Furthermore, spatial analysis was done by overlaying polarimetric features with the existing tropical peatlands identification map to examine the scattering mechanisms of the tropical peatlands.

Tropical peatlands were situated by both surface and volume scattering. In this study, the presence of surface and volume scattering was considered as a key parameter for identifying tropical peatlands, which was therefore extracted as a “shrub class” by performing unsupervised classification. Polarimetric features were used as inputs for unsupervised classification. An entropy based classification scheme was applied for Cloude-Pottier decomposition (Cloude and Pottier 1997), whereas ten classes were derived using the Iterative Self-Organizing Data Analysis Technique (ISODATA) method for the other PD theorems. Afterwards, classes from each decomposition that exhibited similar patterns of shrub areas in the existing land use/cover map were combined as a “shrub class.” Furthermore, the best combination of shrub class was selected using a confusion matrix. A total of 625 points was derived on the reference

map, with each point situated within a 200 x 200 meter mesh (**Figure 3.4**). The best class combination was selected based on accuracy indicators, including Producer's Accuracy (PA), User's Accuracy (UA), Overall Accuracy (OA), and the Kappa coefficient (K). The combination that achieved the most significant accuracy indicators on the shrub class was selected as the best combination.

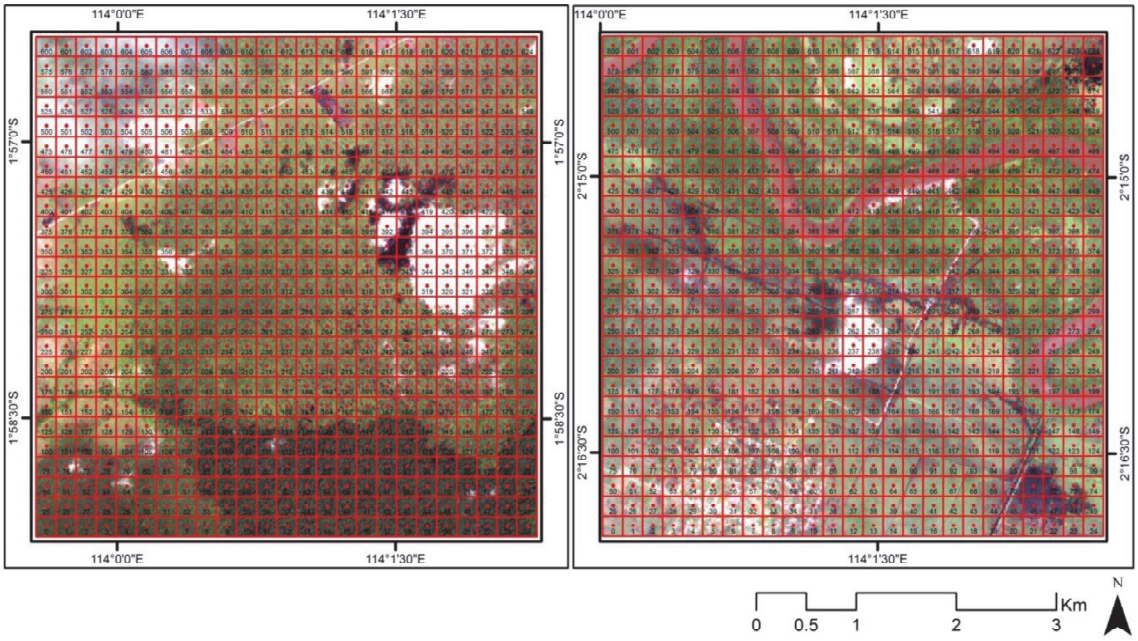

Figure 3.4 ALOS AVNIR-2 imageries of the study area 1 (left) and study area 2 (right) showing the spatial distribution of points used for accuracy assessment purpose.

Concurrently, data were converted to backscatter coefficients (σ^0) in a linear unit to generate the RVI. The RVI has been proposed as a parameter for quantifying the amount of biomass presented in each pixel (Kim and Van Zyl 2004). The equation of the RVI is presented in **Eq. 2.1**. This parameter generally ranges between 0 and 1, and increases with the vegetation cover. The RVI was then overlaid onto the existing tropical peatlands identification map and ground truth data for spatial analysis. A relationship was discovered between the RVI and tropical peatlands whereby particular areas of tropical peatlands tend to have a specific RVI value, and the average RVI of the tropical peatlands is lower than that of other areas. Hence, three interval classes of RVI were derived using the average (avg) and standard deviation (sd) values of the RVI of the tropical peatlands. Each interval class was integrated with the selected shrub class. The integration was conducted by overlaying the interval class of the RVI onto the shrub

class. Afterwards, the intersection of these two elements was extracted as a "peatland class." The most suitable integration of the shrub class and interval class of the RVI was then selected using a confusion matrix. The integration that yielded the most significant accuracy indicators on the peatland class was selected as the most suitable integration. This result was also used to select the best interval class of the RVI in the integration.

A validation using backscatter coefficient was determined to improve the reliability of the selected integration. The backscatter coefficient of tropical peatlands would always produce a higher value in HH channel than those in VV channel (Watanabe et al. 2011). Thus, validation using the backscatter coefficient was done to generate a ratio of the area that produced a higher value in HH channel than in VV channel to the area of the extracted peatland class. This ratio varies between 0% and 100%, and increases with the backscatter coefficient of HH channel. The ratio was calculated as an additional validation for the selected integration.

Finally, the best method for identifying tropical peatlands was developed using the integration of the PD theorem and RVI. The most suitable shrub class derived from unsupervised classification of polarimetric features was integrated with the selected interval class of the RVI. This selected method was then used to generate tropical peatlands identification maps for both study areas. The methodological flow chart of the present study is provided in **Appendix 4**.

3.3 Results and Discussion

3.3.1 Polarimetric features analysis

Three polarimetric features — entropy (H), anisotropy (A), and alpha angle (α) — were generated using the Cloude-Pottier decomposition **(Figure 3.5)**. Surface, double-bounce, and volume scattering parameters were derived for the Freeman-Durden decomposition **(Figure 3.6-a and Figure 3.6-c)**. Four polarimetric parameters—surface, double-bounce, volume, and helix scattering—were produced by the Yamaguchi decomposition **(Figure 3.6-b and Figure 3.6-d)**. These polarimetric features were then overlaid with the existing tropical peatlands map for spatial analysis, which revealed that the α of tropical peatlands was generally a low to medium value, indicating a dominance of surface and volume scattering. This characteristic could also be found on both composite RGB images of the polarimetric features derived by Freeman-Durden

and Yamaguchi decomposition. The presence of sparse to medium vegetation cover means that tropical peatlands generate surface scattering as well as volume scattering. In the present study, this feature was considered a key parameter for the identification of tropical peatlands because the coexistence of surface and volume scattering defined the tropical peatlands units.

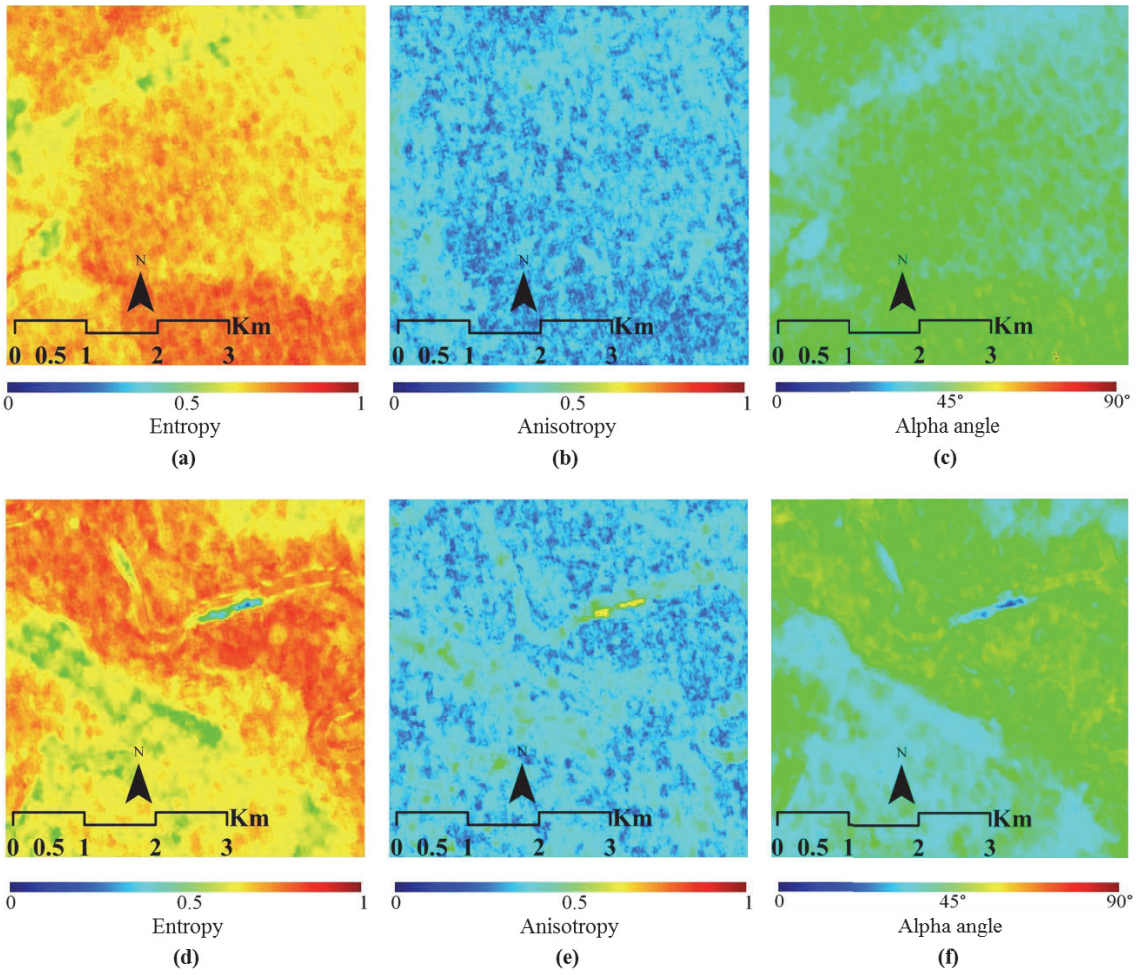

Figure 3.5 Polarimetric features images derived by the Cloud-Pottier decomposition of study area 1 (upper) and study area 2 (lower).

3.3.2 Shrub-class extraction

Table 3.1 shows the combinations of shrub classes, which represent combined classes that exhibited similar patterns of shrub areas on the existing land use/cover map. A total of 12 combinations of shrub class were created for each study area. The best combination of shrub class was selected by an accuracy assessment using a confusion matrix. As shown in **Figure 3.7**, the accuracy indicators of all combinations of the

Freeman-Durden decomposition were relatively higher than those of the other decompositions. This characteristic was obviously evident with K, especially in study area 2. On the contrary, accuracy indicators were low for the Yamaguchi decomposition, which also yielded the lowest K for both study areas. Hence, the combination of classes 2, 3, 4, 5, and 6 of the Freeman-Durden decomposition (coded as 1-f2) was selected as the best combination of shrub class for study area 1, whereas a combination of classes 2, 3, 6, and 7 of the Freeman-Durden decomposition (coded as 2-f4) was selected for study area 2. The 1-f2 combination yielded a PA of 75.4%, a UA of 91.9%, an OA of 76.6%, and a K of 0.68, whereas the 2-f4 combination achieved a PA of 78.8%, a UA of 84.5%, an OA of 78.7%, and a K of 0.62. The selected combinations of shrub classes for the two study areas were derived by the Freeman-Durden decomposition. This decomposition was determined as the most suitable decomposition for extracting the shrub classes.

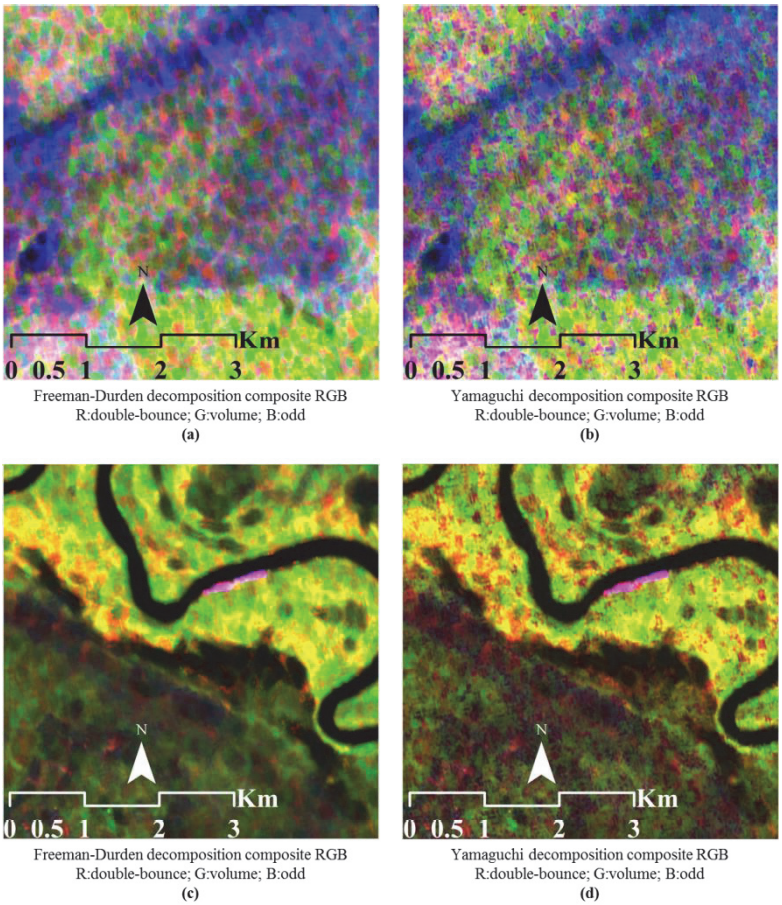

Figure 3.6 Polarimetric features images derived by the Freeman-Durden decomposition and the Yamaguchi decomposition of study area 1 (upper) and study area 2 (lower).

On the other hand, the polarimetric features derived by other decompositions had several issues to be considered. These issues were believed to be the cause of the low level of accuracy of the Cloude-Pottier and Yamaguchi decompositions. The Cloude-Pottier decomposition gave a medium value of α in the smooth surface of a river in study area 2 (**Figure 3.5-f**), where it was expected to be near 0° for surface scattering. Furthermore, an intense noises occurred in the composite RGB image of the polarimetric features of the Yamaguchi decomposition (**Figure 3.6-b** and **Figure 3.6-d**). The additional helix scattering was believed to generate noise, making this decomposition unsuitable for tropical peatlands identification.

Table 3.1 List of combinations of shrub classes for study area 1 and study area 2.

PD theorems	Study area 1		Study area 2	
	Combination of classes	**Code**	**Combination of classes**	**Code**
Cloude-Pottier	5, 6	1-h1	4, 6	2-h1
	6	1-h2	5, 6	2-h2
			4, 5, 6	2-h3
			6	2-h4
Freeman-Durden	2, 3, 4, 5	1-f1	2, 6	2-f1
	2, 3, 4, 5, 6	1-f2	2, 3, 6	2-f2
	2, 3, 4, 5, 10	1-f3	2, 6, 7	2-f3
	3, 4, 5, 6, 10	1-f4	2, 3, 6, 7	2-f4
	2, 3, 4, 5, 6, 10	1-f5		
Yamaguchi	2, 3, 4, 5	1-y1	2, 6	2-y1
	2, 3, 4, 5, 6	1-y2	2, 3, 6	2-y2
	2, 3, 4, 5, 10	1-y3	2, 6, 7	2-y3
	3, 4, 5, 6, 10	1-y4	2, 3, 6, 7	2-y4
	2, 3, 4, 5, 6, 10	1-y5		

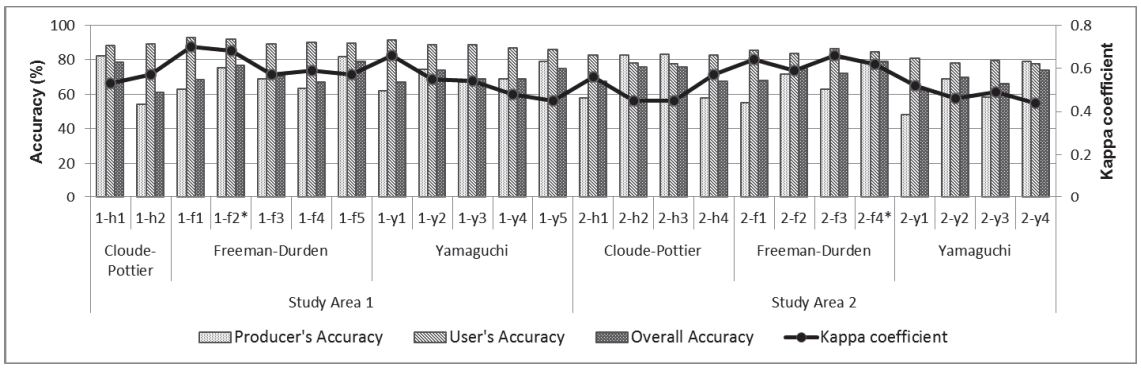

Figure 3.7 Accuracy indicators of combinations of shrub classes; codes with asterisk (*) mark represent the selected combination.

3.3.3 Peatland-class extraction

Three interval classes of RVI were generated using the average (avg) and standard deviation (sd) values of the RVI for tropical peatlands; i.e. avg±0.5sd (coded as narrow-interval), avg±sd (coded as medium-interval), and avg±2sd interval (coded as broad-interval). These interval classes were then integrated with the selected shrub classes (1-f2 and 2-f4). The intersection of the interval class of the RVI and the shrub class was extracted as a peatland class. **Table 3.2** shows the accuracy indicators of peatland class derived from the integrations of the selected shrub class and the interval class of the RVI.

Table 3.2 The accuracy indicators of peatland classes derived from the integrations of selected shrub classes and the interval classes of the RVI.

Shrub Class	Interval class of RVI	PA (%)	UA (%)	OA (%)	K
1-f2	narrow-interval	31.4	86.0	53.8	0.62
	medium-interval	60.0	84.8	68.2	0.59
	broad-interval	75.8	80.9	73.6	0.49
2-f4	narrow-interval	29.7	77.2	58.1	0.52
	medium-interval	55.5	74.4	66.2	0.46
	broad-interval	77.6	76.0	75.2	0.49

For both study areas, the highest K and UA were achieved by the narrow-interval integration. However, this integration also yielded the worst PA and OA. By contrast, relatively good results for all accuracy indicators were obtained with the broad-interval integration. For this reason, the broad-interval integration was selected as the best integration for tropical peatlands identification. Thus, integration of the shrub-class 1-f2 and the broad interval of RVI were selected for the best integration of study area 1, while for study area 2, integration of shrub-class 2-f4 and the broad interval of RVI were selected. The best integration of study area 1 achieved a PA of 75.8%, a UA of 80.9%, an OA of 73.6%, and a K of 0.49, while for study area 2 it obtained a PA of 77.6%, a UA of 76.0%, an OA of 75.2%, and a K of 0.49.

Both integrations also yielded favorable ratios of the validation using the backscatter coefficient. A total of 75% of the extracted peatland class of study area 1 produced a higher value in HH channel than in VV channel, while a total of 68% of the extracted

peatland class of study area 2 produced a higher value in HH channel than in VV channel. Thus, the selected integration for both study areas was confirmed to yield significant results with either the accuracy assessment using the confusion matrix or the validation using the backscatter coefficient.

3.3.4 PD theorems and RVI integration

The selected combination of shrub classes was used to identify tropical peatlands without any integration of the broad-interval class of RVI in order to understand the complementarity of the PD theorems and RVI in tropical peatlands identification. As shown in **Table 3.3**, lower K values were yielded for a peatland class without any addition of the broad-interval class of the RVI. Integration of the broad-interval class of RVI into the identification gave a higher K for the peatland class. The broad interval class of the RVI could distinguish the sparse to medium vegetation cover on tropical peatlands. This information was used to assist the shrub class in discriminating tropical peatlands. For this reason, the addition of a broad interval class of RVI yielded better accuracy when compared to the other interval classes of the RVI. Consequently, in the present study, the broad-interval class of the RVI provided better analysis for use with the integration of selected shrub classes derived from unsupervised classification of polarimetric features of the Freeman-Durden decomposition for tropical peatlands identification.

Table 3.3 Kappa coefficient comparison.

Combination code	Kappa coefficient (K)	
	without RVI integration	with RVI integration
1-f2	0.47	0.49
2-f4	0.46	0.49

3.3.5 Tropical peatlands identification map

As presented on **Figure 3.8**, tropical peatlands identification maps were generated for both study areas using the developed methodology. The tropical peatlands identification maps show two classes: “no peatland” and “peatland.” The “no peatland” class represents the area that was not identified as tropical peatlands, while the “peatland” class indicates the area that was identified as tropical peatlands. Study area 1 had 58.7%

of its total area identified as tropical peatlands, while study area 2 had 54.6% of its total area identified as tropical peatlands. These identification maps could be useful in the support of tropical peatlands monitoring activity, especially with the use of L-band ALOS PALSAR fully polarimetric data.

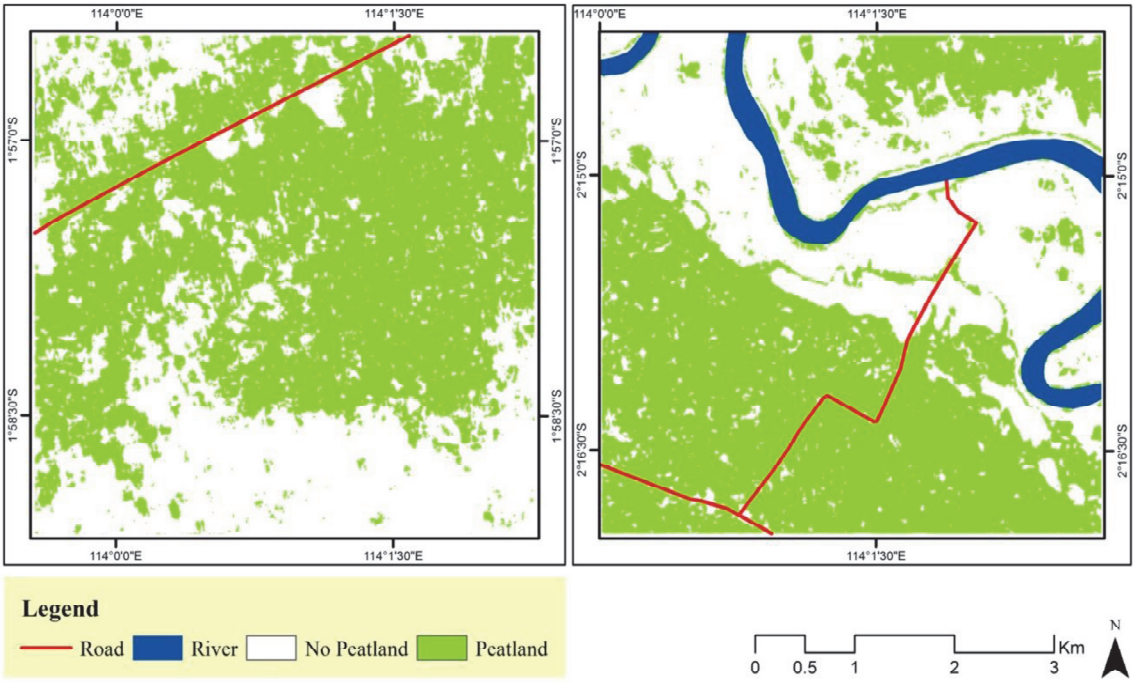

Figure 3.8 Tropical peatlands identification maps derived by using the developed methodology for study area 1 (left) and study area 2 (right).

3.3.6 Tropical peatlands identification method

A methodology has been developed for identification of tropical peatlands that uses the integration of selected shrub classes derived from unsupervised classification of polarimetric features of the Freeman-Durden and the broad interval class of the RVI. This methodology is relatively novel, in the context of tropical peatlands identification that relies on L-band SAR fully polarimetric data. This study resulted in several findings regarding the development of tropical peatlands identification using L-band SAR fully polarimetric data.

First, the Freeman-Durden decomposition was determined as the most suitable PD theorems for tropical peatlands characterization. This decomposition yielded significant accuracy for shrub-class extraction. Second, the broad interval class of the RVI was the most suitable interval class of the RVI as it distinguished the sparse to medium

vegetation cover on tropical peatlands, and was able to assist in assigning the shrub class for distinguishing tropical peatlands. Third, a complementarity between the PD theorems and RVI in the tropical peatlands identification was observed. Integration of the broad-interval class of RVI to the identification resulted in a peatland class with higher accuracy, which evident by the K.

3.4 Conclusion

This study shows that L-band SAR fully polarimetric data could be advantageous for tropical peatlands monitoring activity as an initial response to actualize the sustainable management principles and practices of tropical peatlands, particularly in Indonesia where the largest portion of the tropical peatlands is located. Tropical peatlands characteristics in the scattering mechanisms were extracted using PD theorems. The present study showed that surface and volume scattering were dominant for the tropical peatlands in Central Kalimantan, Indonesia. The presence of sparse to medium vegetation cover meant that tropical peatlands generated both surface scattering and volume scattering as the scattering mechanisms. Furthermore, a relationship between the RVI and tropical peatlands was discovered. This particular area of tropical peatlands tend to have a specific value of RVI, and the average RVI of tropical peatlands is lower than that in other areas.

In this study, a methodology has been developed to identify tropical peatlands using L-band ALOS PALSAR fully polarimetric data. The integration of the selected shrub classes derived from unsupervised classification of polarimetric features of the Freeman-Durden decomposition and the broad interval class of the RVI successfully identified tropical peatlands in two study areas in Central Kalimantan, Indonesia. In addition, tropical peatlands identification maps for both study areas were established using the developed methodology. These results are useful for supporting tropical peatlands monitoring activity, especially in tropical environments that have persistent cloud cover. This study could aid in improving the state of knowledge of tropical peatlands monitoring activity, especially involving the use of L-band SAR fully polarimetric data.

Chapter 4

Polarimetric Synthetic Aperture Radar Application for Tropical Peatlands Classification: A Case Study in Siak Transect, Riau Province, Indonesia

4.1 Introduction

In recent years, there has been considerable interest in the potential of tropical peatlands as carbon storage, as well as the magnitude of their carbon emissions and their important role in climate change processes. These concerns should be responded to via an accurate inventory of tropical peatlands to obtain a better understanding of tropical peatlands management (Page et al. 2007). The accurate inventory of tropical peatlands, such as in mapping spatial distributions of tropical peatlands, is important for properly estimating carbon emissions, for appropriately evaluating the effect of the land use/cover change due to rapid economic development, and for providing information that aids in the sustainable management principles and practices of tropical peatlands, particularly in Indonesia (Page et al. 2011; Shimada et al. 2016b). However, tropical peatlands cover relatively large areas and are primarily located in remote areas that are difficult to access. Therefore, it is challenging to map their spatial distributions (Rudiyanto et al. 2016).

Remote Sensing (RS) is the most effective tool for mapping spatial distributions of tropical peatlands at various spatial and temporal scales, especially when combined with ground truth data (Shimada et al. 2016b). Thus, the RS technique serves as an advantageous tool due to its periodic monitoring system at a wide-scale synoptic view, particularly in remote sites (Lu et al. 2006). Furthermore, the growing availability of the Synthetic Aperture Radar (SAR)-based RS satellites has introduced a new prospect that allows continuous monitoring and cloud-free observations in humid tropical regions (Kuntz 2010), that can be used for mapping spatial distributions of tropical peatlands. Previous studies (Antropov et al. 2012; Antropov et al. 2014) have evaluated the potential of L-band SAR fully polarimetric data for peatlands detection and delineation in the boreal regions. Another study (Wijaya et al. 2010) examined the combination of X-band SAR dual-polarization data and optical data for discriminating tropical

peatlands in Central Kalimantan, Indonesia. Watanabe et al. (2011) used the L-band SAR fully polarimetric data for evaluating the radar scattering mechanism on tropical peatlands in Central Kalimantan, Indonesia. Another report (Dargie et al. 2017) applied the combination of L-band SAR dual-polarization data, optical data, and digital elevation model (DEM)-derived data for mapping spatial distributions of tropical peatlands in the Cuvette Centrale, Congo Basin. However, detailed information is lacking on the performance of L-band SAR dual-polarization and fully polarimetric data for mapping spatial distributions of tropical peatlands.

The L-band SAR dual-polarization data include two channels—horizontal–horizontal (HH) and horizontal–vertical (HV)—of polarization, whereas the fully polarimetric data comprise four channels—HH, HV, vertical–horizontal (VH), and vertical–vertical (VV)—of polarization. These data operated in 1.27 GHz, permitting the cloud penetration ability and reported to be capable of passing through a certain level of vegetation cover to verify the underlying soil characteristics (Takada et al. 2009; Antropov et al. 2011). These potentials make L-band SAR dual-polarization and fully polarimetric data particularly promising for use in tropical peatlands mapping activities.

Thus, in this study, the performance of L-band Advanced Land Observing Satellite (ALOS) Phased Array type L-band SAR (PALSAR) dual-polarization and fully polarimetric data was evaluated for tropical peatlands classification. The performance of the data when utilized as single usage (e.g., only dual-polarization data or only fully polarimetric data), combined (i.e., the combination of dual-polarization and fully polarimetric data), and integrated with an additional feature “distance to river” (i.e., added the topographic-derived feature “distance to river” to the dual-polarization and fully polarimetric data combination) were compared and investigated. Thus, polarimetric features derived after polarimetric decomposition (PD) theorems, backscatter coefficients measurements, and the radar vegetation index (RVI) were evaluated to classify tropical peatlands using the Decision Tree (DT) classifier. In addition, the seasonal variation of tropical peatlands from the viewpoint of L-band SAR dual-polarization data was analyzed to increase the state of knowledge of tropical peatlands for classification. The findings of this study could aid in improving the state of knowledge in tropical peatlands classification, especially when involving the use of L-band SAR dual-polarization and fully polarimetric data.

4.2 Materials and Methods

4.2.1 Study area and data

The study area, 5 km × 10 km in size, was in Siak River Transect, Riau Province, Indonesia (**Figure 4.1**), a rapidly developing region where the tropical peatlands have been intensively converted mostly into oil palm plantations over the last two decades (Sabiham and Kartawisastra 2012). Generally, this area has a flat topography with a surface elevation ranging from 2 to 10 m above sea level. The temperature of this area is 26.2°C per year on average. The annual rainfall of this area varies from 2,200 to 2,600 mm per year, with the lowest and highest monthly rainfall in July (around 110 mm per month) and November (around 290 mm per month), respectively. The common tropical peatlands condition in the study area is provided in **Appendix 5**.

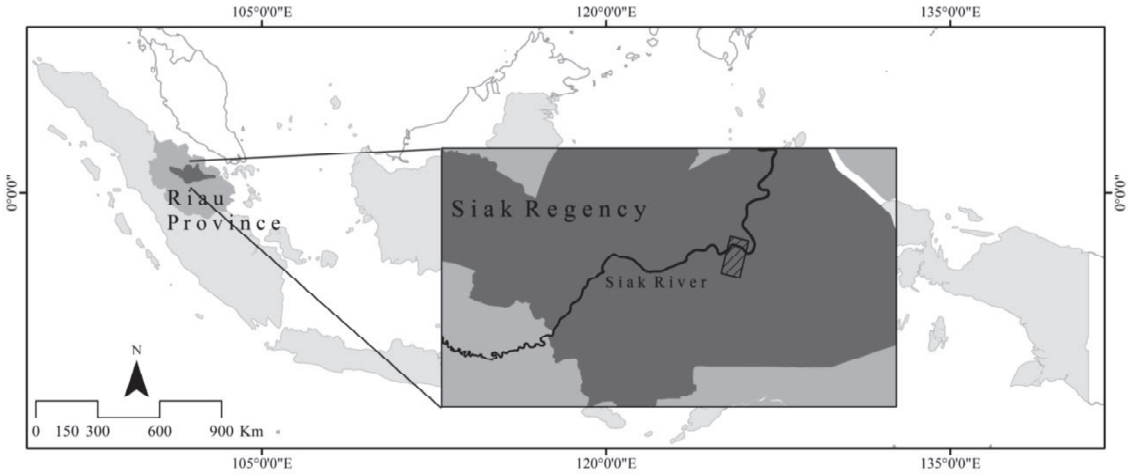

Figure 4.1. Map of Indonesia showing the location of the study area (hatched rectangle) situated in the Siak River Transect, Riau Province, Indonesia.

In this study, two scenes of L-band ALOS PALSAR dual-polarization data and a single scene of L-band ALOS PALSAR fully polarimetric data were used as the primary data. The dual-polarization data were taken during the driest month of the year (ALPSRP236980000, coded as dry scene) and the wettest month of the year (ALPSRP257110000, coded as wet scene), allowing the seasonal variation analysis of tropical peatlands from the viewpoint of L-band SAR dual-polarization data. The single scene of fully polarimetric data (ALPSRP175860000) was taken during the average monthly rainfall.

Moreover, Landsat 5 Thematic Mapper (TM) data were used to update the existing

land use/ cover map by means of visual interpretation and to select the training samples for classification purposes. A total of 2,400 points were derived for training (1,680 points) the algorithm of decision tree classification and for testing (720 points) the accuracy of the classification results (**Figure 4.2**). An existing tropical peatlands distribution map and a topographic map provided by the Indonesian Agency for Agricultural Research and Development (IAARD) were used as reference maps. In addition, a joint ground truth survey with the IAARD was conducted on May 19–22, 2015 to provide basic information about the study area (**Appendix 6**). The list of data used for analysis is shown in **Table 4.1**.

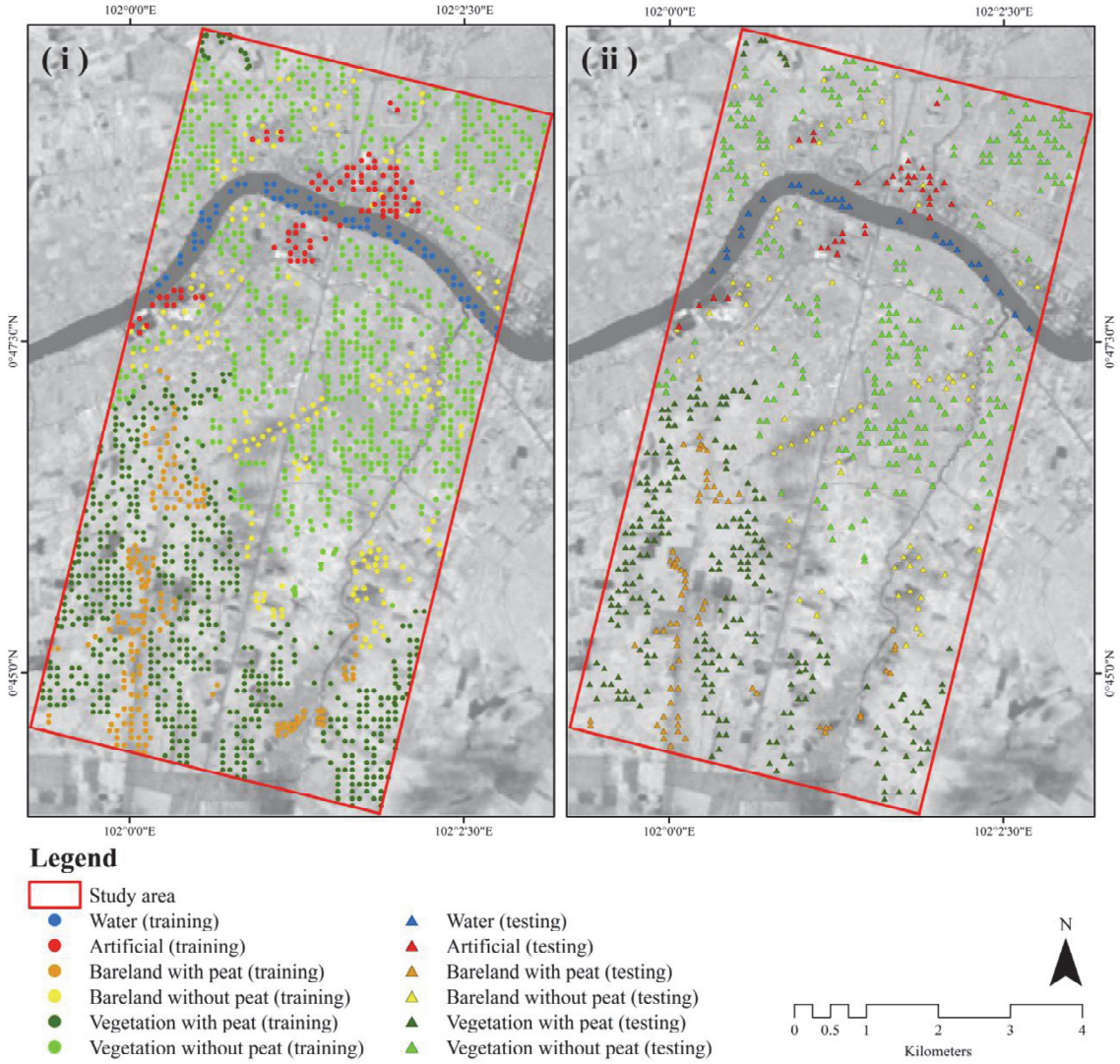

Figure 4.2 Landsat 5 TM image of the study area showing the spatial distribution of (i) training and (ii) testing points.

Table 4.1 List of data used in this study.

Data usage	Data type	Data ID	Acquisition date
Primary data	PALSAR dual-polarization (dry-scene)	ALPSRP236980000	July 6, 2010
	PALSAR dual-polarization (wet-scene)	ALPSRP257110000	November 21, 2010
	PALSAR fully polarimetric	ALPSRP175860000	May 13, 2009
Secondary data	Landsat 5 TM	LT51260592010033BKT00	February 2, 2010
	Landsat 5 TM	LT51260602010289BKT00	October 16, 2010
	ASTER GDEM	ASTGTM2 (Version 2)	October 17, 2011 (Released)

4.2.2 Data processing

L-band ALOS PALSAR data were imported to the PolSARPro Software for image processing. Thus, these data were radiometrically calibrated and multi-looked one time in range and five times in azimuth direction for the dual-polarization data, and one time in range and seven times in azimuth direction for the fully polarimetric data. Speckle noise was reduced by applying a 7 × 7 Lee-refined filter, followed by conversions to the scattering matrix (S2) and a 2 × 2 covariance matrix (C2) for the dual-polarization data, and to the S2, coherency matrix (T3) and a 3 × 3 covariance matrix (C3) for the fully polarimetric data. These matrices were used as inputs for deriving polarimetric features. L-band ALOS PALSAR data were then geocoded using the Advanced Spaceborne Thermal Emission and Reflection radiometer (ASTER) Global Digital Elevation Model (GDEM) to the Universal Transverse Mercator (UTM) Zone 48 North map projection. The methodological flow chart of the present study is provided in **Appendix 7**.

4.2.3 Polarimetric features for dual-polarization data

Polarimetric features for dual-polarization data were derived after PD theorems and backscatter coefficients were obtained. The Cloude–Pottier decomposition (Cloude and Pottier 1996), an eigenvalue/eigenvector-based decomposition, was performed for the dual-polarization data to derive three features, viz. entropy (coded as dFBD_H for the dry-scene data and wFBD_H for the wet-scene data), anisotropy (coded as dFBD_A for the dry-scene data and wFBD_A for the wet-scene data), and alpha angle (coded as dFBDα for the dry-scene data and wFBDα for the wet-scene data). Two features

represent the channels of polarization derived from the dual-polarization data, i.e., HH (coded as dFBD_HH for the dry-scene data and wFBD_HH for the wet-scene data) and HV (coded as dFBD_HV for the dry-scene data and wFBD_HV for the wet-scene data). Each scene of the dual-polarization data (wet and dry scenes) derived five polarimetric features. Thus, a total of 10 polarimetric features were computed using the dual-polarization data for the analysis carried out in this study.

4.2.4 Polarimetric features for fully polarimetric data

Polarimetric features for fully polarimetric data were derived after PD theorems, backscatter coefficients measurements, and the RVI were obtained. Three PD theorems — Cloude–Pottier decomposition (Cloude and Pottier 1996), Freeman–Durden three-component decomposition (Freeman and Burden 1998), and Yamaguchi four-component decomposition (Yamaguchi et al. 2005) — were applied to generate polarimetric features for the fully polarimetric data. Cloude–Pottier decomposition was also performed for the fully polarimetric data and generated three features, namely, entropy (PLR_H), anisotropy (PLR_A), and the alpha angle (PLR_α). The Freeman–Durden decomposition, a physical scattering model-based decomposition, models the covariance matrix (C3) as the contribution of three component scattering mechanisms—surface (f_odd), double-bounce (f_double), and volume (f_volume) scattering mechanisms. The Yamaguchi decomposition scheme incorporates the non-reflection symmetry condition of co-polarization and cross-polarization radar channels thus the covariance matrix (C3) is modeled as four component scattering mechanisms' contributions — surface (y_odd), double-bounce (y_double), volume (y_volume), and helix (y_helix) scattering mechanisms. Four features representing the channels of polarization were derived from the fully polarimetric data, i.e., HH (coded as PLR_HH), HV (coded as PLR_HV), VH (coded as PLR_VH), and VV (coded as PLR_VV).

Three features representing a decomposition approach based on the Pauli matrix were generated (Takada et al. 2009; Clouds and Pottier 1996). These features are HH+VV, HH-VV, and 2HV, associated with surface scattering, double-bounce scattering, and volume scattering, respectively. A depolarization ratio (HV/HH) was calculated that indicated the level of volume scattering (Takada et al. 2009). In addition, the total scattering power (SPAN) in four polarizations of the fully polarimetric data was

generated. The SPAN is an average of HH, HV+VH, and VV, and thus has a lower speckle noise than those polarization channels individually (Lee and Pottier 2009). Concurrently, the RVI was derived for quantifying the amount of biomass presented in each pixel (Kim and Van Zyl 2004). The equation of the RVI is presented in **Eq. 2.1**. This feature generally ranges between 0 and 1 and increases with the vegetation cover. Therefore, a total of 20 polarimetric features were computed from the fully polarimetric data for the analysis carried out in this study. The list of polarimetric features used for analysis is shown in **Table 4.2**.

Table 4.2 List of polarimetric features derived for analysis carried out in this study.

Source	Methods	Feature name	Code name
Fully polarimetric data	Backscatter coefficients	HH	PLR_HH
		HV	PLR_HV
		VH	PLR_VH
		VV	PLR_VV
	Cloude-Pottier decomposition	Entropy	PLR_H
		Anisotropy	PLR_A
		Alpha angle	PLR_α
	Freeman-Durden decomposition	Surface scattering	f_odd
		Double bounce scattering	f_double
		Volume scattering	f_volume
	Yamaguchi decomposition	Surface scattering	y_odd
		Double bounce scattering	y_double
		Volume scattering	y_volume
		Helix scattering	y_helix
	Total scattering power	SPAN	SPAN
	Backscatter coefficients measurements (Pauli Matrix)	Surface scattering	HH+VV
		Double bounce scattering	HH-VV
		Volume scattering	2HV
	Backscatter coefficients measurements	Depolarization ratio	HV/HH
	Radar Vegetation Index	RVI	RVI
Dry-scene dual-polarization data	Backscatter coefficients	HH	dFBD_HH
		HV	dFBD_HV
	Cloude-Pottier decomposition	Entropy	dFBD_H
		Anisotropy	dFBD_A
		Alpha angle	dFBDα
Wet-scene dual-polarization data	Backscatter coefficients	HH	wFBD_HH
		HV	wFBD_HV
	Cloude-Pottier decomposition	Entropy	wFBD_H
		Anisotropy	wFBD_A
		Alpha angle	wFBDα

4.2.5 Image classification

To evaluate the performance of L-band ALOS PALSAR dual-polarization and fully polarimetric data in classifying tropical peatlands, polarimetric features derived by four combinations of data were used in this study to apply to the algorithm of decision tree classification: (i) the combination of the two scenes of dual-polarization data, (ii) the single scene of the fully polarimetric data, (iii) the combination of the two scenes of dual-polarization data and the single scene of the fully polarimetric data, and (iv) the combination of the two scenes of dual-polarization data, the single scene of the fully polarimetric data, and the additional feature "distance to river." These combinations of data were applied in this study to assess the capabilities of each type of data and their combinations in classifying tropical peatlands. Moreover, the integration of the additional feature "distance to river" was meant to evaluate the effectiveness of Geographic Information System (GIS) data integration in the SAR-based tropical peatlands classification. The feature "distance to river" was derived from a GIS data processing, which buffered the center line of the main river stream into three categories, namely, "less than 2 km from river," "2 to 5 km from river," and "more than 5 km from river." Previous studies (Hoover and Vernimmen 2013; Rudiyanto et al. 2016; Shimada et al. 2016a) have found "distance to river" to be an important topographic feature in estimating the peat depth as well as in discriminating spatial distributions of tropical peatlands.

In this study, the Decision Tree (DT) classifier was used for classifying tropical peatlands. According to the concept of DT classification (Friedl and Bradley 1997), the DT is a procedure of classification that recursively partitions a set of data into smaller subdivisions based on a set of criteria determined at each branch in the tree. The DT classifier was characterized as strictly nonparametric and required no-assumptions regarding the distributions of the input data. Moreover, the design of classification is explicit and easy to understand. The main advantages of the DT classifier are its ability to handle complex relations among class properties, its computational speed, and its capability to handle data represented on different measurement scales (Pal and Mather 2003). Thus, the DT is an efficient tool for land cover classification purposes (Mishra et al. 2011). Furthermore, the Distance Factor (DF) was used in this study to evaluate the effectiveness of a feature for separating the class pairs by calculating the distance between the different class mean values compared with the standard deviations. Hence,

if the distance between the different class mean values is large compared with the standard deviations, classes are said to be well separated following the concept of feature separation (Cumming and Van Zyl 1989). The expression for the DF is

$$\mathrm{DF}_{ij} = \frac{|\bar{x}_i - \bar{x}_j|}{\sigma_i + \sigma_j}, \qquad \text{(Eq. 4.1)}$$

where $\bar{x}$ and σ are the mean values and standard deviations, respectively. The quality of the separation between classes *i* and *j* is represented by the value of DF*ij*. Values of DF*ij* of less than 0.8 are considered below average, between 0.8 and 1.5 average, and more than 2.0 close to the complete separation of class pairs (Chen et al. 2007).

In this study, six classes were selected to represent the common land use/cover on the study area from the viewpoint of L-band SAR data. These classes are water, artificial, bareland with peat, bareland without peat, vegetation with peat, and vegetation without peat. Hence, to apply the concept of feature separation on the algorithm of the DT classification, five combinations of class pairs were specified: (1) ("water" plus "artificial") and others ("bareland with peat," "bareland without peat," "vegetation with peat," plus "vegetation without peat"), (2) "water" and "artificial," (3) ("bareland with peat" plus "bareland without peat") and ("vegetation with peat" plus "vegetation without peat"), (4) "bareland with peat" and "bareland without peat," and (5) "vegetation with peat" and "vegetation without peat." These class pairs were then applied to the algorithm of the DT classification to classify each land use/cover class, as shown in **Figure 4.3**.

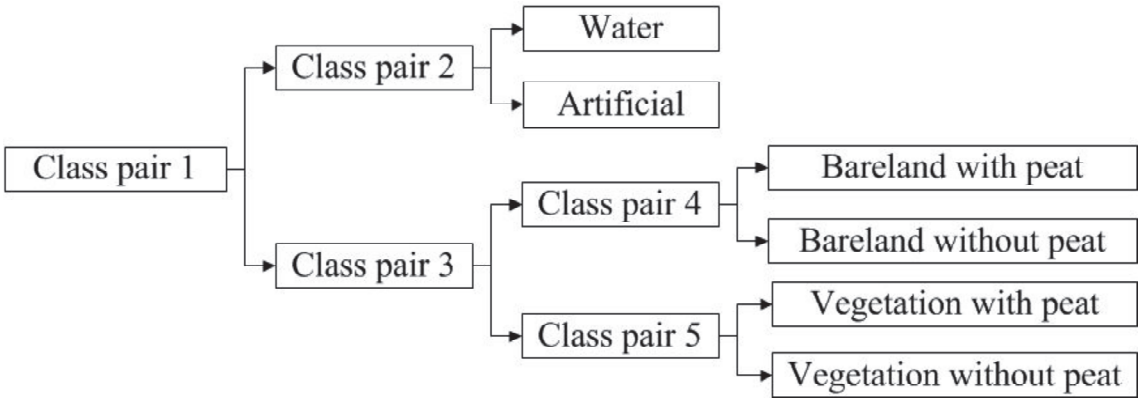

Figure 4.3 The algorithm of the decision tree classification for tropical peatlands classification.

Thus, polarimetric features with a relatively high DF on each class pair were analyzed and applied to the algorithm for DT classification, then the classification results' accuracy was assessed using the available testing points. Features that increase the accuracy of the classification results were then added to the algorithm and vice versa. The confusion matrix was used to perform the accuracy assessment on the classification results by means of deriving the accuracy indicators, namely, Producer's Accuracy (PA), User's Accuracy (UA), Overall Accuracy (OA), and Kappa coefficient (K). These indicators were used to assess the quality of the classification results.

4.3 Results and Discussion

4.3.1 Class pairs' separability

Table 4.3 shows the separability of five class pairs by each polarimetric feature, as measured by the DF. An italic value indicates the low performance of a feature in separating class pairs, whereas a bold value illustrates the average performance. An underlined value indicates the excellent performance of a feature in separating class pairs that equates to a nearly complete separation of class pairs. The values of DF for all class pairs were quite varied, depending on the feature. In general, the DF derived by the fully polarimetric data tends to have a higher value than those derived by the dual-polarization data, particularly for class pairs 1 to 4. However, for the class pair 5, the DF derived by the fully polarimetric data was inferior to those derived by the dual-polarization data. In addition, the quality of DF for class pairs 4 and 5 generated by all polarimetric features was low. The low performance of DF occurred due to the highly overlapping mean and standard deviation values of land use/cover classes in the associated class pairs that corresponded to the stage of identifying the existence of tropical peatlands in a land use/cover class.

4.3.2 Selected feature for classification

4.3.2.1 Data combination (i)

Table 4.4 shows the list of selected features for each combination of data. For dual-polarization data, four polarimetric features — dFBD_HV, wFBD_HV, wFBD_HH, and dFBD_HH — were selected in separating class pair 1. For class pair 2, two polarimetric features were selected, namely, wFBD_HH and dFBD_HH. A total of four

Table 4.3 Separability of five class pairs by each polarimetric feature.

Source	Code name	Distance Factor (DF) of each class pair				
		1	**2**	**3**	**4**	**5**
Fully polarimetric data	PLR_HH	*0.73*	2.30	*0.58*	*0.32*	*0.19*
	PLR_HV	**1.27**	**1.68**	**0.97**	*0.22*	*0.07*
	PLR_VH	**1.26**	**1.68**	**0.94**	*0.19*	*0.13*
	PLR_VV	*0.77*	2.37	*0.27*	*0.32*	*0.18*
	PLR_H	*0.53*	**1.27**	**1.03**	*0.10*	*0.10*
	PLR_A	**1.79**	*0.47*	*0.58*	*0.03*	*0.11*
	PLR_α	*0.15*	**1.73**	*0.76*	*0.12*	*0.15*
	f_odd	*0.10*	2.47	*0.22*	*0.01*	*0.06*
	f_double	*0.07*	*0.37*	*0.09*	*0.00*	*0.06*
	f_volume	**1.36**	2.09	*0.69*	*0.26*	*0.17*
	y_odd	*0.22*	2.62	*0.43*	*0.07*	*0.01*
	y_double	*0.01*	**0.99**	*0.14*	*0.01*	*0.09*
	y_volume	**1.38**	2.09	*0.74*	*0.23*	*0.15*
	y_helix	*0.70*	**1.24**	*0.12*	*0.18*	*0.08*
	SPAN	**1.02**	2.96	*0.02*	*0.16*	*0.20*
	HH+VV	*0.76*	2.41	*0.45*	*0.34*	*0.21*
	HH-VV	*0.10*	*0.11*	*0.45*	*0.01*	*0.04*
	2HV	**1.27**	**1.68**	**0.97**	*0.22*	*0.07*
	HV/HH	*0.03*	*0.42*	*0.08*	*0.06*	*0.22*
	RVI	*0.37*	**1.12**	**1.80**	*0.24*	*0.20*
Dry-scene dual-polarization data	dFBD_HH	**0.92**	**1.65**	*0.04*	*0.20*	*0.18*
	dFBD_HV	**1.30**	**1.35**	*0.58*	*0.24*	*0.15*
	dFBD_H	*0.35*	**0.93**	*0.63*	*0.07*	*0.02*
	dFBD_A	*0.31*	**0.96**	*0.65*	*0.09*	*0.00*
	dFBDα	*0.23*	**0.85**	*0.62*	*0.08*	*0.00*
Wet-scene dual-polarization data	wFBD_HH	**0.94**	**1.80**	*0.05*	*0.26*	*0.29*
	wFBD_HV	**1.26**	**1.63**	*0.61*	*0.23*	*0.22*
	wFBD_H	*0.32*	**1.18**	*0.59*	*0.02*	*0.04*
	wFBD_A	*0.27*	**1.25**	*0.60*	*0.01*	*0.04*
	wFBDα	*0.23*	**1.13**	*0.58*	*0.00*	*0.05*

polarimetric features were selected in separating class pair 3, i.e., dFBD_A, dFBD_H, wFBD_HV, and wFBD_A. In separating class pair 4, wFBD_HH and dFBD_HV were selected. For class pair 5, wFBD_HH and wFBD_HV were selected in the algorithm of the DT for tropical peatlands classification. Therefore, the polarimetric features chosen for dual-polarization data were mainly derived by the backscatter coefficient, whereas those derived by Cloude–Pottier decomposition were selected only in class pair 3. This shows that the backscatter coefficient of the dual-polarization data was dominant among almost all land use/cover classes described in this study for the purpose of tropical peatlands classification.

Table 4.4 List of selected polarimetric features for each data combination.

Class pair	Combinations of data			
	i	ii	iii	iv
1	dFBD_HV, wFBD_HV, wFBD_HH, and dFBD_HH	y_volume and f_volume	y_volume and f_volume	y_volume and f_volume
2	wFBD_HH and dFBD_HH	SPAN and y_odd	SPAN and y_odd	SPAN and y_odd
3	dFBD_A, dFBD_H, wFBD_HV, and wFBD_A	RVI	RVI	RVI
4	wFBD_HH and dFBD_HV	HH+VV, PLR_HH, PLR_VV, and f_volume	HH+VV, PLR_HH, PLR_VV, f_volume, wFBD_HH and dFBD_HV	HH+VV, PLR_HH, PLR_VV, f_volume, wFBD_HH, dFBD_HV, and "distance to river"
5	wFBD_HH and wFBD_HV	HH+VV, RVI, and SPAN	wFBD_HH and HV/HH	wFBD_HH, HV/HH, and "distance to river"

Thus, a total of five classification rules, separating five class pairs, were generated using training points based on the selected polarimetric features for tropical peatlands classification by means of data combination (i). The classification rules were developed using mean and standard deviation values of land use/cover classes for each selected polarimetric feature. These rules are listed as follows:

(i) Rule 1 for separating classes in the class pair 1.
If (dFBD_HV) ≤ (−16.60) dB and (wFBD_HV) ≤ (−16.71) dB and (wFBD_HH) ≤ (−9.06) dB and (dFBD_HH) ≤ (−8.59) dB, Then Class pair 2.

(ii) Rule 2 for separating peat depth classes in the class pair 2.
If (wFBD_HH) ≤ (−15.76) dB and (dFBD_HH) ≤ (−15.45) dB, Then "Water".

(iii) Rule 3 for separating peat depth classes in the class pair 3.
If (dFBD_A) ≥ (0.53) dB and (dFBD_H) ≤ (0.79) dB and (wFBD_HV) ≤ (−13.48) dB and (wFBD_A) ≥ (0.52) dB, Then Class pair 4.

(iv) Rule 4 for separating peat depth classes in the class pair 4.
If (wFBD_HH) ≤ (−8.22) dB and (dFBD_HV) ≤ (−14.19) dB, Then "Bareland with peat".

(v) Rule 5 for separating peat depth classes in the class pair 5.
If (wFBD_HH) ≤ (−7.86) dB and (wFBD_HV) ≤ (−12.61) dB, Then "Vegetation with peat".

These classification rules were then applied to the DT algorithm to obtain classification results of data combination (i).

Moreover, selected features in separating class pairs 4 and 5 described important characteristics in identifying the existence of tropical peatlands as well as in understanding the seasonal variation of tropical peatlands, especially from the viewpoint of L-band SAR dual-polarization data. For class pair 4, in separating the classes "bareland with peat" and "bareland without peat," both features derived by the dry- and wet-scene dual-polarization data were used. Nevertheless, only features derived by the wet-scene dual-polarization data were selected to separate "vegetation with peat" and "vegetation without peat" classes. These characteristics were obviously seen by the value of DF, as shown in **Table 4.3**, whereby the DF of selected features for class pair 4 derived by dry- and wet-scene dual-polarization data was relatively high. However, for class pair 5, the DF of selected features derived by the wet-scene dual-polarization data was higher than the dry scene. Therefore, the existence of tropical peatlands in a land use/cover without the presence of vegetation, such as that in bareland, was not influenced by the seasonal condition as it generates a relatively similar response to backscatter coefficients derived by the wet- and dry-scene dual-polarization data. On the other hand, the existence of tropical peatlands in a land use/cover with the presence of vegetation (or below a vegetation cover) was influenced by the seasonal condition, whereby it was more sensitive to backscatter coefficients derived by the wet-scene dual-polarization data that was taken during the wet season. This finding was valuable in increasing the state of knowledge of tropical peatlands for classification, especially from the viewpoint of L-band SAR dual-polarization data.

4.3.2.2 Data combination (ii)

Regarding the fully polarimetric data, two polarimetric features were selected in separating class pair 1, y_volume and f_volume. To separate class pair 2, SPAN and y_odd were selected. On the other hand, the feature RVI was selected to separate class pair 3. A total of four features were selected in separating class pair 4, i.e., HH+VV, PLR_HH, PLR_VV, and f_volume. In separating class pair 5, three features — HH+VV,

RVI, and SPAN — were selected in the algorithm for tropical peatlands classification. Therefore, the selected polarimetric features for fully polarimetric data showed good complementarity between features derived by Freeman–Durden decomposition, Yamaguchi decomposition, the RVI, the total scattering power, and the co-polarized backscatter coefficient measurements. However, polarimetric features derived by Cloude–Pottier decomposition and cross-polarized backscatter coefficient measurements were not selected due to their low performance in separating class pairs, as they did not have any effect on increasing the accuracy of the classification results. This indicated that the fully polarimetric data had the potential to characterize land use/cover classes described in this study for the purpose of tropical peatlands classification.

Thus, a total of five classification rules, separating five class pairs, were generated using training points based on the selected polarimetric features for tropical peatlands classification by means of data combination (ii). The classification rules were developed using mean and standard deviation values of land use/cover classes for each selected polarimetric feature. These rules are listed as follows:

(i) Rule 1 for separating classes in the class pair 1.
If (y_volume) ≤ (−8.03) dB and (f_volume) ≤ (−7.57) dB, Then Class pair 2.

(ii) Rule 2 for separating peat depth classes in the class pair 2.
If (SPAN) ≤ (−12.39) dB and (y_odd) ≤ (−16.23) dB, Then “Water”.

(iii) Rule 3 for separating peat depth classes in the class pair 3.
If (RVI) ≤ (0.73) dB, Then Class pair 4.

(iv) Rule 4 for separating peat depth classes in the class pair 4.
If (HH+VV) ≤ (−12.03) dB and (PLR_HH) ≤ (−5.00) dB and (PLR_VV) ≤ (−6.84) dB and (f_volume) ≤ (−4.70) dB, Then “Bareland with peat”.

(v) Rule 5 for separating peat depth classes in the class pair 5.
If (HH+VV) ≥ (−15.60) dB and (RVI) ≤ (1.00) dB and (SPAN) ≥ (−3.89) dB, Then “Vegetation with peat”.

These classification rules were then applied to the DT algorithm to obtain classification results of data combination (ii).

4.3.2.3 Data combination (iii)

For the combination of dual-polarization and fully polarimetric data, the selected

polarimetric features in separating the first three class pairs (class pairs 1, 2, and 3) were the same features as those selected in the first three class pairs for the fully polarimetric data. Thus, two polarimetric features — y_volume and f_volume — were selected in separating class pair 1. For class pair 2, two polarimetric features were selected, namely, SPAN and y_odd. In separating class pair 3, the feature RVI was selected. However, to separate class pair 4, six features were selected, HH+VV, PLR_HH, PLR_VV, f_volume, wFBD_HH, and dFBD_HV. For class pair 5, wFBD_HH and the depolarization ratio were selected in the algorithm of the DT for tropical peatlands classification. Therefore, the selected polarimetric features for the combination of dual-polarization and fully polarimetric data indicated a dominance of features derived by the fully polarimetric data, especially those selected in the first three class pairs. Polarimetric features derived by the dual-polarization data were mainly selected in separating class pairs 4 and 5, which was the stage of identifying the existence of tropical peatlands in a land use/cover class. This showed that the dual-polarization data aided the fully polarimetric data in characterizing the existence of tropical peatlands in a land use/cover class.

Thus, a total of five classification rules, separating five class pairs, were generated using training points based on the selected polarimetric features for tropical peatlands classification by means of data combination (iii). The classification rules were developed using mean and standard deviation values of land use/cover classes for each selected polarimetric feature. These rules are listed as follows:

(i) Rule 1 for separating classes in the class pair 1.
If (y_volume) ≤ (−8.03) dB and (f_volume) ≤ (−7.57) dB, Then Class pair 2.

(ii) Rule 2 for separating peat depth classes in the class pair 2.
If (SPAN) ≤ (−12.39) dB and (y_odd) ≤ (−16.23) dB, Then “Water”.

(iii) Rule 3 for separating peat depth classes in the class pair 3.
If (RVI) ≤ (0.73) dB, Then Class pair 4.

(iv) Rule 4 for separating peat depth classes in the class pair 4.
If (HH+VV) ≤ (−12.03) dB and (PLR_HH) ≤ (−5.00) dB and (PLR_VV) ≤ (−6.84) dB and (f_volume) ≤ (−4.70) dB and (wFBD_HH) ≤ (−7.47) dB and (dFBD_HV) ≤ (−13.36) dB, Then “Bareland with peat”.

(v) Rule 5 for separating peat depth classes in the class pair 5.
If (wFBD_HH) ≤ (−7.86) dB and (HV/HH) ≥ (1.70) dB, Then “Vegetation with peat”.

These classification rules were then applied to the DT algorithm to obtain classification results of data combination (iii).

4.3.2.4 Data combination (iv)

For the combination of dual-polarization data, fully polarimetric data, and the additional feature "distance to river," the selected polarimetric features were identical to those selected in the combination of dual-polarization and fully polarimetric data for all class pairs. The feature "distance to river" was added in separating class pairs 4 and 5. In this study, however, only the category "less than 2 km from river" of the feature "distance to river" was applied to the algorithm of the DT classification. The integration of the additional feature "distance to river" was meant to evaluate the effectiveness of GIS data integration in the SAR-based tropical peatlands classification. Therefore, in this study, the feature "distance to river" was hypothesized to produce better classification results along with the use of dual-polarization and fully polarimetric data in tropical peatlands classification.

Thus, a total of five classification rules, separating five class pairs, were generated using training points based on the selected polarimetric features for tropical peatlands classification by means of data combination (iv). The classification rules were developed using mean and standard deviation values of land use/cover classes for each selected polarimetric feature. These rules are listed as follows:

(i) Rule 1 for separating classes in the class pair 1.
If (y_volume) ≤ (−8.03) dB and (f_volume) ≤ (−7.57) dB, Then Class pair 2.

(ii) Rule 2 for separating peat depth classes in the class pair 2.
If (SPAN) ≤ (−12.39) dB and (y_odd) ≤ (−16.23) dB, Then "Water".

(iii) Rule 3 for separating peat depth classes in the class pair 3.
If (RVI) ≤ (0.73) dB, Then Class pair 4.

(iv) Rule 4 for separating peat depth classes in the class pair 4.
If (HH+VV) ≤ (−12.03) dB and (PLR_HH) ≤ (−5.00) dB and (PLR_VV) ≤ (−6.84) dB and (f_volume) ≤ (−4.70) dB and (wFBD_HH) ≤ (−7.47) dB and (dFBD_HV) ≤ (−13.36) dB and ("distance to river") ≥ ("less than 2 km"), Then "Bareland with peat".

(v) Rule 5 for separating peat depth classes in the class pair 5.
If (wFBD_HH) ≤ (−7.86) dB and (HV/HH) ≥ (1.70) dB and ("distance to

river") ≥ ("less than 2 km"), Then "Vegetation with peat".

These classification rules were then applied to the DT algorithm to obtain classification results of data combination (iv).

4.3.3 Results of the image classification

As presented in **Figure 4.4**, the results of tropical peatlands classification from four combinations of data were generated by means of the DT classifier. The classification results showed six land use/cover classes, i.e., water, artificial, bareland with peat, bareland without peat, vegetation with peat, and vegetation without peat. The "bareland with peat" and "vegetation with peat" classes represented land use/cover classes identified with the existence of tropical peatlands, whereby the "bareland without peat" and "vegetation without peat" classes represented land use/cover classes identified as having no tropical peatlands. The classification results of data combinations (i), (ii), (iii), and (iv) had 53.6%, 40.4%, 50.9%, and 32.3% of the total area identified as having tropical peatlands, respectively. The results of tropical peatlands classification derived by the dual-polarization data generated the biggest area identified as having tropical peatlands, whereas those derived by the combination of dual-polarization data, fully polarimetric data, and the additional feature "distance to river" produced the smallest area identified as having tropical peatlands. Thus, in this study, the dual-polarization data tended to generate more tropical peatlands area, whereas the fully polarimetric data tended to generate less tropical peatlands area. In addition, the feature "distance to river" was added to the algorithm of DT classification to ignore the existence of tropical peatlands in less than 2 km from the river stream, so that it influenced the classification results of data combination (iv) producing the smallest area of tropical peatlands.

4.3.4 Accuracies of the image classification

Table 4.5 shows the accuracy indicators of tropical peatlands classification results from four combinations of data by means of the DT classifier. Accuracy indicators were low for the classification results derived by the dual-polarization data, which also yielded the lowest OA and K of 55.0% and 0.39, respectively. In contrast, the accuracy indicators for the classification results generated by the fully polarimetric data produced better accuracy indicators than those produced by the dual-polarization data; the fully polarimetric data gave accuracies of 65.0% and 0.51 for OA and K, respectively.

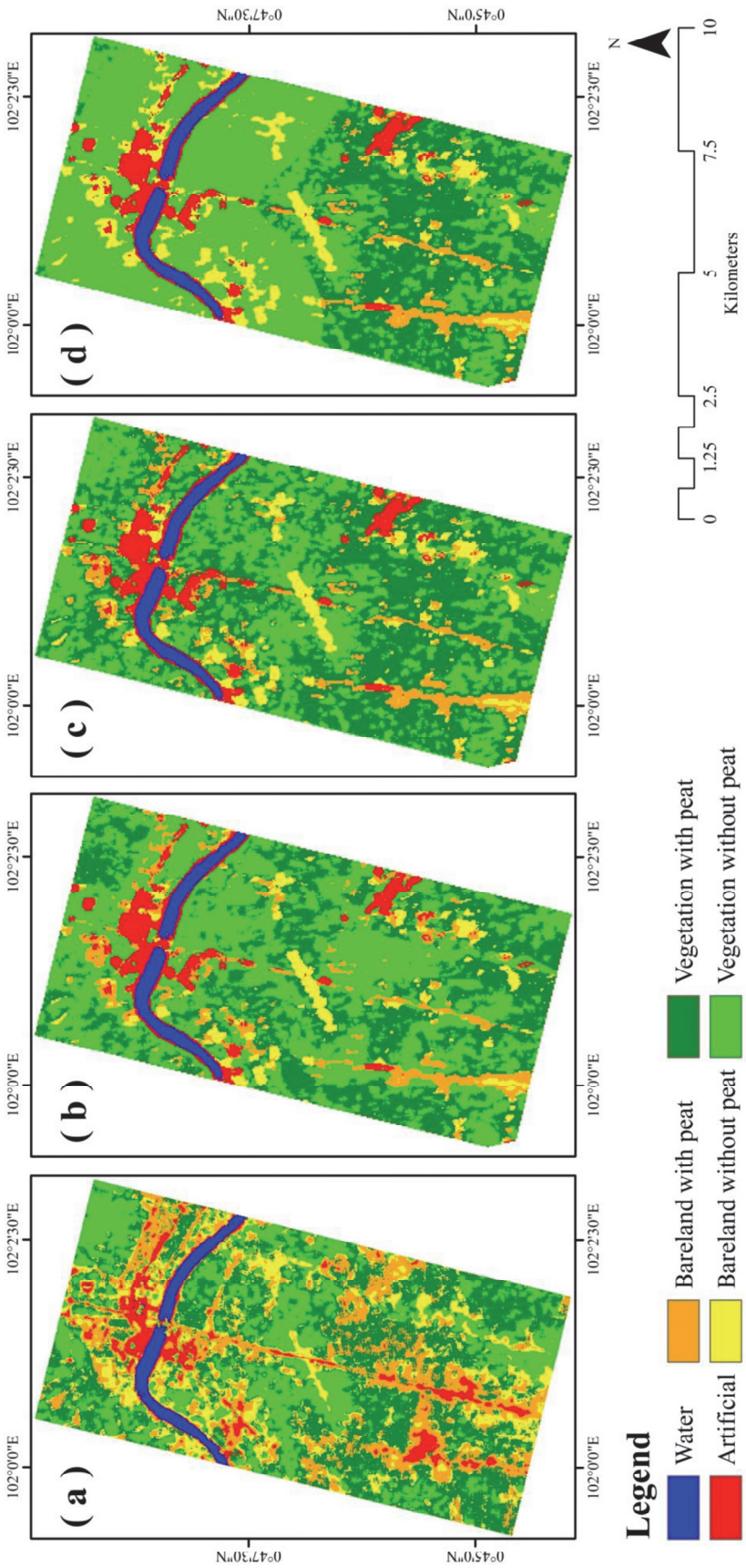

Figure 4.4 Result of tropical peatlands classification for each combination of data: (a) data combination i, (b) data combination ii, (c) data combination iii, and (d) data combination iv.

Table 4.5 Accuracy indicators for tropical peatlands classification for each combination of data.

Class name	Combinations of data							
	i		ii		iii		iv	
	PA (%)	UA (%)	PA (%)	UA (%)	PA (%)	UA (%)	PA (%)	UA (%)
Water	100.0	100.0	100.0	100.0	100.0	100.0	100.0	100.0
Artificial	44.4	55.2	66.7	85.7	66.7	85.7	66.7	85.7
Bareland with peat	46.4	41.6	75.4	64.2	71.0	71.0	66.7	93.9
Bareland without peat	52.6	36.0	62.8	77.8	71.8	74.7	93.6	76.8
Vegetation with peat	56.7	52.5	57.1	60.1	57.1	64.3	52.9	83.0
Vegetation without peat	53.3	67.3	66.3	61.1	75.6	66.2	92.6	67.9
OA (%)	55.0		65.0		69.0		76.0	
Kappa coefficient	0.39		0.51		0.57		0.66	

Significant increases in OA and K were obtained by the classification results derived by the combination of dual-polarization and fully polarimetric data; this combination yielded an OA of 69.0% and a K of 0.57. Thus, accuracy indicators were increased by applying the combination of dual-polarization and fully polarimetric data to the algorithm of DT classification for the SAR-based tropical peatlands classification. This combination showed that the complementarity of dual-polarization and fully polarimetric data produced higher accuracy than the single usage of each type of data for the purpose of tropical peatlands classification by means of the DT classifier. In addition, the best accuracy was obtained by means of integrating the feature "distance to river" into the algorithm of DT classification. The accuracy indicators derived by the combination of dual-polarization data, fully polarimetric data, and the additional feature "distance to river" yielded the best OA and K of 76.0% and 0.66, respectively.

The integration of GIS data in the SAR-based tropical peatlands classification was found to be effective in improving the classification accuracy, whereas the feature "distance to river" ignored the existence of tropical peatlands in less than 2 km calculated from the main river stream. The feature "distance to river" successfully aided the polarimetric features derived by dual-polarization and fully polarimetric data in classifying tropical peatlands and increased the accuracy indicators of the classification results. The category "less than 2 km from river" of the feature "distance to river" was revealed to represent the actual distance of tropical peatlands to exist as measured from the main river stream. Thus, the feature "distance to river" increased the classification accuracy when integrated with the polarimetric features derived by the combination of

dual-polarization and fully polarimetric data by means of the DT classifier. The accuracy indicators derived by the combination of dual-polarization data, fully polarimetric data, and the additional feature “distance to river” were increased by nearly 10% for OA and 15% for K over the best obtained OA and K derived by the SAR-based tropical peatlands classification using the DT classifier.

4.4 Conclusion

This study evaluated the performances of L-band ALOS PALSAR dual-polarization and fully polarimetric data for tropical peatlands classification in response to the scheme of the sustainable management of tropical peatlands, especially in the activity of mapping spatial distributions of tropical peatlands in Indonesia. There were several findings regarding the development of tropical peatlands classification using L-band SAR dual-polarization and fully polarimetric data. First, tropical peatlands is a complex ecosystem to be mapped, especially from the viewpoint of L-band SAR dual-polarization and fully polarimetric data, as they generated highly overlapping means and standard deviations values with no tropical peatlands areas. Thus, in this study, a strict algorithm was successfully applied by means of the DT classifier to classify tropical peatlands involving the use of L-band ALOS PALSAR dual-polarization and fully polarimetric data. Second, the seasonal variation of tropical peatlands was found, in which the existence of tropical peatlands in a land use/cover without the presence of vegetation was not influenced by the seasonal condition. In contrast, the existence of tropical peatlands in a land use/cover with the presence of vegetation (or below a vegetation cover) was influenced by the seasonal condition. Third, the classification results of the dual-polarization data were inferior to the fully polarimetric data, indicating that the fully polarimetric data were more suitable for classifying tropical peatlands. Fourth, the integration of GIS data in the SAR-based tropical peatlands classification was found to be effective in improving the classification accuracy, whereby in this study, the feature “distance to river” increased the classification accuracy when integrated with the polarimetric features derived by the combination of dual-polarization and fully polarimetric data by means of the DT classifier. The results and findings presented in this study could aid in improving the state of knowledge in tropical peatlands classification, especially when involving the use of L-band SAR dual-polarization and fully polarimetric data.

Chapter 5

C-band Dual-polarization Synthetic Aperture Radar Application for Peat Depth Classification: A Case Study in Siak Regency, Riau Province, Indonesia

5.1 Introduction

The importance of tropical peatlands as a long-term carbon sinks and stores, as well as their tendency to become a short-term source of carbon emissions, has been receiving tremendous interest during the past two decades (Osaki et al. 2016; Miettinen et al. 2017). Thus, there is an urgent need to quantify the current carbon status of tropical peatlands to understand their role in relation to the global carbon cycle (Hirano et al. 2016). It is also important to obtain information about peat depth distribution to be able to accurately estimate carbon stock within tropical peatlands, further aiding in understanding the role of tropical peatlands in global environmental change processes (Shimada et al. 2016a). In general, the distribution of peat depth can be obtained by doing manual sampling using a peat auger, an example of in situ measurements (Agus et al. 2011). Nevertheless, this method presents a considerable challenge because conducting extensive in situ measurements at regional, national and global scales is not realistic (Jaenicke et al. 2008). Knowledge of peat depth can sometimes be correlated with properties that are discernible by using a Remote Sensing (RS) application (Lawson et al. 2015). However, little is known regarding the performance of RS applications for classifying peat depth distributions, especially in the tropics.

RS applications can serve as advantageous tools for tropical peatlands monitoring activities, such as peat depth classification, due to periodic monitoring at various spatial and temporal scales, particularly when combined with field measurement data (Shimada et al. 2016a). Furthermore, the recent development of synthetic aperture radar (SAR)-based RS satellites has introduced a new prospect that allows continuous monitoring and cloud-free observations in humid tropical regions (Kuntz 2010). Recently, the use of SAR-based RS applications for peatlands monitoring activities has been increasing rapidly, along with the growing availability of SAR data sets. A previous study evaluated the potential of X-band SAR dual-polarization data and fusion

images with optical data to characterize different peat depths categories in Central Kalimantan, Indonesia (Wijaya et al. 2010). Another report demonstrated the use of L-band Advanced Land Observing Satellite (ALOS) Phased Array type L-band SAR (PALSAR) for wide-area mapping of tropical forest and land cover, including several categories for tropical peatlands on Borneo Island (Hoekman et al. 2010). Other reports have evaluated the performance of L-band ALOS PALSAR for peatlands detection and delineation in the boreal regions (Antropov et al. 2012; Antropov et al. 2014). A previous report also applied the L-band ALOS PALSAR to examine a radar scattering mechanism on tropical peatlands in Central Kalimantan, Indonesia (Watanabe et al. 2011). Another study examined the combination of L-band ALOS PALSAR data, optical data and digital elevation model (DEM)-derived data for mapping the extent of tropical peatlands in Cuvette Centrale, Congo Basin (Dargie et al. 2017). Despite all the previous research, detailed information is lacking on the potential C-band SAR dual-polarization data have for classifying peat depth distribution within the tropical peatlands.

The C-band Sentinel-1 data provided by the European Space Agency (ESA) are of interest because they are freely available and have global coverage. The Sentinel-1 mission encompasses a constellation of two polar-orbiting satellites (Sentinel-1A and Sentinel-1B). This data collection method operates at a center frequency of 5.405 GHz and includes two polarization channels — vertical transmit-horizontal receive (VH) and vertical transmit-vertical receive (VV) — with a very short repeat cycle (12 days with one satellite and 6 days with two) and rapid product delivery. These characteristics make C-band Sentinel-1 data particularly promising for use in tropical peatlands monitoring activity, particularly for classifying peat depth distributions. Therefore, in this study, the potential of C-band Sentinel-1 data was evaluated for peat depth classification on oil palm plantations in Siak Regency, Riau Province, Indonesia. Particularly, features derived after the ground-range radar cross section (sigma-naught or σ^0) and slant-range perpendicular radar cross section (gamma-naught or γ^0) for both polarization channels of C-band Sentinel-1 data were compared and evaluated, monthly during 2015, for discriminating peat depth classes using the Decision Tree (DT) classifier. In addition, the seasonal variation of peat depth classes, from the viewpoint of C-band SAR dual-polarization data, was analyzed for better understanding of the relationship between peat depth classification and seasonal effects. The results and

findings of this study could aid in increasing the foundation of knowledge regarding peat depth classification, involving the use of C-band SAR dual-polarization data, to improve the sustainable management of tropical peatlands.

5.2 Materials

5.2.1 Study area

In Indonesia, there are 14.91 million ha of tropical peatlands that distributed along the low altitudes in the coastal and sub-coastal areas of Sumatra (6.44 million ha, 43%), Kalimantan (4.78 million ha, 32%) and Papua (3.69 million ha, 25%) (Ritung et al. 2012). Riau Province in Sumatra dominates the provincial level of tropical peatlands distribution, consisting of around 3.86 million ha (26%). This study considers the area of Siak Regency, a rapidly developing region in the central part of Riau Province, where the tropical peatlands have been intensively converted into mostly oil palm and timber plantations over the last two decades (Sabiham and Kartawisastra 2012; Irawan and Tacconi 2016).

In general, this area has a flat topography and low altitude ranging from 2 to 10 m above sea level. The average temperature of this area is around 26.2^{o}C per year, with an annual rainfall that varies from 2,200 to 2,600 mm per year. However, in 2015, this area was affected by a very strong El Niño, leading to rainfall anomalies and a more severe dry season (Englhart et al. 2016).

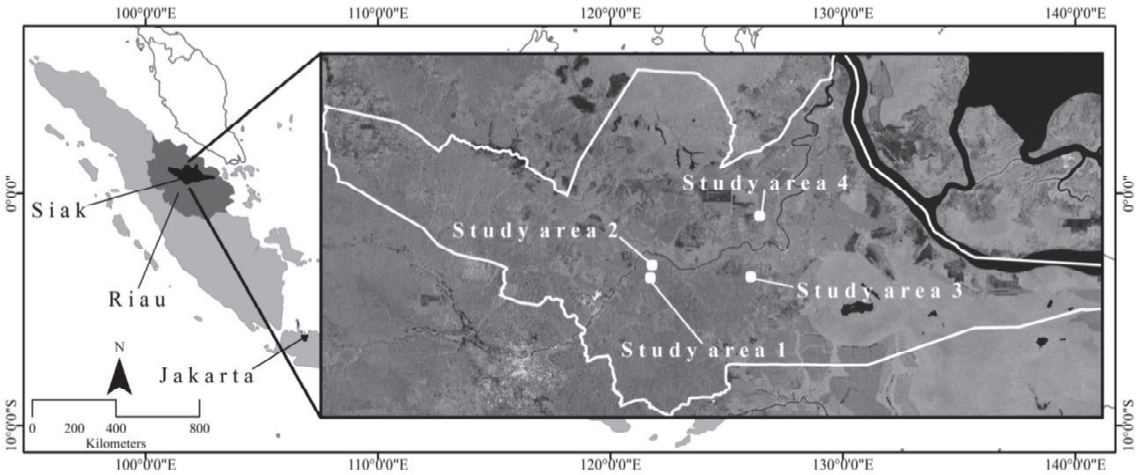

Figure 5.1 Map of Indonesia showing the location of the study areas in Siak regency, Riau Province, Indonesia.

Four study areas, 1 × 1 km in size, were selected to represent the condition of tropical peatlands in Siak Regency, Riau Province, Indonesia (**Figure 5.1**). These study areas are situated in large-scale oil palm plantations with similar types of growing stages. Furthermore, to represent peat depth categories, each study area is located on distinct types of peat depth classes as categorized by the Indonesian Agency for Agricultural Research and Development (IAARD) (Ritung et al. 2012). Thus, study area 1 is situated in a shallow-peat class (0.5 to 1 m of peat depth), study area 2 is situated in a medium-peat class (1 to 2 m of peat depth), study area 3 is situated in a deep-peat class (2 to 4 m of peat depth), and study area 4 is situated in a very deep-peat class (more than 4 m of peat depth).

5.2.2 Data

In this study, there were 12 scenes of C-band Sentinel-1 data, acquired between January and December 2015, served as 12-months observations. Thus, each scene, with a specific acquisition date, was used to represent a monthly observation to provide monthly analyses. These scenes were used as the primary data. The C-band Sentinel-1 data were collected using the settings of level-1 Ground Range Detected (GRD) and the acquisition mode of Interferometric Wide (IW) swath (Dimov et al. 2016). Moreover, Tropical Rainfall Measuring Mission (TRMM) 3B43 version 7 data were used to calculate the amount of monthly rainfall in the study areas (Huffman et al. 2010). Landsat 8 Operational Land Imager (OLI) data and high-resolution satellite images on Google Earth were used to obtain basic information of the study areas by means of visual interpretation and to select training and testing points for DT classification.

Thus, a total of 600 points (150 points for each study area) were derived for training the algorithm (400 points) and testing the accuracy of the classification results (200 points) (**Figure 5.2**). Each point was located within a 100 × 100 m mesh, with manual adjustments made to avoid points situated on plantation roads. These points represented the detected pixels in the C-band SAR dual-polarization imagery. In addition, an existing peat depth and distribution map, provided by the IAARD, was used as reference map. The list of data used for analyses is shown in **Table 5.1**.

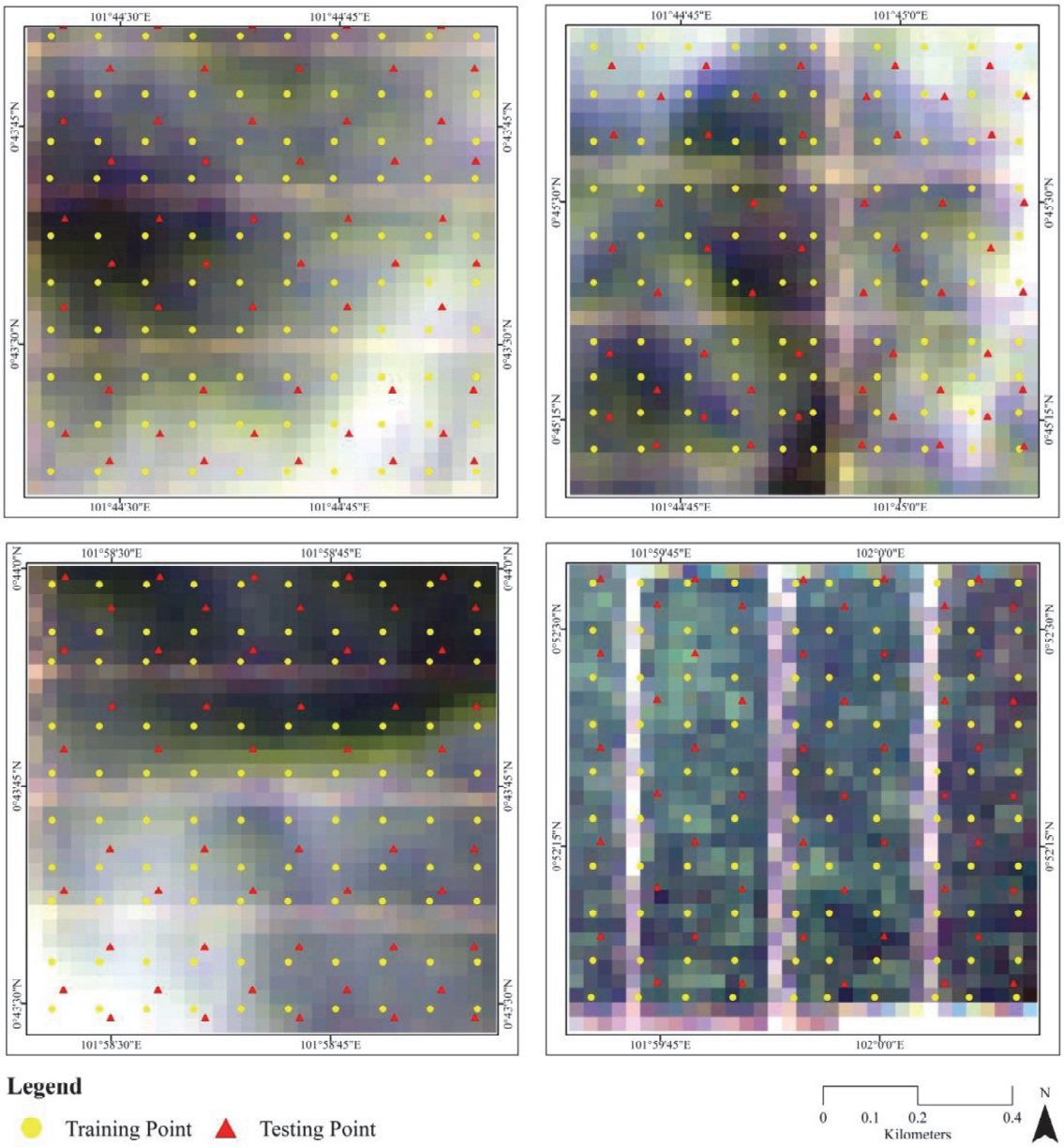

Figure 5.2 Landsat 8 OLI imageries of the study area 1 (upper left), study area 2 (upper right), study area 3 (lower left), and study area 4 (lower right), showing the spatial distribution of training and testing points.

5.3 Methodology

5.3.1 Image processing steps

The C-band Sentinel-1 data were imported into the European Space Agency (ESA) Sentinel Application Platform (SNAP) software for image processing (Luis et al. 2017). First, the data were radiometrically calibrated and converted from digital pixel values to radiometrically-calibrated backscatter by means of a calibration vector provided in the

Table 5.1 List of data used for analyses carried out in this study.

Data usage	Source	Acquisition date
Primary data	C-band Sentinel-1 data (Sentinel-1A satellite, dual-polarization)	Jan. 3, 2015 Feb. 19, 2015 Mar. 4, 2015 Apr. 21, 2015 May 15, 2015 Jun. 8, 2015 Jul. 26, 2015 Aug. 18, 2015 Sep. 11, 2015 Oct. 6, 2015 Nov. 11, 2015 Dec. 29, 2015
Secondary data	TRMM 3B43 version 7 (Monthly 0.25 x 0.25 degree, mm/hour of rainfall rate)	Monthly data between January to December 2015
	Landsat 8 OLI	Jul. 10, 2015 Jul. 26, 2015 Aug. 2, 2015
	High-resolution satellite images accessed on Google Earth	Jul. 25, 2014 Jul. 5, 2015 Aug. 26, 2016

data product. In this study, the C-band Sentinel-1 data were converted to ground-range radar cross section (sigma-naught or σ^0) and slant-range perpendicular radar cross section (gamma-naught or γ^0) values, in decibel units (dB), for both channels of polarization prior to data analyses. Both σ^0 and γ^0 are measures used to express radar backscatter coefficients. However, σ^0 is defined as the radar cross section per unit area in the ground-range, whereas γ^0 is defined as radar cross section per unit area of the incident wavefront (perpendicular to the slant-range), to minimize the incidence angle dependency of the radar backscatter for a distributed target (Shimada 2010; El-Darymli et al. 2014). Furthermore, the data were terrain corrected using Shuttle Radar Topography Mission (SRTM) DEM 3 arc-seconds (Farr et al. 2007) and geocoded to the Universal Transverse Mercator (UTM) zone 48 North map projection with pixel spacing of 10×10 m. Speckle noise was reduced by applying a 7×7 window size Lee filter (Lee and Pottier 2009). In addition, to provide rainfall information for the study areas, the precipitation layers of TRMM 3B43 version 7 data acquired between January and December 2015 were extracted. Rainfall rate conversions from mm/hour to mm/month were calculated. The data were then subset into the boundaries of the study areas so that monthly rainfall information could be generated for the analyses carried out in this study. The methodological flow chart of the present study is provided in **Appendix 8**.

5.3.2 Feature description

In this study, the σ^0 and γ^0 images, for both polarization channels, derived using the C-band Sentinel-1 data, were considered as features. To allow for monthly analysis, each σ^0 or γ^0 image for a particular polarization channel on a specific acquisition date was considered as one feature (e.g., a σ^0 image for the VH polarization channel acquired on January 3, 2015 was considered as one feature and coded as sVH01; a γ^0 image for the VV polarization channel acquired on November 11, 2015 was considered as one feature and coded as gVV11). Thus, a total of 48 features were derived, using the C-band Sentinel-1 data, for the analyses carried out in this study. The list of features used for analyses is shown in **Table 5.2**.

Table 5.2 List of features used for analyses, derived using sigma naught (σ^0) and gamma naught (γ^0) images, for both polarization channels.

Polarization channel	Acquisition date	Sigma-naught code name	Gamma-naught code name
VH	Jan. 3, 2015	sVH01	gVH01
	Feb. 19, 2015	sVH02	gVH02
	Mar. 4, 2015	sVH03	gVH03
	Apr. 21, 2015	sVH04	gVH04
	May 15, 2015	sVH05	gVH05
	Jun. 8, 2015	sVH06	gVH06
	Jul. 26, 2015	sVH07	gVH07
	Aug. 18, 2015	sVH08	gVH08
	Sep. 11, 2015	sVH09	gVH09
	Oct. 6, 2015	sVH10	gVH10
	Nov. 11, 2015	sVH11	gVH11
	Dec. 29, 2015	sVH12	gVH12
VV	Jan. 3, 2015	sVV01	gVV01
	Feb. 19, 2015	sVV02	gVV02
	Mar. 4, 2015	sVV03	gVV03
	Apr. 21, 2015	sVV04	gVV04
	May 15, 2015	sVV05	gVV05
	Jun. 8, 2015	sVV06	gVV06
	Jul. 26, 2015	sVV07	gVV07
	Aug. 18, 2015	sVV08	gVV08
	Sep. 11, 2015	sVV09	gVV09
	Oct. 6, 2015	sVV10	gVV10
	Nov. 11, 2015	sVV11	gVV11
	Dec. 29, 2015	sVV12	gVV12

5.3.3 Decision tree (DT) classification

To classify the peat depth classes using C-band Sentinel-1 data, DT classifier was used due to its ability to handle complex relations among class properties, its computational efficiency and its conceptual simplicity (Friedl and Bradley 1997). DT is a classification procedure that recursively separates a set of data into smaller subcategories based on a set of rules determined at each branch in the tree. DT classifier requires no assumptions regarding the distributions of input data, making it suitable for classifying SAR data (Simard et al. 2000). Furthermore, DT algorithm diagrams are explicit and easy to understand, particularly when evaluating feature contributions and relations in a classification procedure (Simard et al. 2002).

5.3.4 Distance factor (DF) extraction

In this study, the Distance Factor (DF) was generated to assess the effectiveness of a feature for separating classes, particularly on DT classification. The DF measures the distance between the different class mean values compared to the standard deviations. Thus, if a DF is large, classes are said to be well-separated, according to the concept of feature separation (Cumming and Van Zyl 1989). The equation of the DF is defined in **Eq. 4.1**. The performance of the separation between classes *i* and *j* is represented by the value DF*ij*. A higher DF*ij* means that a feature has better performance separating the associate class pairs (Chen et al. 2007). Thus, in this study, features that yielded the highest DF value on each class pair for each polarization channel were analyzed and applied to the DT algorithm.

In the present study, to apply the concept of feature separation on the DT algorithm, three combinations of class pairs were specified (i.e., (A) “shallow-peat” plus “medium-peat” and “deep peat” plus “very-deep peat”, (B) “shallow-peat” and “medium-peat,” and (C) “deep-peat” and “very-deep peat.” The class pairs were then applied to the DT algorithm to identify each peat depth class. In addition, the selected features for each class pair were analyzed to understand the effect seasonal variation has upon peat depth classifications. Hence, the monthly rainfall information, derived from the TRMM 3B43 version 7 data, was used for seasonal analysis purposes.

5.3.5 Accuracy assessment

An accuracy assessment was performed for the classification results using a

confusion matrix generated by testing points (Congalton 1991). Thus, accuracy indicators were derived to evaluate the quality of classification results (i.e., Producer's Accuracy (PA), User's Accuracy (UA), Overall Accuracy (OA) and the Kappa coefficient (K)). The PA and UA represent the measures of omission and commission error for each class, respectively. The OA was computed by creating a ratio of the total number of correct pixels to the total number of pixels in the confusion matrix, which correspond to the correctly classified areas of the classified image. Last, the K describes the degree of matching between the reference data set and the classification.

5.4 Results and discussion

5.4.1 Comparison of sigma-naught and gamma naught features

Table 5.3 shows the DF values for class pair (A), derived using σ^0 and γ^0 features, for both polarization channels. The values in bold indicate the highest DF values in each category. Generally, the DF values of class pair (A) were varied, depending on the feature used to derive them. The sVH06 (σ^0_{VH} in June) and sVV06 (σ^0_{VV} in June) features yielded the highest DF values for those derived using σ^0_{VH} and σ^0_{VV} features, respectively. On the other hand, the gVH06 (γ^0_{VH} in June) and gVV06 (γ^0_{VV} in June) features produced the highest DF values for those derived using γ^0_{VH} and γ^0_{VV} features, respectively.

Thus, by comparing the highest DF values of class pair (A), derived using σ^0 and γ^0 features, for both polarization channels, it was found that γ^0 features yielded much higher DF values for class pair (A), for both polarization channels, than those produced by σ^0 features. By applying γ^0 features, the highest DF values of class pair (A) increased as much as 11.5% and 13.3% for VH and VV polarizations, respectively. Hence, in this study, γ^0 features were used for developing a methodology for classifying peat depth due to the features having better performance in discriminating peat depth classes.

5.4.2 Selected features for the classification

Table 5.4 shows the DF values for all class pairs, derived by γ^0 features, for both polarization channels. The values in bold indicate the highest DF values in each category. The highest values were selected to be analyzed and applied to the DT

Table 5.3 The distance factor (DF) values for class pair (A), derived using sigma naught (σ^0) and gamma naught (γ^0) features, for both polarization channels.

Feature		Class pair (A)	
Polarization channel	**Acquisition date**	**Sigma naught**	**Gamma naught**
VH	Jan. 3, 2015	0.18	0.12
	Feb. 19, 2015	0.51	0.44
	Mar. 4, 2015	0.44	0.50
	Apr. 21, 2015	0.05	0.01
	May 15, 2015	0.10	0.04
	Jun. 8, 2015	**0.52**	**0.58**
	Jul. 26, 2015	0.41	0.35
	Aug. 18, 2015	0.15	0.08
	Sep. 11, 2015	0.22	0.15
	Oct. 6, 2015	0.11	0.17
	Nov. 11, 2015	0.06	0.13
	Dec. 29, 2015	0.04	0.09
VV	Jan. 3, 2015	0.06	0.12
	Feb. 19, 2015	0.40	0.33
	Mar. 4, 2015	0.41	0.46
	Apr. 21, 2015	0.19	0.25
	May 15, 2015	0.03	0.02
	Jun. 8, 2015	**0.45**	**0.51**
	Jul. 26, 2015	0.04	0.11
	Aug. 18, 2015	0.31	0.24
	Sep. 11, 2015	0.32	0.25
	Oct. 6, 2015	0.32	0.37
	Nov. 11, 2015	0.09	0.15
	Dec. 29, 2015	0.00	0.07

algorithm. In general, the DF values for all class pairs varied, depending on the features used to derive them. For class pair (A), as mentioned before, the gVH06 (γ^0_{VH} in June) and gVV06 (γ^0_{VV} in June) features yielded the highest DF values for VH and VV polarization, respectively. On the other hand, for class pair (B), the gVH03 (γ^0_{VH} in March) and gVV04 (γ^0_{VV} in April) features produced the highest DF values for VH and VV polarization, respectively. Furthermore, for class pair (C), the gVH06 (γ^0_{VH} in June) and gVV09 (γ^0_{VV} in September) features generated the highest DF values for VH and VV polarization, respectively. These features were selected and applied to the DT algorithm for classifying peat depth classes.

In addition, by examining the highest DF values for all class pairs, derived by γ^0 features, for both polarization channels, it was found that γ^0_{VH} features produced much higher DF values than those generated by γ^0_{VV} features, indicating that the γ^0_{VH} features yielded a better performance in discriminating peat depth classes. However,

Table 5.4 The distance factor (DF) values for all class pairs, derived using gamma-naught (γ^0) features, for both polarization channels.

Feature		Class pair		
Polarization channel	**Code name**	**(A)**	**(B)**	**(C)**
VH	gVH01	0.12	0.23	0.18
	gVH02	0.44	0.22	0.31
	gVH03	0.50	**0.75**	0.08
	gVH04	0.01	0.28	0.59
	gVH05	0.04	0.60	0.15
	gVH06	**0.58**	0.05	**0.60**
	gVH07	0.35	0.34	0.43
	gVH08	0.08	0.48	0.20
	gVH09	0.15	0.40	0.18
	gVH10	0.17	0.27	0.07
	gVH11	0.13	0.07	0.41
	gVH12	0.09	0.13	0.57
VV	gVV01	0.12	0.34	0.28
	gVV02	0.33	0.48	0.44
	gVV03	0.46	0.62	0.55
	gVV04	0.25	**0.71**	0.04
	gVV05	0.02	0.65	0.42
	gVV06	**0.51**	0.38	0.05
	gVV07	0.11	0.38	0.29
	gVV08	0.24	0.50	0.51
	gVV09	0.25	0.48	**0.56**
	gVV10	0.37	0.30	0.48
	gVV11	0.15	0.36	0.12
	gVV12	0.07	0.28	0.07

in this study, all γ^0 features that obtained the highest DF values for both polarization channels were applied to the DT algorithm. Moreover, among all the class pairs, class pair (B) yielded the highest DF values for both polarization channels, indicating that the mean and standard deviation values of the shallow- and medium-peat classes represented in class pair (B) overlapped less, obtaining a higher DF values than those derived in the other class pairs.

5.4.3 Seasonal variation of the selected features

To understand the effect of seasonal variation on the selected features for peat depth classification, monthly rainfall information derived from the TRMM 3B43 version 7 data was used for seasonal analysis purposes. In 2015, a year with a very strong El Niño, the annual rainfall was as low as 1,992 mm, with an average monthly rainfall of 166 mm. For the seasonal analyses carried out in this study, months with below average monthly rainfall were said to be “less rain” months, whereas those with above average

rainfall were said to be “much rain” months. Hence, the less rain months are January (149 mm/month), February (141 mm/month), May (146 mm/month), June (119 mm/month), July (46mm/month), September (52mm/month), and October (78mm/month), whereas the much rain months are March (269 mm/month), August (222 mm/month), November (330 mm/month), and December (254 mm/month).

For class pair (A) (derived by both σ^0 and γ^0), features acquired in June yielded the highest DF value for both polarization channels. Thus, for the initial separation of peat depth classes represented in class pair (A), features derived in the less rain months were prominent. In contrast, for class pair (B), features acquired in March and April produced the highest DF value for VH and VV polarization, respectively. Hence, for more detailed separation of peat depth classes, (i.e., separating the shallow- and medium-peat classes) features derived in the much rain months were suitable. On the other hand, for class pair (C), features acquired in June and September generated the highest DF value for VH and VV polarization, respectively. Therefore, features derived in the less rain months were suitable for separating the deep- and very deep-peat classes. In this study, it was discovered that seasonal variation influenced feature selection for peat depth classification, particularly when analyzing C-band SAR dual-polarization data.

5.4.4 Results of the classification

The selected features for peat depth classification were the gVH06 (γ^0_{VV} in June) and gVV06 (γ^0_{VV} in June), for separating classes in the class pair (A). Subsequently, the gVH03 (γ^0_{VH} in March) and gVV04 (γ^0_{VV} in April) were selected for discriminating peat depth classes in the class pair (B). Afterwards, the gVH06 (γ^0_{VH} in June) and gVV09 (γ^0_{VV} in September) were selected for separating peat depth classes in the class pair (C). Thus, a total of three classification rules, separating three class pairs, were generated using training points based on the selected features for peat depth classification. The classification rules were developed using mean and standard deviation values of peat depth classes for each selected feature. These rules are listed as follows:

(i) Rule 1 for separating classes in the class pair (A).
If gVH06 (γ^0_{VH} in June) ≥ (−13.20) dB and gVV06 (γ^0_{VV} in June) ≥ (−4.97) dB,
Then Class pair (B).

(ii) Rule 2 for separating peat depth classes in the class pair (B).
If gVH03 (γ^0_{VH} in March) ≥ (−13.55) dB and gVV04 (γ^0_{VV} in April) ≥ (−5.31)

dB, Then Shallow peat.

(iii) Rule 3 for separating peat depth classes in the class pair (C).
If gVH06 (γ^0_{VH} in June) ≥ (−12.71) dB and gVV09 (γ^0_{VV} in September) ≤ (−4.88) dB, Then Deep peat.

These classification rules were then applied to the DT algorithm to obtain classification results. The classification rules and DT algorithm diagram developed in this study are shown in **Figure 5.3**. Afterwards, as shown in **Figure 5.4**, results of the peat depth classification of all study areas were successfully generated by means of DT classification. These results presented four peat depth classes (i.e., shallow peat (0.5 to 1 m of peat depth), medium peat (1 to 2 m of peat depth), deep peat (2 to 4 m of peat depth), and very-deep peat (more than 4 m of peat depth).

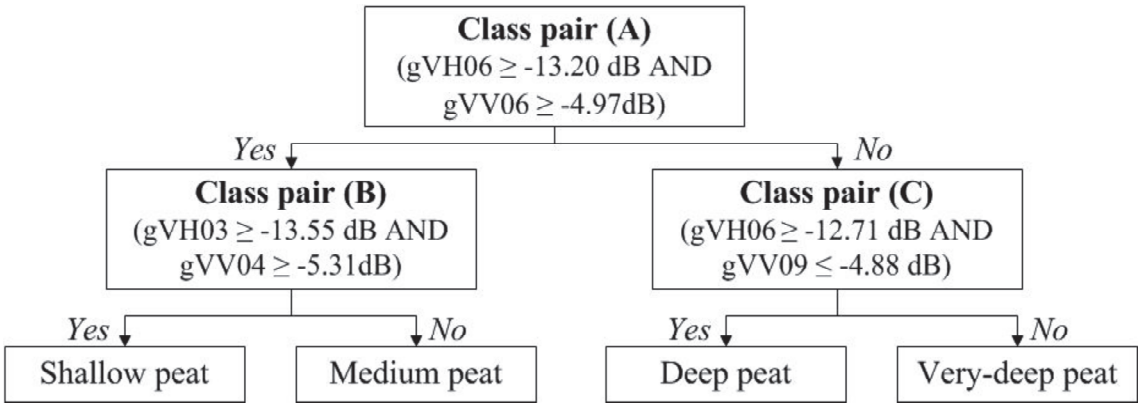

Figure 5.3 The classification rules and the decision tree (DT) algorithm diagram developed in this study.

In addition, **Table 5.5** shows the pixel percentage of each peat depth class calculated in each study area. Thus, by comparing the actual peat depth condition of each study area and the pixel percentage of peat depth classes computed on the associated study area, it was found that the developed methodology was always successful in matching the actual peat depth condition with the highest pixel percentage of peat depth classes produced. Hence, in study area 1, an area situated in shallow peat, the highest pixel percentage (56.37%) was yielded for the shallow-peat class. Subsequently, in study area 2, an area situated in medium peat, the highest pixel percentage (43.17%) was produced for the medium-peat class. Next, in study area 3, an area situated in deep peat, the highest pixel percentage (48.42%) was generated for the deep-peat class. Last, in study

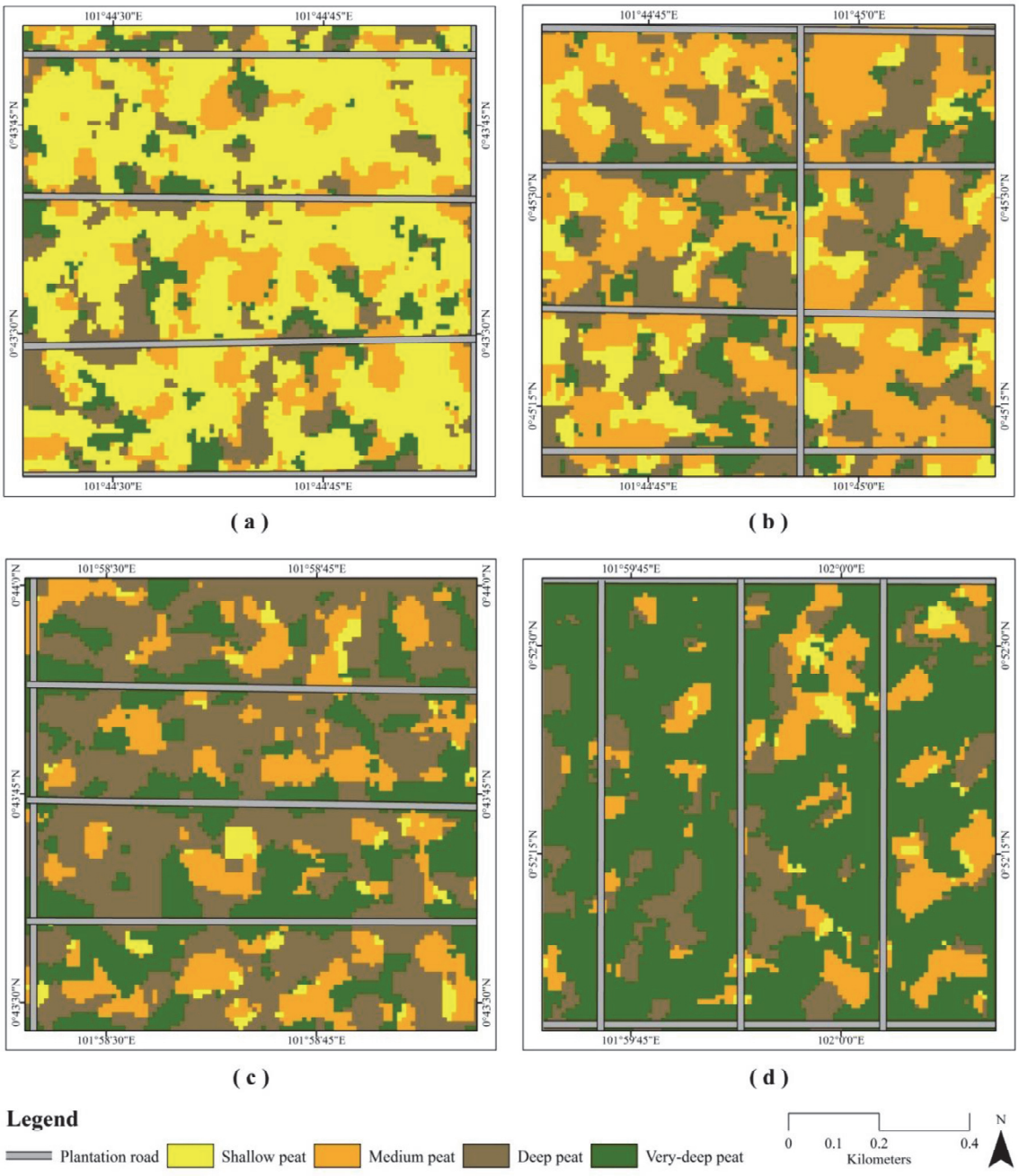

Figure 5.4 The result of the peat depth classification of (a) study area 1, (b) study area 2, (c) study area 3, and (d) study area 4.

area 4, an area situated in very deep peat, the highest pixel percentage (70.76%) was yielded for the very deep-peat class. Furthermore, the best performance of the developed methodology was found in very deep-peat areas, represented in study area 4, as the methodology generated much higher pixel percentages of peat depth classes that matched with actual peat depth conditions, compared to those derived in other study areas.

Table 5.5 The pixel percentage of each peat depth class calculated in each study area. The values in bold indicate the highest pixel percentage of peat depth classes produced on each study area.

Study area	Pixel percentage (%)			
	Shallow peat	Medium peat	Deep peat	Very-deep peat
1	**56.37**	18.45	14.81	10.37
2	11.74	**43.17**	31.81	13.28
3	2.82	18.42	**48.42**	30.34
4	1.84	13.44	13.96	**70.76**

5.4.5 Accuracies of the classification

Table 5.6 shows the confusion matrix and accuracy indicators for peat depth classifications by means of DT classification. The accuracy assessment was conducted by using the testing points situated in the study areas, evaluating the performance of the developed peat depth classifications method. Thus, the very deep-peat class obtained the best accuracy, with 76% and 67.86%, PA and UA, respectively, followed by the shallow-peat class that yielded a PA of 64% and UA of 80%. Subsequently, the deep-peat class produced a PA of 58% and UA of 59.18%, whereas the medium-peat class yielded the lowest PA and UA, of 54% and 49.09%, respectively. This result showed that the C-band SAR dual-polarization data have potential for classifying peat depth classes, particularly on oil palm plantations, due to its ability to produce the best accuracy for the very deep-peat class that is difficult to be distinguished among peat depth classes (Shimada et al. 2016a). In addition, the developed methodology gave accuracies of 63% and 0.51, for OA and K, respectively. This value of K was considered as a moderate agreement of a classification result (Viera and Garret 2005). Furthermore, the accuracy assessment result agreed with the analysis result for the pixel percentage of peat depth classes generated on each study area as presented in **Sub-subsection 5.4.4**, whereby the developed methodology consistently gave the best performance for the very deep-peat areas.

5.5 Conclusion

This study evaluated the potential of C-band Sentinel-1 data for peat depth classification on oil palm plantations, by using a SAR-based RS application, in response to the emerging tropical peatlands monitoring activities. Several findings were obtained

Table 5.6 The confusion matrix and accuracy indicators for peat depth classifications using the decision tree (DT) classification.

Class	Reference				Total	PA (%)	UA (%)
	Shallow peat	Medium peat	Deep peat	Very-deep peat			
Shallow peat	32	7	1	0	40	64.00	80.00
Medium peat	11	27	11	6	55	54.00	49.09
Deep peat	3	11	29	6	49	58.00	59.18
Very-deep peat	4	5	9	38	56	76.00	67.86
Total	50	50	50	50	200		
OA (%)	63.00						
Kappa coefficient	0.51						

relating to the development of peat depth classification using C-band SAR dual-polarization data. First, the present study showed that the γ^0 features yielded better performance in discriminating peat depth classes. By comparing the highest DF values of class pair (A), derived using σ^0 and γ^0 features, for both polarization channels, it was found that γ^0 features yielded much higher DF values for class pair (A), for both polarization channels, than those produced by σ^0 features. Thus, by applying γ^0 features, the DF values of class pair (A) increased as much as 11.5% and 13.3% for VH and VV polarizations, respectively. Second, it was discovered that seasonal variation was influencing feature selection for peat depth classification. Both γ^0_{VH} and γ^0_{VV}, in the much rain months, were selected for separating the shallow- and medium-peat classes in class pair (B), whereas both γ^0_{VH} and γ^0_{VV}, in the less rain months, were selected for discriminating the deep- and very deep-peat classes in class pair (C). Third, the developed methodology gave the best accuracy for the very deep-peat class, with 76% and 67.86%, producer's accuracy (PA) and user's accuracy (UA), respectively, followed by the shallow-peat class that yielded a PA of 64% and UA of 80%. Subsequently, the deep-peat class produced a PA of 58% and UA of 59.18%, whereas the medium-peat class yielded the lowest PA and UA, of 54% and 49.09%, respectively. Moreover, it was discovered that the developed methodology was always successful in matching the actual peat depth condition with the highest pixel percentage of peat depth classes

generated. Furthermore, accuracy assessment results agreed with the analysis results for the pixel percentage of peat depth classes produced in each study area, whereby the developed methodology was consistent in providing the best performance for very deep-peat areas. The results and findings in this study show that the C-band Sentinel-1 data are suitable for classifying peat depth classes, particularly on oil palm plantations, and might serve as an efficient tool in peat depth classification used for sustainable management of tropical peatlands.

Chapter 6

General Discussion and Recommendation

6.1 Discussion and conclusion

The present study has investigated the performances of SAR-based RS applications for tropical peatlands monitoring activity as an initial response to actualize the sustainable management principles and practices of tropical peatlands, particularly in Indonesia where the largest portion of the tropical peatlands is located. This study was addressed to provide a comprehensive understanding in connection with the utilization of potential SAR data (i.e., L-band ALOS PALSAR and C-band Sentinel-1 data) to improve the foundation of knowledge regarding tropical peatlands monitoring activity in Indonesia, especially for use in tropical peatlands identification and classification, as well as in peat depth classification. Thus, the primary objectives of the present study are listed as follows:

1. to explore the ability of L-band ALOS PALSAR fully polarimetric data for tropical peatlands identification,
2. to evaluate the performance of L-band ALOS PALSAR dual-polarization and fully polarimetric data for tropical peatlands classification, and
3. to investigate the potential of C-band Sentinel-1 data for peat depth classification,

in response to the emerging SAR-based RS applications for tropical peatlands monitoring activity.

To obtain the first primary objective, the first topic of this study (as discussed in Chapter 3) has been focused on two specific objectives. The first specific objective, associated with the first topic of this study, was *to explore the characteristic of tropical peatlands from the viewpoint of L-band ALOS PALSAR fully polarimetric data.* The present study showed that the surface and volume scattering were dominant for characterizing tropical peatlands, particularly those situated in Central Kalimantan, Indonesia. Hence, the presence of sparse to medium vegetation cover indicates that tropical peatlands generated both surface scattering and volume scattering as the dominant scattering mechanisms. Moreover, a relationship between the radar vegetation index (RVI) and tropical peatlands was discovered. These particular areas of tropical peatlands tend to have a specific value of the RVI, and the average RVI of tropical

peatlands is lower than that in other areas.

Afterwards, the second specific objective, associated with the first topic of this study, was *to develop methodology for tropical peatlands identification using L-band ALOS PALSAR fully polarimetric data.* In this study, a methodology has been developed to identify tropical peatlands using L-band ALOS PALSAR fully polarimetric data. Overall, the combination of classes derived from the unsupervised classification of polarimetric features of Freeman-Durden decomposition, integrated with the broad interval class of RVI that represents the amount of vegetation cover in the scattering mechanisms, successfully identified tropical peatlands. Subsequently, the tropical peatlands identified in the study area 1 yielded a producer's accuracy (PA) of 75.8% and a user's accuracy (UA) of 80.9%, whereas those in the study area 2 gave accuracies of 77.6% and 76.0% for PA and UA, respectively. In addition, tropical peatlands identification maps for both study areas were established using the developed methodology. These results indicate that L-band SAR fully polarimetric data is advantageous for monitoring tropical peatlands, particularly in humid tropical regions such as in Indonesia.

To obtain the second primary objective, the second topic of this study (as reported in Chapter 4) has been concentrated on two specific objectives. The first specific objective, associated with the second topic of this study, was *to develop methodology for tropical peatlands classification by means of four combinations of L-band ALOS PALSAR data: (i) the combination of two scenes of dual-polarization data, (ii) the single scene of fully polarimetric data, (iii) the combination of two scenes of dual-polarization data and the single scene of the fully polarimetric data, and (iv) the combination of two scenes of dual-polarization data, the single scene of the fully polarimetric data, and the additional topographic-derived feature "distance to river."* Thus, for the combination of two scenes of dual-polarization data, the polarimetric features chosen for these data were mainly derived by backscatter coefficients, whereas those derived by Cloude–Pottier decomposition were selected only in the class pair 3 ("bareland with peat" plus "bareland without peat" and "vegetation with peat" plus "vegetation without peat"). This shows that backscatter coefficients of the dual-polarization data were dominant among almost all land use/cover classes described in this study for the purpose of tropical peatlands classification. For the single scene of fully polarimetric data, a good complementarity was shown between polarimetric features derived by Freeman–Durden

decomposition, Yamaguchi decomposition, the RVI, the total scattering power, and the co-polarized backscatter coefficient measurements. However, polarimetric features derived by Cloude–Pottier decomposition and cross-polarized backscatter coefficient measurements were not selected due to their low performances in separating class pairs, as well as they did not have any effect on increasing the accuracy of the classification results. This indicated that the fully polarimetric data had the potential to characterize land use/cover classes described in this study for the purpose of tropical peatlands classification. For the combination of two scenes of dual-polarization data and the single scene of the fully polarimetric data, the selected polarimetric features for the combination of dual-polarization and fully polarimetric data indicated a dominance of features derived by the fully polarimetric data, especially those selected in the first three class pairs. Polarimetric features derived by the dual-polarization data were mainly selected in separating class pairs 4 ("bareland with peat" and "bareland without peat") and 5 ("vegetation with peat" and "vegetation without peat"), which were the stages of identifying the existence of tropical peatlands in a land use/cover class. This showed that the dual-polarization data aided the fully polarimetric data in characterizing the existence of tropical peatlands in a land use/cover class. Lastly, for the combination of two scenes of dual-polarization data, the single scene of the fully polarimetric data, and the additional topographic-derived feature "distance to river," the selected polarimetric features were identical to those selected in the combination of dual-polarization and fully polarimetric data for all class pairs. The feature "distance to river" was added in separating class pairs 4 and 5. In this study, however, only the category "less than 2 km from river" of the feature "distance to river" was applied to the algorithm of the decision tree classification. The integration of the additional feature "distance to river" was meant to evaluate the effectiveness of GIS data integration in the SAR-based tropical peatlands classification. Thus, in this study, the feature "distance to river" was hypothesized to produce better classification results along with the use of dual-polarization and fully polarimetric data in tropical peatlands classification.

Subsequently, the second specific objective, associated with the second topic of this study, was *to compare and investigate the performance of L-band ALOS PALSAR data for tropical peatlands classification when utilized as single usage, combined, and integrated with topographic-derived feature.* The present study showed that the classification results of the dual-polarization data were inferior to that using the fully

polarimetric data, indicating that the fully polarimetric data were more suitable for classifying tropical peatlands. Furthermore, polarimetric features generated by the combination of dual-polarization and fully polarimetric data yielded an overall accuracy (OA) of 69% and a kappa coefficient (K) of 0.57. Thus, accuracy indicators were increased by applying the combination of dual-polarization and fully polarimetric data to the algorithm of decision tree classification for the SAR-based tropical peatlands classification. However, the best accuracy was obtained by means of integrating the feature "distance to river" into the algorithm of decision tree classification. The accuracy indicators derived by the combination of dual-polarization data, fully polarimetric data, and the additional feature "distance to river" yielded the best OA and K of 76.0% and 0.66, respectively. To conclude, the accuracy indicators derived by the combination of dual-polarization data, fully polarimetric data, and the additional feature "distance to river" were increased by nearly 10% for OA and 15% for K over the best obtained OA and K derived by the SAR-based tropical peatlands classification using the decision tree classifier. These results indicated that the methodology in this study might serve as an efficient tool in tropical peatlands classification, especially when involving the use of L-band SAR dual-polarization and fully polarimetric data.

To obtain the third primary objective, the third topic of this study (as described in Chapter 5) has been determined on two specific objectives. The first specific objective, associated with the third topic of this study, was *to compare and evaluate the performance of features derived after the ground-range radar cross section (sigma naught or σ^0) and slant-range perpendicular radar cross section (gamma naught or γ^0) of C-band Sentinel-1 data for discriminating peat depth classes.* The present study showed that the γ^0 features yielded better performance in discriminating peat depth classes. By comparing the highest DF values of class pair (A) ("shallow-peat" plus "medium-peat" and "deep peat" plus "very-deep peat"), derived using σ^0 and γ^0 features, for both polarization channels, it was found that γ^0 features yielded much higher DF values for class pair (A), for both polarization channels, than those produced by σ^0 features. Furthermore, by applying γ^0 features, the DF values of class pair (A) increased as much as 11.5% and 13.3% for VH and VV polarizations, respectively. Thus, in this study, γ^0 features were used for developing a methodology for classifying peat depth due to the features having better performance in discriminating peat depth classes.

Thereafter, the second specific objective, associated with the third topic of this study,

was *to develop methodology for peat depth classification on oil palm plantations using C-band Sentinel-1 data.* In this study, the selected features for peat depth classification were the gVH06 (γ^0_{VH} in June) and gVV06 (γ^0_{VV} in June), for separating classes in the class pair (A). Subsequently, the gVH03 (γ^0_{VH} in March) and gVV04 (γ^0_{VV} in April) were selected for discriminating peat depth classes in the class pair (B) ("shallow-peat" and "medium-peat"). Afterwards, the gVH06 (γ^0_{VH} in June) and gVV09 (γ^0_{VV} in September) were selected for separating peat depth classes in the class pair (C) ("deep-peat" and "very-deep peat"). In addition, the developed methodology gave the best accuracy for the very deep-peat class, with 76% and 67.86%, PA and UA, respectively, followed by the shallow-peat class that yielded a PA of 64% and UA of 80%. Subsequently, the deep-peat class produced a PA of 58% and UA of 59.18%, whereas the medium-peat class yielded the lowest PA and UA, of 54% and 49.09%, respectively. This study showed that the C-band SAR dual-polarization data have potential for classifying peat depth classes, particularly on oil palm plantations, and might serve as an efficient tool in peat depth classification used for sustainable management of tropical peatlands.

To conclude, the present study has been evaluated potentials of SAR-based RS applications for tropical peatlands monitoring activity in Indonesia, and has been successfully developed methodologies to identify and to classify tropical peatlands, as well as to classify their peat depth categories. In general, the results and findings of this study could aid in increasing the foundation of knowledge regarding the tropical peatlands monitoring activity, involving the use of both L- and C-band SAR data, as an initial response to actualize the sustainable management principles and practices of tropical peatlands in Indonesia. Finally, this study might serve as a contribution to the development of the emerging SAR-based RS applications for monitoring environmental issues in agriculture, especially in the studies of tropical peatlands monitoring activity in Indonesia.

6.2 Recommendation

This study provided a comprehensive understanding in connection with the utilization of L- and C-band SAR data to improve the foundation of knowledge regarding tropical peatlands monitoring activity in Indonesia, especially for use in tropical peatlands identification and classification, as well as in peat depth classification. This study has

successfully demonstrated the ability of L-band ALOS PALSAR fully polarimetric data for tropical peatlands identification in humid tropical regions, such as in Indonesia. It is therefore recommended to apply L-band SAR fully polarimetric data for characterizing and for discriminating tropical peatlands in tropical environments that have persistent cloud cover. Furthermore, this study shows that the integration of GIS data (e.g., topographic-derived feature) in the SAR-based RS application for tropical peatlands classification was found to be effective in improving the classification accuracy. Thus, it is also recommended to utilize the combination of multi-polarization SAR data and GIS data for obtaining a reliable monitoring technique in tropical peatlands classification. In addition, this study has obtained a positive result in verifying the potential of C-band Sentinel-1 data for peat depth classification in oil palm plantations in Indonesia, whereby the γ^0 features were used for developing methodology for classifying peat depth due to the γ^0 features having a better performance in discriminating peat depth classes compared to those using the σ^0 features. Hence, it is recommended to apply the γ^0 features for discriminating peat depth classes in oil palm plantations by means of C-band SAR dual-polarization data. Lastly, along with the growing interests of SAR-based RS applications for tropical peatlands monitoring activity, further study regarding the complementarity between multi-frequency SAR data for tropical peatlands monitoring activity is recommended to further improve the foundation of knowledge regarding SAR-based RS applications towards the implementation of sustainable management principles and practices of tropical peatlands.

References

Agus, F., Hairiah, K., and Mulyani, A. (2011). *Measuring carbon stock in peat soils: practical guidelines*. Bogor, Indonesia: World Agroforestry Centre (ICRAF) Southeast Asia Regional Program and Indonesian Centre for Agricultural Land Resources Research and Development.

Anderson, J. A. R. (1983). The tropical peat swamps of western Malesia. In A. J. P. Gore (Eds). *Ecosystems of the world: mires: swamp, bog, fen and moor* (Vol. 4B, pp. 181–199). New York: Elsevier.

Andriesse, J. P. (1988). Nature and management of tropical peat soils. In *FAO Soils Bulletin 59*. Rome, Italy: Food and Agricultural Organisation of the United Nations.

Antropov, O., Rauste, Y., and Häme, T. (2011). Volume scattering modeling in PolSAR decompositions: Study of ALOS PALSAR data over boreal forest. *IEEE Transactions on Geoscience and Remote Sensing*, 49(10), 3338– 3348.

Antropov, O., Rauste, Y., Praks, J., Hallikainen, M., Häme, T. (2012). Peatland delineation under forest canopy with polsar data using model based decomposition technique. In *Proceeding IEEE International Geoscience and Remote Sensing Symposium* (pp. 4918–4921).

Antropov, O., Rauste, Y., Astola, H., Praks, J., Häme, T., Hallikainen, M. T. (2014). Land cover and soil type mapping from spaceborne PolSAR data at L-band with probabilistic neural network. *IEEE Transactions on Geoscience and Remote Sensing*, 52(9), 5256–5270.

Austin, K., Sheppard, S., and Stolle, F. (2012). *Indonesia's moratorium on new forest concessions: Key findings and next steps*. Retrieved from https:// wri.org/sites/default/files/indonesia_moratorium_on_new_forest_con cessions.pdf

Carmenta, R., Zabala, A., Daeli, W., and Phelps, J. (2017). Perceptions across scales of governance and the Indonesian peatland fires. *Global environmental Change*, 46, 50-59.

CCRS – Center for Remote Sensing Canada. (2014). *Fundamentals of Remote Sensing*. Canada: Canada Center for Remote Sensing.

Chen, J., Lin, H., and Pei, Z. (2007). Application of ENVISAT ASAR data in mapping rice crop growth in southern China. *IEEE Geoscience and Remote Sensing Letters*, 4(3), 431-435.

Cloude, S. R., and Pottier, E. (1996). A review of target decomposition theorems in radar polarimetry. *IEEE transactions on geoscience and remote sensing*, 34,

498-518.

Cloude, S. R., and Pottier, E. (1997) An entropy based classification scheme for land applications of polarimetric SAR. *IEEE transactions on geoscience and remote sensing*, 35, 68–78.

Congalton, R. G. (1991). A review of accessing the accuracy of classifications of remotely sensed data. *Remote Sensing Environment*, 37, 35-46.

Cumming, I. G., and Van Zyl, J. J. (1989). Feature utility in polarimetric radar image classification. In *Proceeding IEEE International Geoscience and Remote Sensing Symposium* (pp. 1841–1846).

Dargie, G. C, Lewis, S. L., Lawson, I. T., Mitchard, E. T. A., Page, S. E., Bocko, Y. E., and Ifo, S. A. (2017). Age, extent and carbon storage of the central Congo Basin peatland complex. *Nature,* 542(2), 86–90.

Dimov, D., Kuhn, J., and Conrad, C. (2016). Assessment of cropping system diversity in the Fergana Valley through image fusion of Landsat 8 and Sentinel-1. *ISPRS Annals of the Photogrammetry, Remote Sensing and Spatial Information Sciences*, III(7), 173-180.

El-Darymli, K., McGuire, P., Gill, E., Power, D., and Moloney, C. (2014). Understanding the significance of radiometric calibration for synthetic aperture radar imagery. In *Canadian Conference on Electrical and Computer Engineering*. Toronto, Canada.

Englhart, S., Staengel, M., and Siegert, F. (2016). Estimation of fire affected areas and carbon emissions on the basis of Sentinel-1. In *Proceedings of the 15th International Peat Congress 2016: Poster Presentations* (pp. 370-374). Kuching, Sarawak, Malaysia.

Farr, T. G., Rosen, P. A., Caro, E., Crippen, R., Duren, R., Hensley, S., Kobrick, M., Paller, M., Rodriguez, E., Roth, L., Seal, D., Shaffer, S., Shimada, J., Umland, J., Werner, M., Oskin, M., Burbank, D., Alsdorf, D. (2007). The shuttle radar topography mission. *Reviews of Geophysics*, 45(2), RG2004.

Freeman, A., and Durden, A. L. (1998). A three-component scattering model for polarimetric SAR data. *IEEE Transactions on Geoscience and Remote Sensing*, 36, 963-973.

Friedl, M. A., and Brodley, C. E. (1997). Decision tree classification of land cover from remotely sensed data. *Remote Sensing of Environment*, 61, 399–409.

Hirano, T., Sundari, S., and Yamada, H. (2016). CO_2 balance of tropical peat ecosystems. In M. Osaki and N. Tsuji (Ed.), *Tropical Peatland Ecosystems* (pp. 329-338). Tokyo, Japan: Springer.

Hoekman, D., and Vissers, M. (2007). ALOS PALSAR radar observation of tropical peat swamp forest as a monitoring tool for environmental protection and

restoration. In *International Geoscience and Remote Sensing Symposium held in Barcelona, Spain on 23-28 July 2007* (pp. 3710-3714). IEEE International.

Hoekman, D. H., Vissers, M. A. M., and Wielaard, N. (2010). PALSAR wide-area mapping of borneo: methodology and map validation. *IEEE Journal of Selected Topics in Applied Earth Observations and Remote Sensing*. 3(4), 605-617.

Hooijer, A., and Vernimmen, R. (2013). *Peatland maps: accuracy assessment and recommendations (TA-QANS)*. Netherlands: Deltares & Euroconsult Mott MacDonald.

Huffman, G.J., Adler, R.F., Bolvin, D.T., Nelkin, E.J. (2010).The TRMM Multi-satellite Precipitation Analysis (TMPA). In F. Hossain and M. Gebremichael (Ed.), *Satellite Rainfall Applications for Surface Hydrology* (pp. 3-22), Springer Verlag.

Huijnen, V., Wooster, M.J., Kaiser, J.W., Gaveau, D.L.A., Flemming, J., Parrington, M., Inness, A., Murdiyarso, D., Main, B., Van Weele, M. (2016). Fire carbon emissions over maritime southeast Asia in 2015 largest since 1997. *Scientific Reports*, 6, 26886.

Irawan, S., and Tacconi, L. (2016). *Intergovernmental fiscal transfer, forest conservation and climate change*. Cheltenham, UK: Edward Elgar.

Jaenicke, J. (2010). *3D modelling and monitoring of Indonesian peatlands aiming at global climate change mitigation.* Ludwig Maximilians University of Munich, Germany.

Jaenicke, J., Rieley, J. O., Mott, C., Kimman, P., and Siegert, F. (2008). Determination of the amount of carbon stored in Indonesian peatlands. *Geoderma*, 147, 151-158.

Jauhiainen, J., Hidenori, T., Juha, E. P. H., Pertti, J. M., and Harri, V. (2005). Carbon fluxes from a tropical peat swamp forest floor. *Global Change Biology*, 11, 1788-1797.

Joosten, H., and Clarke, D. (2002). *Wise use of mires and peatlands - Backgrounds and Principles, including a Framework for Decision-making*. Jyväskylä, Finland: International Mire Conservation Group / International Peat Society.

Kim, Y., and Van Zyl, J. (2004). Vegetation effects on soil moisture estimation. In *International Geoscience and Remote Sensing Symposium held in Anchorage, USA on 20-24September 2004* (Vol. 2, pp. 800-802). IEEE International.

Kuntz, S. (2010). Potential of spaceborne SAR for monitoring the tropical environments. *Tropical Ecology*, 51(1), 3-10.

Lawson, I. T., Kelly, T. J., Aplin, P., Boom, A., Dargie, G., Draper, F. C. H., Hassan, P. N. Z. B. P., Hoyos-Santillan, J., Kaduk, J., Large, D., Murphy, W., Page, S. E., Roucoux, K. H., Sjögersten, S., Tansey, K., Waldram, M., Wedeux, B. M. M., and Wheeler, J. (2015). Improving estimates of tropical peatland area, carbon

storage, and greenhouse gas fluxes. *Wetlands Ecology Management*, 23, 327-346.

Lee, J. S., and Pottier, E. (2009). *Polarimetric radar imaging: From basics to applications*. United States of America: CRC Press Taylor and Francis Group.

Lillesand, T., Kiefer, R., and Chipman, J. W. (2008). *Remote Sensing and Image Interpretation* (Sixth ed.). USA: John Wiley and Sons, Inc.

Lohberger, S., Stängel, M., Atwood, W. C., and Siegert, F. (2017). Spatial evaluation of Indonesia's 2015 fire-affected area and estimated carbon emissions using Sentinel-1. Global Change Biology, 2017;00:1-11.

Lu, D. (2006). The potential and challenge of remote sensing-based biomass estimation. *International Journal of Remote Sensing*, 27(7), 1297-1328.

Luis, V., Lu, J., Foumelis, M., and Engdahl, M. (2017). ESA's multi-mission Sentinel-1 Toolbox. In *Proceedings of the 19th EGU General Assembly* (19398). Vienna, Austria.

Maltby, E. (1997). Developing guidelines for the integrated management and sustainable utilization of tropical lowland peatlands, In J. O. Rieley, and S. E. Page (Eds.). *Biodiversity and sustainability of tropical peatlands - Proceedings of the International Symposium on Tropical Peatlands*, *04-08.09.1995* (pp. 9-18). Palangka Raya, Indonesia: Samara Publishing, Cardigan.

McColl, K., Entekhabi, D., and Piles, M. (2014). Uncertainty analysis of soil moisture and vegetation indices using aquarius scatterometer observations. *IEEE transactions on geoscience and remote sensing,* 52(7), 4259-4272.

Miettinen, J., Shi, C., Liew, S.C. (2016). Land cover distribution in the peatlands of Peninsular Malaysia, Sumatra and Borneo in 2015 with changes since 1990. Global Ecology and Conservation, 6, 67–78.

Miettinen, J., Hooijer, A., Vernimmen, R., Liew, S. C., and Page, S. E. (2017). From carbon sink to carbon source: extensive peat oxidation in insular Southeast Asia since 1990. *Environmental Research Letters*, 12 (024014), 1-10.

Mishra, P., Singh, D., and Yamaguchi, Y. (2011). Land cover classification of Palsar images by knowledge based decision tree classifier and supervised classifiers based on SAR observables. *Progress in Electromagnetics Research B,* 30, 47-70.

Najiyati, S., Muslihat, L., and Suryadiputra, I. N. N. (2005). Panduan pengelolaan lahan gambut untuk pertanian berkelanjutan. Bogor: Wetlands International – Indonesia Programme.

Noor, M. (2012). Sejarah Pembukaan Lahan Gambut untuk Pertanian di Indonesia. In E. Husen, M. Anda, M. Noor, H. S. Mamat, Maswar, A. Fahmi, and Y. Sulaiman

(Eds.). *Pengelolaan Lahan Gambut Berkelanjutan* (pp. 399-412). Bogor, Indonesia: BBSDLP.

Notohadiprawiro, T. (1998). Conflict between problem-solving and optimising approach to land resources development policies – the case of Central Kalimantan Wetlands, In *Proceedings of the International Symposium: Spirit of Peatlands, 7-9 September 1998* (pp. 14-24). Jyväskylä, Finland.

Nugroho, K. (2012). Sejarah Penelitian Gambut dan Aspek Lingkungan. In E. Husen, M. Anda, M. Noor, H. S. Mamat, Maswar, A. Fahmi, and Y. Sulaiman (Eds.). *Pengelolaan Lahan Gambut Berkelanjutan* (pp. 173-184). Bogor, Indonesia: BBSDLP.

Osaki, M., and Tsuji, N. (2016). *Tropical Peatland Ecosystems*. Tokyo, Japan: Springer.

Osaki, M., Nursyamsi, D., Noor, M., Wahyunto, and Segah, H. (2016a). Peatland in Indonesia. In M. Osaki and N. Tsuji (Eds.), *Tropical Peatland Ecosystems* (pp. 49-58). Tokyo, Japan: Springer.

Osaki, M., Hirose, K., Segah, H., and Helmy, F. (2016b). Tropical peat and peatland definition in Indonesia. In M. Osaki and N. Tsuji (Eds.), *Tropical Peatland Ecosystems* (pp. 137-147). Tokyo, Japan: Springer.

Page, S. E., Banks, C. J., and Rieley, J.O. (2007). Tropical Peatlands: Distribution, Extent and Carbon Storage-Uncertainties and Knowledge Gaps. *Peatlands International,* 2, 26–27.

Page, S. E., Rieley, J. O., and Banks, C. J. (2011). Global and regional importance of tropical peatland carbon pool. *Global Change Biology*, 17(2), 798-818.

Page, S. E., Siegert, F., Rieley, J. O., Boehm, H. V., Jaya, A., and Limin, S. (2002). The amount of carbon released from peat and forest fires in Indonesia during 1997. *Nature,* 420, 61-65.

Page, S.E., and Rieley, J.O. (1998). Tropical peatlands: a review of their natural resource functions, with particular reference to Southeast Asia. *International Peat Journal*, 8, 95-106.

Pal, M., and Mather, P. M. (2003). An assessment of the effectiveness of decision tree methods for land cover classification. *Remote Sensing of Environment*, 86, 554–565.

Rieley, J. O. (2007). Tropical peatland - the amazing dual ecosystem: co-existence and mutual benefit. In *Proceedings of The International Symposium and Workshop on Tropical Peatland edited by J. O. Rieley, C. J. Banks, and B. Ragjagukguk, held in Yogyakarta, Indonesia, on 27-29 August 2007* (pp. 1-14). EU CARBOPEAT and RESTORPEAT Partnership.

Rieley, J. O., and Page, S.E. (2005). Wise Use of Tropical Peatlands - Focus on Southeast Asia. Wageningen: ALTERRA.

Rieley, J. O., and Page, S. E. (2016). Tropical peatland of the World. In M. Osaki and N. Tsuji (Eds.), *Tropical Peatland Ecosystems* (pp. 3-32). Tokyo, Japan: Springer.

Rieley, J. O., Wüst, R. A. J., Jauhiainen J., Page, S. E., Wösten, H., Hooijer, A., Siegert, F., Limin, S. H., Vasander, H., and Stahlhut, M. (2008). Tropical peatlands: carbon stores, carbon gas emission and contribution to climate change processes. In M. Strack (Eds.). *Peatlands and Climate Changes* (pp. 148-181). International Peat Society.

Ritung, S., Wahyunto, and Nugroho, K. (2012). Karakteristik dan sebaran lahan gambut di Sumatera, Kalimantan dan Papua. In E. Husen, M. Anda, M. Noor, H. S. Mamat, Maswar, A. Fahmi, and Y. Sulaiman (Eds.). *Pengelolaan Lahan Gambut Berkelanjutan* (pp. 47-62). Bogor, Indonesia: BBSDLP.

Romshoo, S. A., Shimada, M., and Igarashi, T. (2002). Peatland ecosystem characterization employing L-band SAR. *Geoscience and Remote Sensing Symposium, IEEE*, 3, 1795-1797.

Rudiyanto, Minasny, B., Setiawan, B. I., Arif, C., Saptomo, S. K., and Chadirin, Y. (2016). Digital mapping for cost-effective and accurate prediction of the depth and carbon stocks in Indonesian peatlands. *Geoderma*, 272, 20-31.

Rydin, H., and Jeglum, J. (2006). *The biology of peatlands*. United Kingdom: Oxford University Press.

Sabiham, S., and Kartawisastra, S. (2012). Peatland management for oil palm development in indonesia. *Indonesian Journal of Land Resources*, 6(2), 55–66.

Shimada, M. (2010). Ortho-rectification and slope correction of SAR data using DEM and its accuracy evaluation. *IEEE Journal of Selected Topics in Applied Earth Observations and Remote Sensing*, 3(3), 657-671.

Shimada, S., Takahashi, H., and Osaki, M. (2016a). Carbon Stock Estimate. In M. Osaki and N. Tsuji (Eds.), *Tropical Peatland Ecosystems* (pp. 353-365). Tokyo, Japan: Springer.

Shimada, S., Takada, M., and Takahashi, H. (2016b). Peat Mapping. In M. Osaki and N. Tsuji (Eds.), *Tropical Peatland Ecosystems* (pp. 455-467). Tokyo, Japan: Springer.

Siegert, F., Zhukov, B., Oertel, D., Limin, S., Page, S. E., Rieley, J. O. (2004). Peat fires detected by the BIRD satellite. *International Journal of Remote Sensing*, 25, 3221–3230.

Simard, M., Grandi, G. D., Saatchi, S., and Mayaux, P. (2002). Mapping tropical coastal vegetation using JERS-1 and ERS-1 radar data with a decision tree classifier. *International Journal of Remote Sensing*, 23(7), 1461-1474.

Simard, M., Saatchi, S. S., and Grandi, G. D. (2000). The use of decision tree and multiscale texture for classification of JERS-1 SAR data over tropical forest. *IEEE Transactions on Geoscience and Remote Sensing*, 38(5), 2310-2321.

Takada, M., Mishima, Y., and Natsume, S. (2009). Estimation of surface soil properties in peatland using ALOS/PALSAR. *Landscape and Ecological Engineering*, 5(1), 45-58.

Van Der Werf, G. (2015). Indonesian fire season progression. Global Fire Data Updates [Online]. Available from: http://www.globalfiredata.org/updates.html [Accessed October 25 2015].

Viera, J. A. and Garrett, J. M. (2005). Understanding interobserver agreement: The kappa statistic. *Family Medicine*, 37(5), 360-363.

Wahyunto, and Agus, F. A. (2012). ALOS satellite data to explore areal extent of peatland. Case study: Kubu Rata District, West Kalimantan Province. In *Report and proceedings of ALOS application and verification project in Indonesia* (pp. 26-31). LAPAN and JAXA.

Watanabe, M., Kushida, K., Yonezawa, C., Sato, M., and Fukuda, M. (2011). PALSAR full-polarimetric observation for peatland. *Asian Journal of Geoinformatics*, 11(3).

Wijaya, A., Marpu, P. R., and Gloaguen, R. (2010). Discrimination of Peatlands in tropical swamp forests using dual-polarimetric SAR and Landsat ETM data. *International Journal of Image and Data Fusion*, 1(3), 257-270.

Yamaguchi, Y., Moriyama, T., Ishido, M., and Yamada, H. (2005). Four-component scattering model for polarimetric SAR image decomposition. *IEEE Transactions on Geoscience and Remote Sensing,* 43(8), 1699-1706.

List of Publications

CHAPTER 3

Author : **Dandy Aditya Novresiandi,** Ryota Nagasawa

Title : Tropical peatland identification using ALOS PALSAR imageries - A case study in Kahayan River catchment area, Central Kalimantan, Indonesia -

Journal : Journal of The Japanese Agricultural Systems Society, 2016, Vol. 32, No.1, pp. 1-9.

CHAPTER 4

Author : **Dandy Aditya Novresiandi,** Ryota Nagasawa

Title : Polarimetric synthetic aperture radar application for tropical peatlands classification: a case study in Siak River Transect, Riau Province, Indonesia

Journal : Journal of Applied Remote Sensing, 2017, Vol. 11, No. 1, 016040, pp. 1-13, doi: 10.1117/1.JRS.11.016040

CHAPTER 5

Author : **Dandy Aditya Novresiandi,** Ryota Nagasawa

Title : C-Band Dual-Polarization Synthetic Aperture Radar Application for Peat Depth Classification: A Case Study in Siak Regency, Riau Province, Indonesia

Journal : Progress in Electromagnetics Research M, 2017, Vol. 61, pp. 29-41

Appendices

Appendix 1 The common tropical peatlands condition in the study area 1 presented in Chapter 3.

Appendix 2 The common tropical peatlands condition in the study area 2 presented in Chapter 3.

Appendix 3 Photographs of the ground truth survey's activity for the study presented in Chapter 3, include (a) peat depth measurement, (b) current land use/cover observation, (c) peat maturity measurement, (d) soil moisture measurement, (e) observation and documentation on surrounding environment, and (f) sample points collection.

(a)

(b)

(c)

(d)

(e)

(f)

Appendix 4 The methodological flow chart of the study presented in Chapter 3.

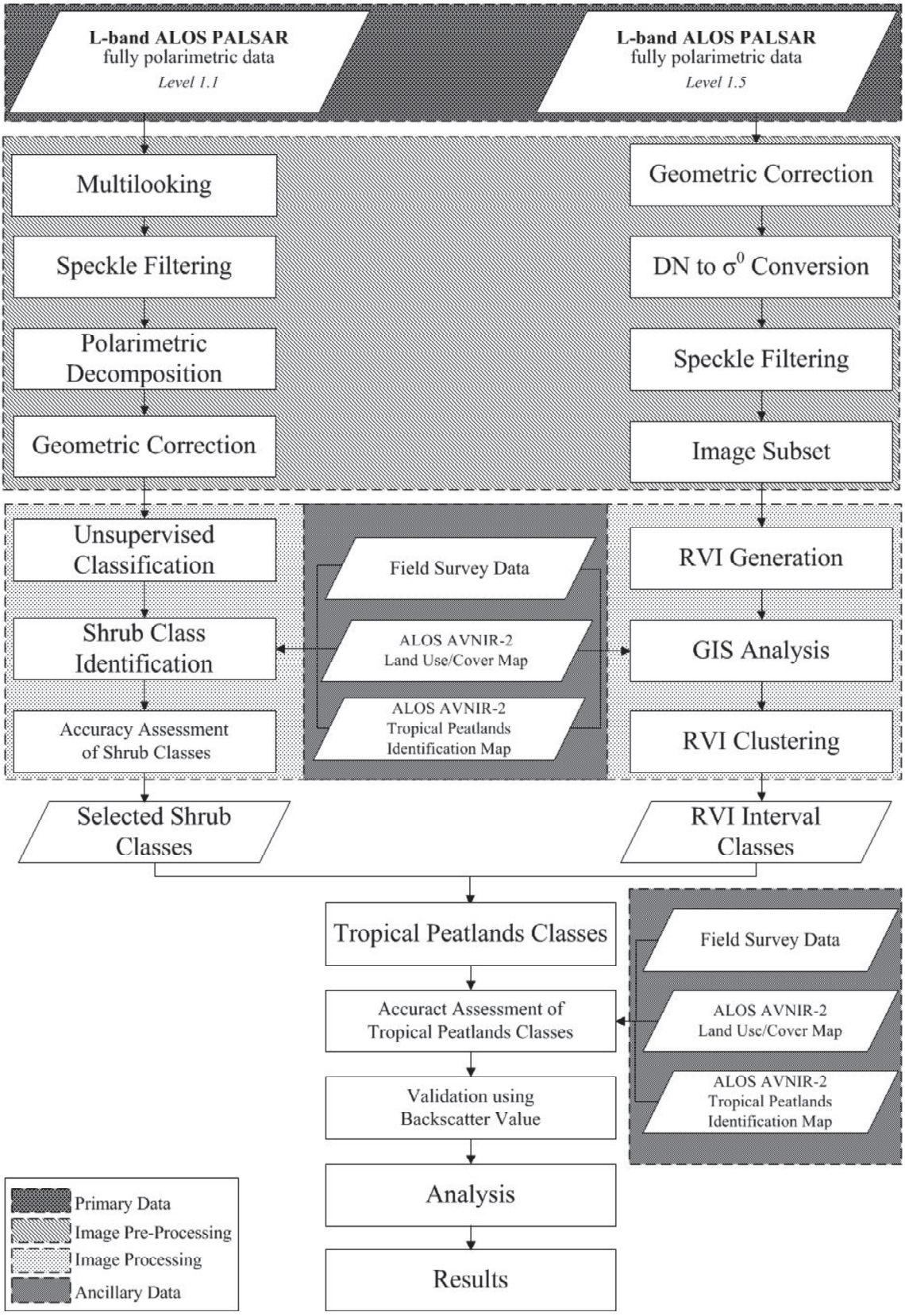

Appendix 5 The common tropical peatlands condition in the study area presented in Chapter 4.

Appendix 6 Photographs of the joint ground truth survey's activity for the study presented in Chapter 4, include, (a) coordination with local government, (b) coordination with IAARD, (c) current land use/cover observation, (d) peat maturity measurement, (e) observation and documentation on surrounding environment, and (f) peat drilling with soil auger.

(a)

(b)

(c)

(d)

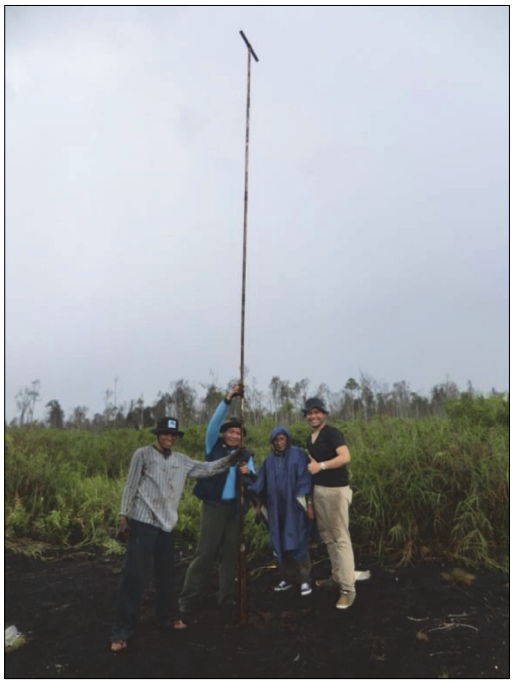

(e)

(f)

Appendix 7 The methodological flow chart of the study presented in Chapter 4.

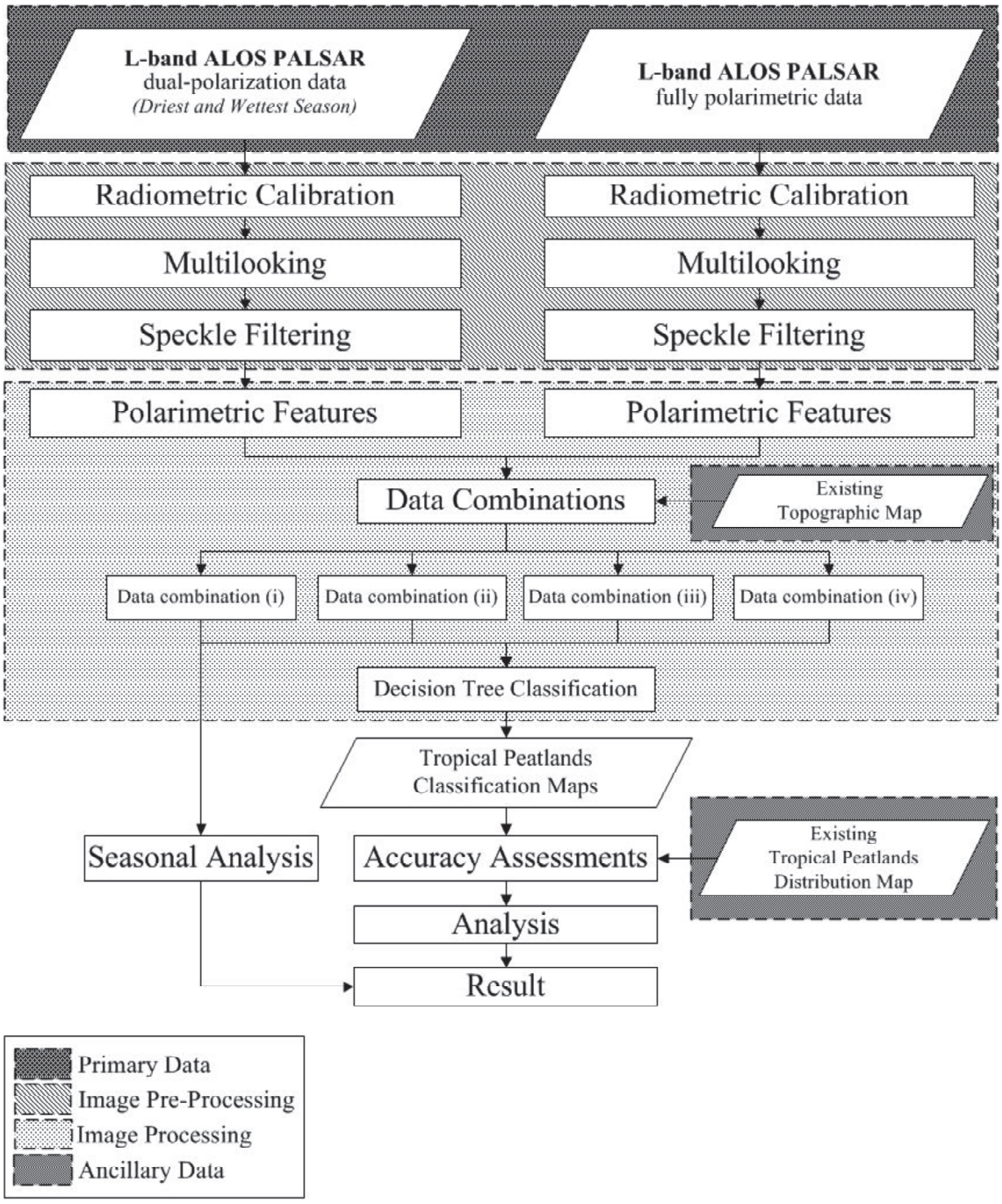

Appendix 8 The methodological flow chart of the study presented in Chapter 5.

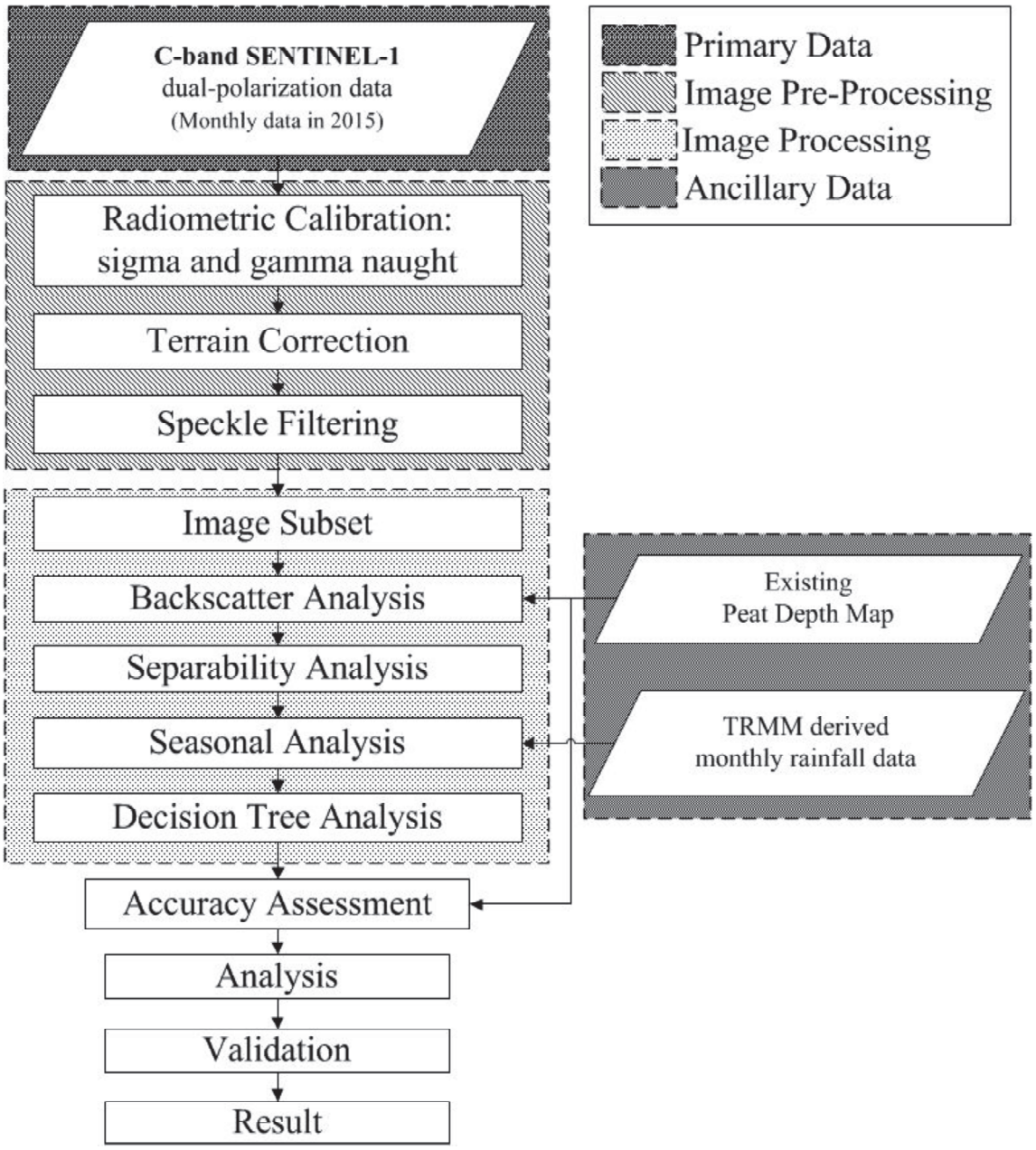

Summary

Tropical peatlands acknowledged as one of key ecosystems among the high-carbon reservoir ecosystems due to their huge carbon and water storage, their effect on coastal ecosystems, and their role in preserving bio-resources and biodiversity. Furthermore, tropical peatlands play an important role in the global carbon balance, and thus have a direct relationship with global climate change processes. Unfortunately, tropical peatlands are now being subjected to a rapid economic development without full consideration to the sustainable management principles and practices of tropical peatlands, which has led to large increases in carbon emission.

Concurrently, the importance of tropical peatlands as a long-term carbon sinks and stores, their tendency to become a short-term source of carbon emission, and their significant role in climate change processes, have been receiving tremendous interest during the past two decades. These concerns should be initially responded to via an accurate inventory of tropical peatlands to obtain a better understanding of the sustainable management principles and practices of tropical peatlands, as well as to improve the foundation of knowledge in tropical peatlands monitoring activity. Nevertheless, tropical peatlands cover relatively large areas and are primarily located in remote areas that are difficult to access. Thus, it is obviously challenging to develop reliable methodologies for monitoring the vast areas of tropical peatlands, especially in Indonesia where the largest portion of the tropical peatlands is located.

Remote sensing (RS) application is recognized as one of the most suitable tool to monitor the vast areas of tropical peatlands, as in situ measurements are generally time-consuming, labor-intensive and limited by accessibility. Furthermore, the recent development of synthetic aperture radar (SAR)-based RS satellites has introduced an advanced prospect that enables continuous monitoring and cloud-free observation in humid tropical regions, particularly for tropical peatlands monitoring activity in Indonesia. The primary objectives of this study are to explore the ability of L-band Advanced Land Observing Satellite (ALOS) Phased Array type L-band SAR (PALSAR) fully polarimetric data for tropical peatlands identification, to evaluate the performance of L-band ALOS PALSAR dual-polarization and fully polarimetric data for tropical peatlands classification, as well as to investigate the potential of C-band dual-polarization Sentinel-1 data for peat depth classification, in response to the

emerging SAR-based RS applications for tropical peatlands monitoring activity.

The first topic of this study was carried out to investigate the use of L-band ALOS PALSAR fully polarimetric data for identifying tropical peatlands in two study areas situated in Kahayan River catchment area, Central Kalimantan Province, Indonesia. Specifically, three polarimetric decomposition (PD) theorems and the radar vegetation index (RVI) were evaluated for their capability to identify tropical peatlands characteristics from the viewpoint of L-band SAR fully polarimetric data. This study has suggested that SAR-based RS application serves as an efficient tool in tropical peatlands identification, such that the combination of classes derived from unsupervised classification of polarimetric features of Freeman-Durden tree-component decomposition integrated with the broad-interval (calculated by mean and standard deviation values) class of RVI value that generated from L-band ALOS PALSAR fully polarimetric data was successfully identified the existence of tropical peatlands. Thus, the tropical peatlands identified in study area 1 yielded a producer's accuracy (PA) of 75.8% and a user's accuracy (UA) of 80.9%, whereas those in study area 2 gave accuracies of 77.6% and 76.0% for PA and UA, respectively.

The second topic of the present study evaluated the performance of L-band ALOS PALSAR dual-polarization data, fully polarimetric data, and their data combinations for tropical peatlands classification in Siak River transect, Riau Province, Indonesia. Thus, polarimetric features derived after PD theorems, backscatter coefficients measurements, and the RVI were evaluated to classify tropical peatlands using the decision tree (DT) classifier. This study has found that the classification results of the dual-polarization data were inferior to the fully polarimetric data, indicating that the fully polarimetric data were more suitable for classifying tropical peatlands. Furthermore, the integration of topographic-derived data in the SAR-based tropical peatlands classification was found to be effective in improving the classification accuracy, whereby in this study, the feature "distance to river" increased the classification accuracy by nearly 10% for overall accuracy (OA) and 15% for Kappa coefficient (K) when integrated with the polarimetric features derived by the combination of dual-polarization and fully polarimetric data by means of the DT classifier. Additionally, the seasonal variation of tropical peatlands was discovered, in which the existence of tropical peatlands in a land use/cover without the presence of vegetation was not influenced by the seasonal condition. In contrast, the existence of tropical peatlands in a land use/cover with the

presence of vegetation was influenced by the seasonal condition.

The third topic of this study examined the potential of C-band dual-polarization Sentinel-1 data for peat depth classification on oil palm plantations in Siak Regency, Riau Province, Indonesia. Particularly, the ground-range radar cross section (σ^0) and slant-range perpendicular radar cross section (γ^0) for both polarization channels — vertical transmit-horizontal receive (VH) and vertical transmit-vertical receive (VV) — of Sentinel-1 data were compared and evaluated, on monthly basis, during 2015, for discriminating peat depth classes using the DT classifier. This study has suggested that γ^0 features yielded better performance in discriminating peat depth classes. By applying γ^0 features, the distance factor (DF) values of the initial class pair increased as much as 11.5% and 13.3% for VH and VV polarizations, respectively. Furthermore, the classification results gave the best accuracy for the very deep-peat class, with 76% and 67.86%, of PA and UA, respectively, followed by the shallow-peat class that yielded a PA of 64% and UA of 80%. Subsequently, the deep-peat class produced a PA of 58% and UA of 59.18%, whereas the medium-peat class yielded the lowest PA and UA, of 54% and 49.09%, respectively. In addition, the seasonal variation of rainfall intensity was discovered to be influencing feature selection for peat depth classification. Thus, the combination of γ^0 features derived in the much rain months was selected for separating the shallow- and medium-peat classes, whereas those derived in the less rain months was selected for discriminating the deep- and very deep-peat classes.

To conclude, the present study has been successfully developed methodologies for tropical peatlands identification by means of L-band SAR fully polarimetric data, for tropical peatlands classification by using L-band SAR dual-polarization and fully polarimetric data, as well as for peat depth classification on oil palm plantations by utilizing C-band SAR dual-polarization data. In general, the results and findings of this study could aid in increasing the foundation of knowledge regarding the tropical peatlands monitoring activity, involving the use of both L- and C-band SAR data, as an initial response to actualize the sustainable management principles and practices of tropical peatlands in Indonesia. Finally, this study might serve as a contribution to the development of the emerging SAR-based RS applications for monitoring environmental issues in agriculture, especially in the studies of tropical peatlands monitoring activity.

Keywords: ALOS PALSAR, Sentinel-1, dual-polarization, fully polarimetric, polarimetric decomposition, radar vegetation index, decision tree classification

Japanese Summary

熱帯泥炭地は膨大な土壌炭素・地下水を貯留しており，海岸地域における炭素貯留生態系のなかでも重要な位置を占め，地球温暖化に関わる炭素収支に大きな役割を果たしている。しかしながら，近年の急速な経済発展に伴い熱帯地域における泥炭地の開発は適切な生態系管理に対する配慮もなされぬまま著しく進展し，大量の CO^2 を大気に放出する危険性が高まっている。炭素貯留庫としての熱帯泥炭地では，その不適切な管理から発生する膨大な CO^2 排出量は地球全体の気候変動に与える影響は極めて憂慮される地球環境問題であり，過去 20 年にわたって大きな関心事として注目されている。特に，インドネシアは地球上の熱帯地域に分布する泥炭地面積の半分以上を占めているにもかかわらず，その持続可能な管理手法やモニタリングについてはこれまでに適切な行動・配慮が施されてきたとは言い難い状況にある。

衛星リモートセンシングは，広大な泥炭地においてその全容を把握するモニタリングツールとして極めて有効な手法である。特に，合成開口レーダー(SAR)を用いた手法は全天候型で雲被覆の影響を受けることなく経時観測が可能であるためにインドネシアのような熱帯地域での活用は極めて有効である。そこで，本研究の目的は日本の ALOS 衛星に搭載された L バンド SAR データの 2 偏波および４（全）偏波合成データを用いて熱帯泥炭地を分類・抽出し，さらに C バンドセンサーを搭載した Sentinel-1 衛星の SAR 画像から泥炭層厚の区分を試み，衛星リモートセンシングによる熱帯地域の泥炭地モニタリングの利用可能性を評価することにある。

本研究での 1 番目の議論は，L バンド SAR（ALOS PALSAR）の全偏波合成手法を用いた熱帯泥炭地の分類・抽出手法開発に関する検討である。研究対象地域は，中央カリマンタン州のカハヤン川流域に広がる低湿地で行われた。3 種の偏波合成とレーダー植生指数（RVI）の手法を試み，Freeman-Durden の偏波合成と L バンド SAR の RVI の中央値と標準偏差値を用いた教師なし分類手法が熱帯泥炭地の特徴抽出を行うのに有用であることがわかった。その分類精度は，対象地域１と対象地域２の 2 か所においてそれぞれプロデューサー精度で 75.7%と 77.6%，ユーザー精度で 80.9%と 76.0%の値を得，統計的に泥炭地抽出の実行可能性が実証された。

本研究での 2 番目の議論は，L バンド SAR の 2 偏波と全偏波画像を用いた熱帯泥炭地の空間的分布をマッピングする手法検討である。研究対象地域は，リアウ州のシアック川の流域である。画像分類手法としては，偏波合成による偏波の特性，後方散乱量および RVI 値を用いたディシジョンツリー分類が試みられた。これに地形データを加味することによって分類精度は向上し，さらに河川からのバッファー距離を用いることで総合精度（OA）で 10%近く，カッパー係数（K）で 15%の精度の改善が得られ，熱帯泥炭地の図化が可能になった。

本研究での 3 番目の議論は，C バンド SAR の 2 偏波画像を用いた泥炭層厚の分類に関する検討である。ここでは，上記研究地域と同様にシアック県のオイルパームプランテーション地域において検討を行った。Sentinel-1 画像の多季節データの水平偏波(VH)と垂直偏波(VV)のうち ground-range radar cross section（σ^0）と slant-range perpendicular radar cross section（γ^0)を用いてディシジョンツリー分類により泥炭層厚の分類を試みた。その結果，パラメータとしては γ^0 特性が有効であることが示され，初期値の distance factor (DF)は VH,VV の偏波合成に対してそれぞれ 11.5%と 13.3%上昇した。さらに，泥炭層厚クラスの分類精度はプロデューサー精度で 76%，ユーザー精度で 67.86%を得て高精度で分類できることが分かった。このうち，浅層の泥炭層についてはプロデューサー精度が 64%，ユーザー精度で 80%，より深層の泥炭層で 58%と 59.1%，中層のそれでは 54%と 49.09%の精度値を得る結果となった。こうしたことから，C バンド SAR の 2 偏波画像を用いることによってオイルパームが展開する泥炭地の層厚をある程度の精度で分類区分・図化できることが明らかにされた。

包括的な結論として，SAR を基調とした衛星リモートセンシング手法では，熱帯地域の泥炭地の空間的分布や泥炭層厚の区分を有効的に行えることが明らかにされた。その効用は L バンドと C バンドデータを併用することによってより効果的であり，インドネシアのような熱帯泥炭地の今後の持続的生態系管理に SAR リモートセンシングが極めて有用であることが示された。

キーワード：ALOS PALSAR, Sentinel-1, ２偏波合成, ４（全）偏波合成, ポラリメトリック（偏波）合成, レーダー植生指数, ディシジョンツリー分類